

CENTRAL LIBRARY

TEZPUR DIST. LIBRARY

Accession No. I 323

Date _____

**THERMOCHEMICAL CONVERSION OF BIOENERGY
BYPRODUCTS TO BIO-OIL AND BIOMATERIALS**

**A THESIS SUBMITTED IN PARTIAL FULFILLMENT OF THE
REQUIREMENTS FOR THE DEGREE OF
DOCTOR OF PHILOSOPHY**

RAHUL SINGH CHUTIA
Registration Number 042 of 2010



**SCHOOL OF ENGINEERING
DEPARTMENT OF ENERGY
TEZPURUNIVERSITY
DECEMBER, 2013**

**I WANT TO DEDICATE THIS THESIS TO MY PARENTS WHOSE SKY FULL LOVE
AND PRINCIPLE OF LIFE INSPIRED ME TO DO THIS EVENTFUL WORK
SUCCESSFULLY.**

Rahul

DECLARATION

I do hereby declare that the thesis entitled "*Thermochemical Conversion of Bioenergy Byproducts to Bio-oil and Biomaterials*", being submitted to the Department of Energy, Tezpur University, is a record of original research work carried out by me. All sources of assistance have been assigned due acknowledgment. I also declare that neither this work as a whole nor a part of it has been submitted to any other University or Institute for any other degree, diploma or award.

Place : Tezpur University, Tezpur

Rahul Singh Chutia
(Rahul Singh Chutia)

Date : 31/12/2013



TEZPUR UNIVERSITY

(A Central University established by an Act of Parliament)
NAPAAM, TEZPUR-784028, ASSAM

CERTIFICATE BY THE SUPERVISOR(S)

This is to certify that the matter embodied in the thesis entitled ***“Thermochemical Conversion of Bioenergy Byproducts to Bio-oil and Biomaterials”*** submitted to the School of Engineering, Tezpur University in partial fulfillment for the award of the degree of Doctor of Philosophy in **Energy**, is a record of research work carried out by **Mr. Rahul Singh Chutia** under our supervision and guidance.

All help received by him from various sources have been duly acknowledged.

No part of this thesis has been submitted elsewhere for award of any other degree.

Signature of:

Handwritten signature of Dr. Rupam Kataki in black ink.

Supervisor: Dr. Rupam Kataki

Designation: Associate Professor

School: Engineering

Department: Energy

Date:

Handwritten signature of Dr. Thallada Bhaskar in black ink.

Co-Supervisor: Dr. Thallada Bhaskar

Designation: Senior Scientist & Head

Affiliation: Thermo-catalytic Processes Area,
Bio-Fuels Division (BFD), CSIR-Indian Institute
of Petroleum, Dehradun 248005 .

Date:



TEZPUR UNIVERSITY
(A Central University established by an Act of Parliament)
NAPAAM, TEZPUR-784028
DISTRICT : SONITPUR :: ASSAM :: INDIA
Ph: 03712-267004, 267005 Fax: 03712-267005, 267006

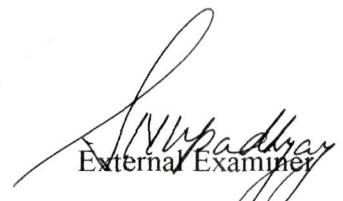
CERTIFICATE

This is to certify that the thesis entitled "*Thermochemical Conversion of Bioenergy Byproducts to Bio-oil and Biomaterials*" submitted to the Tezpur University in the Department of Energy under the School of Engineering; in partial fulfillment for the award of the Degree of Doctor of Philosophy in **Energy**, has been examined by us on 03-03-15 and found to be satisfactory.

The committee recommends for the award of the degree of Doctor of Philosophy.


Principal Supervisor

Date: 03-03-2015


External Examiner
03/03/2015
Date:

ACKNOWLEDGEMENT

In the endeavor of the journey towards my doctoral work, this thesis has been kept on track and seen through to completion with the support and encouragement of numerous people including my supervisors, well-wishers, friends, colleagues and different laboratories. It is a pleasant opportunity to express my wholehearted thanks to all those people who made this thesis possible and contributed in different ways.

I am greatly indebted to my venerable supervisor Dr. R. Kataki and co-supervisor Dr. T. Bhaskar, for their keen interest, constant guidance and encouragement, authoritative discussion during the entire course of my Ph. D. programme and innumerable constructive suggestions and help during the preparation of this manuscript.

I would also like to thank my doctoral committee members, Prof. S. K. Samdarshi and Prof. D. Deka of department of Energy and Dr. A. J. Thakur, Department of chemical sciences for serving as my doctoral committee members and their valuable advice, helpful suggestions, comments and encouragement.

I convey my sincere gratitude and thanks to Prof. D. Deka, Head, Prof. S. K. Samdarshi and Prof. D. C. Baruah, former heads, Dept of Energy for providing me the necessary facilities to carry out my research work. I would also like to thank Mr. S. Mahapatra, Mr. P. K. Choudhury and Dr. P. Kalita of Department of Energy for their support, encouragement and valuable advices.

Most of the results described in this thesis would not have been obtained without a close collaboration with few laboratories. I owe a great deal of appreciation and gratitude to Director of CSIR-Indian Institute of Petroleum, Dehradun for giving me the opportunity to do a part of this research work at biofuels division. I would also thank Director, CSIR-North East Institute of Science & Technology, Mr. H. K. Baruah of Oil India Limited, Duliajan, Dr. J. Chetia of dibrugarh University for their support while facilitating the infrastructure for sample testing.

I offer my special to all my lab-mates Prasen da, Munu, Maumita, Sarat, Neon, Rumi, Debashis, Ruprekha, Deepak, Vivek and Debojeet for providing a stimulating

and fun filled environment. Special thanks to Neon, Rumi and Ruprekha for their help during preparation of this thesis.

It is my pleasure to offer gratitude and thanks to Biswajit gogoi, Technical officer, Tapanjit Borah, Technical Assistant, T. Lahon, Lab assistant, Chittaranjan gogoi, Office Assistant, Department of Energy, Tezpur University, for their co-operation and encouragement.

I received great help from my friends, Pitambar da, Tapan da, Ruhit, Mayur, Samrat ji, Barman ji, Rajib, Madhuryya, Dushyanta, Subhasit, Anup, Diganta, Pranjal, Shyam, Champak, Hemanga and all my fellow researcher friends, department of Energy, during the entire period of my Ph.D work. Special thanks to Pitambar da, Mayur, Ruhit, Madhuryya and Rajib for their suggestions and help in every phases of my Ph.D work.

I express my gratitude and thanks to baidew (Mrs. Mankia Das) for her care and encouragement.

I express my sincere thanks to Lakhya da for his efforts and timely help during the preparation of the manuscripts.

Last but not least, I am grateful to my most beloved Ma, Papa, bhonti, Apu and all my family members and childhood friend particularly my Koka (Late Grandfather), Aapa, Mama, Mami, Daisy ba, Dimpal, Moni Ba, Abhijit da, Papu, pallab, Manuj, Aicharjya for their timely inspiration, love, care and support during the uncompromising time of my research work.

I am highly thankful to Tezpur University for its initial financial support in the form of Institutional Fellowship, University grants commission (UGC), New Delhi, for providing financial assistance in the form of Meritorious Students Fellowship and Ministry of New and Renewable Energy, Govt. of India, for providing financial grant in the form of National Renewable Energy fellowship which supported me to pursue my doctoral research conveniently.

(Rahul Singh Chutia)

ABSTRACT

Currently, a great deal of interest is focused on renewable energy worldwide, due to continuous diminution in the availability of conventional fossil based resources coupled with increasing cost of extraction from these sources and ever increasing pollution due to utilization of fossil resources. For these reasons, search for a new and sustainable alternative renewable source of energy has been geared up and one of the aspects with enormous potential for gratifying mankind's energy need is biomass sources due to its easy availability, easy process ability and environment friendly nature. Again biomass is the fourth largest energy source in the world and due to their high reactivity and volatility; they can be easily processed to produce fuels and value added chemicals. Moreover, biomass has been serving human civilization from antiquity as a primary source of energy either in the form of wood and dung for cooking and heating, charcoal for metallurgy, and animal feeds for food and transportation. As a result, biomass is considered to be one of the most attractive and promising renewable energy resource.

As of now, the existent available bio-energy feedstock cannot suffice for the petro-crude reservoirs; consequently new feedstock for the same will serve as a cumulative step for addressing the long documented problem of energy production and supply. For an agriculture based economy like India, the vista of utilization of feedstocks like agricultural residues to various forms of fuel as a supplement for conventional fossil based fuel is attractive, as it has numerous advantages suitable for achieving energy and benefiting in environmental, agricultural and trade policies. This is also important as these resources are otherwise low-value perishable products. It is indeed with this purpose that two bioenergy byproducts i.e. deoiled cakes of *Mesua ferrea* (MFDC) and *Pongamia glabra* (PGDC) are selected for present investigation via pyrolysis conversion technique. *Mesua ferrea* and *Pongamia glabra* are two oil bearing forest tree species having been extensively researched for their utilization for biodiesel production. Deoiled seed

cakes of these two species are biomass resources with little or no reported use so far. Again, successful utilization of any biofuel mission fundamentally depends on the availability of feedstock. The greatest share of production costs of biofuel is linked with the feedstock. Consequently, availability of low-cost and good quality non-edible feedstock is critical to large-scale commercial use of biofuel. In this regard, feasibility of conversion of deoiled seed cakes to liquid fuel as well as value added chemicals and other biomaterials is being tried as one of the route of value addition of these otherwise waste bio-resources.

Various experimental and characterization techniques were adopted for the feedstocks under investigation and the pyrolysis products i.e. bio-oil and biochar generated. The biomass feedstock used in this investigation was characterized and its thermal decomposition behavior together with pyrolytic conversion through catalytic and non-catalytic routes was studied. Characterization of the solid and liquid products obtained via pyrolysis of MFDC and PGDC was also carried out. It was found that low moisture, ash content and high volatile matter as compared to some other feedstock suggest MFDC and PGDC as a potential candidate for pyrolysis for production of liquid hydrocarbons. The gross calorific value of MFDC and PGDC (18.7 & 16.9 MJ/kg respectively) and proximate analysis confirms the suitability of the feedstock for exploitation of biocrudes/biochemicals production. To calculate the activation energy the entire thermogravimetric curve for both the feedstock was divided into four regions viz. S_I, S_{II}, S_{III} and S_{IV} since every single slope change on a TG curve indicates the beginning of a new stage. The average activation energy for MFDC calculated from Arrhenius, Coats-Redfern, FWO and Global independent reactions model are found to be 54.1, 64.1, 94.0 and 43.8 kJ/mol for S_{II} and 169.6, 252.6, 146.9 and 256.8 kJ/mol for S_{III}, respectively. The average activation energy for PGDC of stage S_{II} was calculated as 91.7, 130.8, 127.7 and 76.1 kJ/mol and 96.6, 193.2, 128.7 and 256.8 kJ/mol for S_{III} by Arrhenius, FWO, Coats-Redfern methods and Global independent reactions model respectively. Both the feedstock under investigation showed almost similar pyrolytic behavior which is evident from the pyrolysis experiments. The maximum liquid yield of 32 and 30% was observed for MFDC and PGDC respectively at

500°C with a heating rate of 40°C/min. However application of catalyst decreased the liquid product yield while char yield increased for both the feedstocks. Bio-oil obtained from MFDC and PGDC via catalytic pyrolysis have higher carbon, hydrogen and lower oxygen content as compared to bio-oil obtained via non-catalytic pyrolysis. Furthermore, catalytic pyrolysis derived bio-oil contained higher aromatic content than non-catalytic pyrolysis derived bio-oil. HZSM-5 catalyst showed a higher selectivity towards aromaticity than Mordenite and Y-zeolite. Pyrolysis of mixed feedstock showed good result with a yield of 30.4% at 500°C. The bio-oil from the mixed feedstock showed similar properties with individual bio-oil. However, as expected differences in composition to that of PGDC and MFDC bio-oil are found through NMR and GC-MS.

The generated liquid product i.e. bio-oil was studied for its applicability as a chemical feedstock and screened for its antimicrobial activity against four microorganisms namely *Escherichia coli*, *Saccharomyces cerevisiae*, *Candida albicans* and *Staphylococcus aureus*. Bio-oil from MFDC and PGDC recorded the most effective Zone of Inhibition against *Staphylococcus aureus* viz., 28 and 29 mm, respectively. Both the bio-oils were more effective in terms of antimicrobial efficacy. The results of this study showed the presence of bio-active agents in bio-oil which may lead to development of new pharmaceuticals.

The MFDC biochar which was produced as a byproduct in the pyrolysis process was applied as a support material for catalyst. The biochars of MFDC and PGDC obtained at optimum condition have a porous structure, and the surface area of MFDC and PGDC biochars were 7.5 and 7.2 m²/g, respectively. The pore volumes of MFDC and PGDC biochars were 0.051 and 0.046 cm³/g, respectively. The biochars from both feedstocks showed a higher pH (~11) value at higher pyrolysis temperature which led the biochar to be used as a liming agent, for the soil that are highly acidic in nature.

An attempt was made to utilize the co-product of MFDC and PGDC pyrolysis as a catalyst support and employ biochar supported CaO as a heterogeneous catalyst in the production of biodiesel from *Mesua ferrea* derived

oil. The catalyst reported was synthesized entirely by processing waste materials. The active part of the catalyst (i.e., CaO) was derived from waste shells of *Turbonilla striatula* and the support (i.e., activated biochar) was prepared from MFDC. Use of this novel approach makes the biodiesel synthesis process environmentally benign. It showed high activity and very high yield upto 96% was achieved in 6 h using 3 wt.% catalyst 12/1 (methanol/oil molar ratio) at reaction temperature of 65°C.

Apart from these, limitations for the current study and some important outcomes from MFDC and PGDC pyrolysis are recorded. Finally, some recommendations for future work of research in biomass pyrolysis are suggested.

Table of Contents

Acknowledgement	I-II
Abstract	III-VI
Table of Content	VII-XI
List of Tables	XII-XIII
List of Figures	XIV-XVIII
List of Abbreviations	XIX

Chapter 1: Introduction

1.1	Need for renewables	1-1
1.2	Importance of biomass as a source of renewable energy	1-4
1.2.1	Importance of biomass and the biobased society	1-5
1.2.2	India's energy concern, renewable energy intervention and national biofuel policy	1-6
1.3	Various pathways of biomass conversion	1-10
1.4	Pyrolysis process	1-11
1.5	Historical background	1-12
1.6	Mechanism of pyrolysis	1-12
1.7	Pyrolysis products	1-14
1.7.1	Liquid product (Bio-oil)	1-15
1.7.2	Gases	1-17
1.7.3	Solid product (Char)	1-17
1.8	Feedstock suitability and justification of the work	1-17
1.9	Research objectives	1-20
	References	1-21

Chapter 2: Review of literature

2.1	Biomass for energy production	2-1
2.2	Liquid fuel/hydrocarbon production from biomass pyrolysis	2-3
2.3	Types of feedstock	2-4
2.4	Biomass pyrolysis kinetics	2-9
2.5	Factors affecting pyrolysis liquid product	2-10
2.5.1	Processing parameters	2-10
2.5.1.1	Temperature	2-10
2.5.1.2	Particle size	2-11
2.5.1.3	Heating rate	2-11
2.5.1.4	Inert gas flow rate	2-12
2.5.1.5	Initial moisture content of biomass feedstock	2-13
2.5.2	Non-processing parameters	2-13
2.5.2.1	Biomass composition	2-13
2.5.2.2	Mineral matter/metal ions in biomass feedstock	2-14
2.6	Effect of parameters on pyrolysis solid product (biochar)	2-15
2.6.1	Structural and chemical composition	2-15
2.6.2	Biochar porosity and surface area	2-15
2.6.3	pH of biochar	2-16
2.7	Catalytic pyrolysis	2-16
2.8	Chemistry of catalytic pyrolysis	2-17
2.9	Factors affecting biomass catalytic pyrolysis	2-18
2.9.1	Porosity and acidity of catalyst	2-18
2.9.2	Hydrogen to carbon effective ratio	2-19
2.9.3	Reaction temperature and heating rate	2-21
2.9.4	Catalyst-to-feed ratio	2-21

2.9.5	Catalyst surface area	2-22
2.9.6	Incorporation of metal to catalyst	2-22
References		2-25

Chapter 3: Materials and Methods

3.1	Methodology flow diagram	3-1
3.2	Description of tree species	3-2
3.2.1	<i>Mesua ferrea</i>	3-2
3.2.2	<i>Pongamia glabra</i>	3-3
3.3	Materials and analytical methods	3-5
3.3.1	Sample preparation	3-5
3.3.2	Determination of moisture content	3-5
3.3.3	Determination of ash content	3-5
3.3.4	Determination of volatile matter	3-6
3.3.5	Determination of fixed Carbon	3-6
3.3.6	Higher heating value (HHV)	3-7
3.3.7	Determination of net calorific value (NCV)	3-7
3.3.8	Biochemical analysis of biomass samples	3-7
3.3.9	Determination of biochar pH	3-8
3.3.10	Determination of acid sites	3-8
3.3.11	Total acid number	3-9
3.4	Kinetic modeling	3-9
3.4.1	Arrhenius method	3-10
3.4.2	Coats-Redfern method	3-11
3.4.3	FWO method	3-11
3.4.4	Global independent reactions model (Multilinear regression analysis method)	3-12
3.5	Pyrolysis experiment	3-13
3.5.1	Non-catalytic pyrolysis	3-15
3.5.2	Catalytic pyrolysis	3-15

3.6	Instrumental characterization	3-15
3.7	Assesment of antimicroblal activity	3-17
3.7.1	Preparation of cultures	3-17
3.7.2	Agar well diffusion method	3-18
3.7.3	Determination of minimum inhibitory concentration (MIC)	3-18
3.7.4	Statistical analysis	3-19
	References	3-20

Chapter 4: Results and Discussion

Chapter 4(a)

4-1.1	Physico-chemical and thermal decomposition studies of MFDC and PGDC	4-1
4-1.1.1	Thermal degradation behavior of MFDC biomass	4-5
4-1.1.2	Thermal degradation behavior of PGDC biomass	4-11
4-1.2	Pyrolysis of MFDC and PGDC	4-15
4-1.2.1	Influence of pyrolysis parameters on product yields of MFDC pyrolysis	4-16
4-1.2.2	Influence of pyrolysis parameters on product yields of PGDC pyrolysis	4-19
4-1.2.3	Influence of feedstock particle on liquid product yields of MFDC and PGDC pyrolysis	4-22
4-1.2.4	Influence of catalyst on product yield and elemental composition	4-24
4-1.3	Characterization of bio-oil	4-25
4-1.4	Characterization of biochar	4-41
4-1.5	Pyrolysis of mixed feedstock	4-49
	References	4-56

Chapter 4(b)

4-2.1	Prospect of utilization of bio-oil	4-62
	References	4-69

Chapter 4(c)

4-3	Prospect of utilization of biochar	4-71
4-3.1	Introduction	4-71
4-3.2	Preparation of catalyst and characterization	4-72
	References	4-76

Chapter 5: Summary and Conclusions

5.1	MFDC and PGDC as potential bioenergy feedstock	5-1
5.2	Pyrolytic valorization of MFDC and PGDC	5-3
5.3	Prospect of utilization of bio-oil and biochar	5-5
5.4	Conclusions	5-6
5.5	Scope of future work	5-7

Appendix	i-vi
-----------------	-------------

List of Publications	vii-x
-----------------------------	--------------

LIST OF TABLES

Table no.	Contents	Page no.
Table 1.1	Product yield from different mode of pyrolysis process	1-15
Table 1.2	Typical properties of wood pyrolysis bio-oil and heavy fuel-oil	1-16
Table 1.3	Production of non-edible seeds and residues in India	1-19
Table 2.1	The diversity of the feedstock types used for pyrolysis along with their compositional analysis	2-5
Table 3.1	Important features of <i>P. glabra</i> and <i>M. ferrea</i> seed oil	3-4
Table 3.2	Catalysts properties	3-15
Table 3.3	GC-MS analyzer details	3-16
Table 4.1	Properties of MFDC and PGDC biomass	4-3
Table 4.2	Properties of active pyrolysis stages for MFDC	4-7
Table 4.3	Kinetic parameters for MFDC calculated by Arrhenius, Coats-Redfern and multilinear regression analysis method	4-8
Table 4.4	Activation energy for MFDC calculated by FWO method (kJ/mol)	4-10
Table 4.5	Properties of active pyrolysis stages for PGDC	4-12
Table 4.6	Kinetic parameters table for PGDC calculated by Arrhenius, Coats-Redfern and multilinear regression analysis method	4-13
Table 4.7	Activation energy for PGDC calculated by FWO method (kJ/mol)	4-15
Table 4.8	Product distribution of pyrolysis of MFDC	4-17
Table 4.9	Product distribution of pyrolysis of PGDC	4-21

Table no.	Contents	Page no.
Table 4.10	Elemental composition of bio-oil	4-25
Table 4.11	Properties of the pyrolysis product	4-26
Table 4.12	FTIR spectral data of bio-oil	4-29
Table 4.13	Percentage of hydrogen based on ¹ H-NMR analysis of MFDC, PGDC bio-oil and conventional petrol, diesel and crude oil, grouped according to chemical shift range	4-33
Table 4.14	Percentage of carbon based on ¹³ C-NMR analysis of MFDC, PGDC bio-oil and conventional petrol, diesel and crude oil, grouped according to chemical shift range	4-34
Table 4.15	Chemical compounds in MFDC-500 bio-oil (GC-MS)	4-39
Table 4.16	Chemical compounds in PGDC-500 bio-oil (GC-MS)	4-40
Table 4.17	Elemental analysis of biochar co-produced from pyrolysis of MFDC	4-41
Table 4.18	Elemental analysis of biochar co-produced from pyrolysis of PGDC	4-43
Table 4.19	Comparison of properties of the (MFDC+PGDC) with MFDC and PGDC bio-oil	4-49
Table 4.20	Percentage of hydrogen based on ¹ H-NMR analysis of (MFDC+PGDC) bio-oil and individual bio-oil, grouped according to chemical shift range	4-51
Table 4.21	Percentage of carbon based on ¹³ C-NMR analysis of (MFDC+PGDC) bio-oil and individual bio-oil, grouped according to chemical shift range	4-52
Table 4.22	Chemical compounds in (MFDC+PGDC) bio-oil (GC-MS)	4-53
Table 4.23	Percentage of distillation cut point of bio-oil obtained via simulated distillation	4-54
Table 4.24	Bioassay results for antimicrobial activity of MFDC and PGDC bio-oil	4-63
Table 4.25	Influence of different parameters on biodiesel yield	4-75

LIST OF FIGURES

Figure no.	Contents	Page no.
Figure 1.1	Renewable Energy Share of Global Final Energy Consumption, 2010	1-2
Figure 1.2	Energy consumption in the United States, China, and India, 1990-2035 (quadrillion Btu)	1-3
Figure 1.3	A schematic of various processes to transform a variety of biomass into liquid hydrocarbon	1-11
Figure 1.4	Biomass pyrolysis process adopted from reference [14] with due permission from RSC publishing	1-13
Figure 1.5	Mechanism of pyrolysis adopted from reference [27] with due permission from Wiley publishing	1-14
Figure 1.6	Chemical composition of bio-oils adopted from reference [23] with due permission from ACS publishing	1-16
Figure 2.1	Thermo-chemical conversion processes and end products	2-2
Figure 2.2	A schematic of pyrolysis process to transform a variety of biomass feedstocks	2-3
Figure 2.3	Catalytic upgrading of biomass	2-17
Figure 2.4	Reaction chemistry for the catalytic fast pyrolysis of cellulose on solid acid catalyst [adapted from reference [121] with due permission from springer]	2-18
Figure 3.1	Flow diagram of methodology adopted in the study	3-1
Figure 3.2(a)	<i>Mesua ferrea</i> tree	3-2
Figure 3.2(b)	<i>Mesua ferrea</i> seed	3-2
Figure 3.2(c)	<i>Mesua ferrea</i> deoiled cake	3-2

Contd...

Figure no.	Contents	Page no.
Figure 3.3(a)	<i>Pongamia</i> tree	3-3
Figure 3.3(b)	<i>Pongamia</i> seed	3-3
Figure 3.3(c)	<i>Pongamia glabra</i> deoiled cake	3-3
Figure 3.4	Schematic of pyrolysis experimental setup	3-14
Figure 3.5(a)	Pyrolysis experimental setup	3-14
Figure 3.5(b)	Separation of pyrolytic liquid	3-14
Figure 4.1	FTIR spectra of PGDC and MFDC biomass	4-4
Figure 4.2	TG profile of MFDC at different heating rates	4-6
Figure 4.3	DTG profile of MFDC at different heating rates	4-6
Figure 4.4	Plots obtained by FWO method for determination of activation energy of MFDC at S _{II}	4-9
Figure 4.5	Plots obtained by FWO method for determination of activation energy of MFDC at S _{III}	4-10
Figure 4.6	TG profile of PGDC at different heating rates	4-11
Figure 4.7	DTG profile of PGDC at different heating rates	4-12
Figure 4.8	Plots obtained by FWO method for determination of activation energy of PGDC at S _{II}	4-14
Figure 4.9	Plots obtained by FWO method for determination of activation energy of PGDC at S _{III}	4-15
Figure 4.10	Effect of temperature and heating rate on liquid product yield of MFDC pyrolysis	4-16
Figure 4.11	Effect of temperature and heating rate on solid product yield of MFDC pyrolysis	4-16

Contd...

Figure no.	Contents	Page no.
Figure 4.12	Effect of temperature and heating rate on gaseous product yield of MFDC pyrolysis	4-17
Figure 4.13	Effect of temperature and heating rate on liquid product yield of PGDC pyrolysis	4-19
Figure 4.14	Effect of temperature and heating rate on solid product yield of PGDC pyrolysis	4-20
Figure 4.15	Effect of temperature and heating rate on gaseous product yield of PGDC pyrolysis	4-20
Figure 4.16	Effect of particle size on liquid product yield of MFDC pyrolysis	4-23
Figure 4.17	Effect of particle size on liquid product yield of PGDC pyrolysis	4-23
Figure 4.18	Influence of catalysts on product yields of MFDC pyrolysis	4-24
Figure 4.19	Influence of catalysts on product yields of PGDC pyrolysis	4-24
Figure 4.20	FTIR spectrum of MFDC bio-oil at different temperature	4-27
Figure 4.21	FTIR spectrum of PGDC bio-oil at 500°C	4-28
Figure 4.22	FTIR spectrum of MFDC bio-oil at 500°C	4-28
Figure 4.23	Comparison of ¹ H-NMR spectral distribution of functional groups of MFDC bio-oil	4-35
Figure 4.24	Comparison of ¹³ C-NMR spectral distribution of functional groups of MFDC bio-oil	4-35
Figure 4.25	Comparison of ¹ H-NMR spectral distribution of functional groups of PGDC bio-oil	4-36
Figure 4.26	Comparison of ¹³ C-NMR spectral distribution of functional groups of PGDC bio-oil	4-36
Figure 4.27	Total ion chromatogram of MFDC bio-oil	4-38
		Contd...

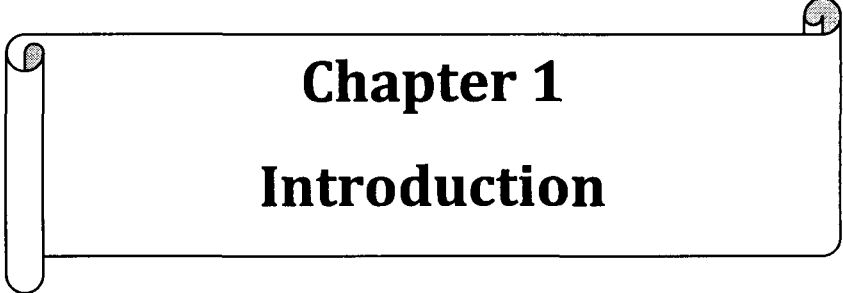
Figure no.	Contents	Page no.
Figure 4.28	Total ion chromatogram of PGDC bio-oil	4-38
Figure 4.29	Van-krevelen diagram for MFDC biochar	4-41
Figure 4.30	Van-krevelen diagram for PGDC biochar	4-43
Figure 4.31	Inorganic element constituents of MFDC biochar at different temperature	4-44
Figure 4.32	Inorganic element constituents of PGDC biochar at different temperature	4-44
Figure 4.33	FTIR spectrum of MFDC biochar at different temperature	4-45
Figure 4.34	XRD pattern of MFDC biochar at different temperature	4-46
Figure 4.35	XRD pattern of PGDC biochar at different temperature	4-47
Figure 4.36	SEM micrographs of MFDC biochar at different temperature	4-48
Figure 4.37	SEM micrographs of PGDC biochar at different temperature	4-48
Figure 4.38	FTIR spectrum of (MFDC+PGDC) bio-oil compared with bio-oil from MFDC and PGDC	4-50
Figure 4.39	Total ion chromatogram of MFDC+PGDC (1:1) bio-oil	4-53
Figure 4.40	Distillation characteristics of bio-oil obtained via simulated distillation	4-54
Figure 4.41	Antimicrobial activity histogram for MFDC and PGDC bio-oil samples	4-63
Figure 4.42	Inhibition zones of MFDC bio-oil against <i>E. coli</i> , <i>S. aureus</i> , <i>S. cerevisiae</i> and <i>C. albicans</i>	4-64
Figure 4.43	Inhibition zones of PGDC bio-oil against <i>E. coli</i> , <i>S. aureus</i> , <i>S. cerevisiae</i> and <i>C. albicans</i>	4-65
Figure 4.44	FTIR of MFDC and PGDC bio-oil	4-67

Contd...

Figure no.	Contents	Page no.
Figure 4.45	XRD patterns of active phase and supported catalyst	4-74
Figure 4.46	EDX spectra of BCh-CaO catalyst	4-74
Figure 4.47	SEM images of activated biochar and BCh-CaO catalyst	4-74

LIST OF ABBREVIATIONS

BET	Brunauer-Emmett-Teller
C-cycle	Carbon cycle
DTG	Differential thermogravimetric
FTIR	Fourier transformed infrared
FWO	Flynn-Wall-Ozawa
GC-MS	Gas chromatography-Mass spectrometry
GHG	Greenhouse gas
IEO	International Energy Outlook
MFDC	<i>Mesua ferrea</i> deoiled cake
MFDC-500	Bio-oil/biochar obtained at pyrolytic temperature of 500°C
MFDC+PGDC	Feedstock of <i>Mesua ferrea</i> and <i>Pongamia glabra</i> deoiled cake mixed with 1:1 ratio
PGDC	<i>Pongamia glabra</i> deoiled cake
PGDC-500	Bio-oil/biochar obtained at pyrolytic temperature of 500°C
REN21	Renewable energy policy network for the 21st century
SEM	Scanning electron microscope
S _I	Initial degradation stage of a DTG curve
S _{II}	First zone of active pyrolysis
S _{III}	Second zone of active pyrolysis
S _{IV}	Zone of passive pyrolysis
T _{end}	Ending temperature of a particular zone of active pyrolysis
TGA	Thermogravimetric analysis
TIC	Total ion chromatogram
T _{max}	Temperature where maximum mass loss rate occur
T _{onset}	Starting temperature of a particular zone of active pyrolysis
W _{max}	maximum mass loss rate
XRD	X-ray diffraction



Chapter 1
Introduction

Chapter 1 : Introduction

1.1 Need for renewables

The history of human civilization can be directly correlated to the progressive development of new energy sources and their associated conversion technologies. The principal energy sources of antiquity were all derived directly from the sun: human and animal muscle power, wood, flowing water and wind. About 300 years ago, the industrial revolution began with stationary wind-powered and water-powered technologies, which were essentially replaced by fossil hydrocarbons: coal in the nineteenth century, oil since the twentieth century, and now, increasingly, natural gas. The global use of hydrocarbons for fuel by humans has increased nearly 800-fold since 1750 and about 12-fold in the twentieth century [1].

Over the past century, the world has enjoyed cheap and abundant energy supplies through the adoption of fossil energy economy and fossil fuels (oil, coal and natural gas) represent the primary energy sources in the world as shown in Figure 1.1. The 1900s have been declared as the ‘‘Petroleum Century’’, with both positive and negative connotations [2].

Today, energy demand has been growing worldwide tremendously. In a report prepared by U.S. Energy Information Administration [3], it was projected that the world energy consumption will increase by 56% from 524 quadrillion Btu in 2010 to 630 quadrillion Btu in 2020 and 820 quadrillion Btu in 2040. According to the report, the role of coal is expected to remain important but natural gas, petroleum and other liquid fuels will play a major role as the largest global energy source with an increase of 28.3 million barrel per day and energy consumption together in China and India will account for half of the projected increase as depicted in Figure 1.2 [3].

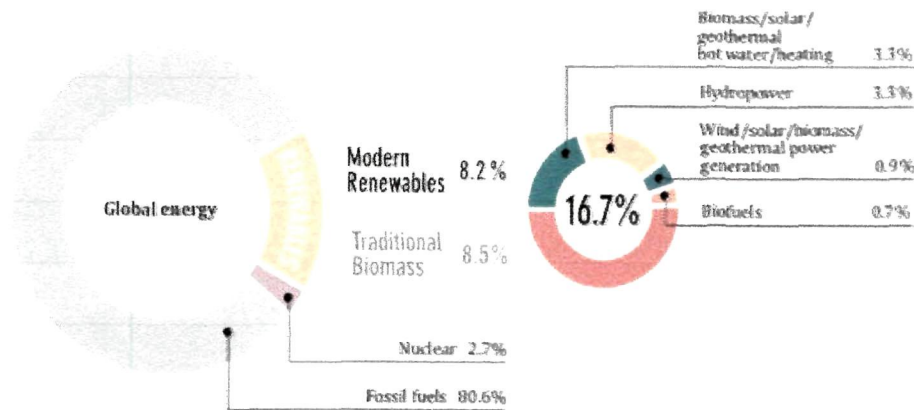


Figure 1.1: Renewable energy share of global final energy consumption, 2010 [4].

Moreover, the exponential increase in the fossil fuel consumption worldwide has resulted in a higher emission of greenhouse gases (GHGs) which has led to global environmental damages such as imbalance of natural Carbon-cycle, the global warming, ozone depletion, climate change and urban smog and emerges as a major challenge for mitigation. There is new and stronger evidence that most of the global warming observed over the last 50 years is anthropogenic [5]. It is reported that during the past 20 years, about three quarters of human-derived CO₂ emissions were due to the burning of fossil fuels [6].

Environmental concerns increase significantly over the past decade, particularly after the Earth Summit '92 [7, 8]. These environmental implications are being felt and observed in our day to day life in the form of changing weather patterns, more severe winters and summers globally, foggy conditions in several parts of the world for a prolonged period during winter months. The combustion of fossil fuel also has an adverse effect on human health due to the increase of air pollution, acid rains,

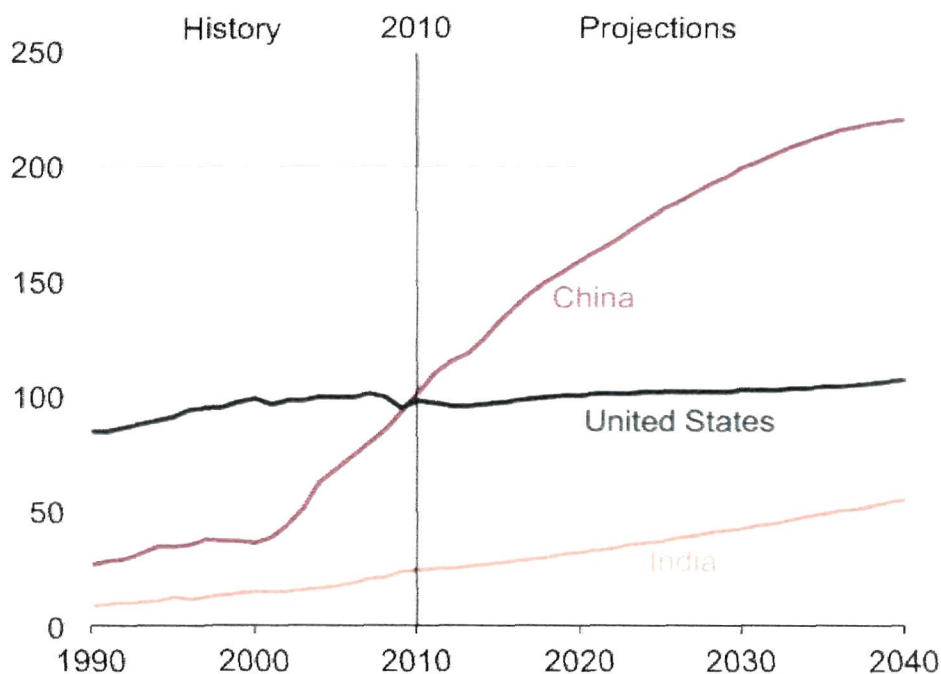


Figure 1.2: Energy consumption in the United States, China, and India, 1990-2040 (quadrillion Btu).

buildup of carbon dioxide, changing heat balance of earth etc. Hence, the world is currently confronted with the twin crisis of fossil fuel depletion and environmental degradation. Progressive depletion of fossil fuels with increasing energy consumption and GHG emission have led to a move towards alternative energy sources which are renewable, sustainable, efficient and cost-effective with lesser emissions [9, 10].

In this backdrop, the interest towards renewable resources and subsequent development of hydroelectric, solar, wave, geothermal and wind energy that can potentially limit the use of fossil fuels have been built-up [11].

Renewable energy can be particularly appropriate for developing countries. In rural areas, particularly in remote locations, transmission and distribution of energy generated from fossil fuels can be difficult and expensive. Producing renewable energy locally can offer a viable alternative. Renewable energy can facilitate economic and social development in communities but only if the projects are intelligently designed and carefully planned with local input and cooperation.

Biomass remains to be the oldest sources of energy with very specific properties unlike other renewable resources. It is the only source of renewable energy which has the potential to fulfill the mankind's demand for hydrocarbons for manufacturing goods ranging from plastics and chemicals to biofuels and other products usually derived from modern petroleum refinery. Among these diverse products that biomass can offer, bio-fuels are important because they can replace petroleum fuels. Biomass and biofuels can be used as a substitute for fossil fuels to generate heat, power and/or chemicals. Generally speaking, biofuels provide many benefits, including sustainability, reduction of GHG emissions, regional development, social structure, diversification of agriculture and security of supply of energy.

1.2 Importance of biomass as a source of renewable energy

Biomass is the most abundant renewable energy resources in the world and provides approximately 50 exajoule or ~10% of all global energy [12]. In India, biomass resource potential is assessed at 500 MT/year and about 30% of the same is estimated surplus biomass availability creating a potential of about 18,000 MW electricity generation [13]. Biomass resources and their utilization offer a new paradigm of research in the changing world faced with diverse problems related to fossil fuel use for most of the energy needs of the existing society.

Rural bioenergy is still the predominant form of energy used by people in the less developed countries, and bioenergy from biomass accounts for about 15% of the

world's primary energy consumption and about 38% of the primary energy consumption in developing countries. Furthermore, bioenergy often accounts for more than 90% of the total rural energy supplies in some developing countries. Biomass and bioenergy use in developing country perspectives are mostly in the form of traditional biomass dominated by firewood, charcoal, dung, twigs and shrubs etc. and is also associated with problems like indoor air pollution related health hazards. Unsustainable extraction of these traditional biomass from forests is also thought to be one of the reasons of forest depletion. In developed countries, there is a growing trend towards employing a range modern technologies and efficient bioenergy conversion processes to produce biofuels, however their cost competitiveness with fossil fuel is yet to be achieved.

Energy is vital for various stages of development and all societies require affordable and sustainable source of quality energy to meet the basic human needs (e.g. lighting, cooking, space comfort, mobility, communication) and to serve productive processes causing least pollution to the environment in which they live. Biomass-derived energy can provide a solution in terms of diversity of products that can be produced by employing modern technologies and replace conventional sources such as coal and petroleum with large social and environmental benefits.

1.2.1 Importance of biomass and the biobased society

Renewable feedstocks supplied a significant portion of the global energy and chemical need before the beginning of petrochemical era. It was in the 1920-1930's, the Chemurgy movement in the United States promoted the use of biomass as a source of chemicals with the belief that "anything that can be made from a hydrocarbon could be made from a carbohydrate". The incentive was to find an economic way to use farm surpluses [1]. It is only in the relatively short period between 1920 and 1950 that mankind have witnessed the transition to a non-renewable based economy that heavily depends on fossil resources. However, since the first oil crisis in the 1970's, decreasing resources, global warming and environmental pollution associated with the

use of fossil fuels are growing motivations for the transition to renewable based energy resources. Among the renewable resources, lignocellulosic biomass is particularly suited as an abundant, low cost feedstock for production of bio-based chemicals, fuels and energy to substitute fossil resources. A drawback of the growing consumption of biomass for energy is the increase in price for the biomass feedstock. This conflicts with the need of biorefineries for low cost raw materials. Biomass alone is probably not able to solve the world's power needs but can satisfy its need for the synthesis of carbon containing raw materials because its unique composition makes it especially suitable for the extraction of value-added chemicals and materials that can replace petrochemicals partially if not completely [4, 14]. Therefore, production of such chemicals from lignocellulosic biomass enhances the economic viability of a society whose energy and material needs depend on renewables.

1.2.2 India's energy concern, renewable energy intervention and national biofuel policy

There is an increased demand of energy requirements in India during the recent years due to rapid population outgrowth and substantial development of crucial sectors of its economy. Development activities in rural and sub-urban areas, modernization of cities and metros is the major energy consumers besides the growing energy demand in the households and industrial sectors. For an economy to develop and survive, there is the need of constant supply of energy requirements. But, in India, the rate of energy supply does not meet the actual energy needs. In 2011-12, India's total energy requirement was 546 MTOE and this demand has been projected to be increased more than 200% in 2031-32 [15]. Taking a historical prospective, Kumar and Jain [16], have reported that during the period of 1970-71 to 2006-07, coal consumption in India has increased from 71.2 MT to 462.7 Million tonnes (MT), crude-petroleum consumption gone up from 18.4 MT to 146.5 MT and the natural gas consumption rose from 0.64 Giga cubic meters (GCM) to 31.36 GCM. Similarly, electricity consumption has also increased from a level of 43.7 TWh to 443.1 TWh during the same period. Contrary to

the demand, indigenous energy reserves of India are not adequate to meet the requirements and therefore, the country is fairly dependent on foreign import of energy resources. For instance, crude-oil reserve of India is only 0.80 billion tonnes against world reserve of 235.8 billion tonnes at the end of year 2012; while against the consumption of 156.53 MT, production was only 37.86 MT in 2012-13 [17]. As such, the country is highly dependent on import of crude oil. It was reported that net imports of crude oil have increased from 99.41 MT during 2005-06 to 184.80 MT during 2012-13. Although more than 70% of its crude oil requirements and part of the petroleum products is met from imports, India has developed sufficient processing capacity over the years to produce different petroleum products so as to become a net exporter of petroleum products [18].

Renewable energy, which was so far designated as “alternate energy” can be a viable answer to address the above problems. India has immense potential to develop its renewable sources of energy which comprises wind, solar, water, biomass and waste energy. Out of the total installed capacity of 2,36,380 MW for power generation, around 24,914 MW i.e. ~11% is derived from renewable energy sources. The renewable energy sector is expected to grow significantly in the coming years. During 2008, around 8% of the total energy mix was contributed by renewable energy sources, whereas it has reached 12.9% in a period of 5 years only because of various subsidies for the renewable energy sector provided by the government. However, apart from this contribution in the national electric installed capacity, renewable energy based decentralized and distributed applications have benefited millions of people in Indian villages by meeting their cooking, lighting and other energy needs in an environment friendly manner [19].

Biofuels will remain as an important option in the renewable energy mix in India. Bio-fuels provide a strategic advantage to promote sustainable development and to supplement conventional energy sources in meeting the rapidly increasing requirements for transportation fuels associated with high economic growth, as well as

in meeting the energy needs of India's vast rural population. Bio-fuels can increasingly satisfy these energy needs in an environmentally benign and cost-effective manner while reducing dependence on import of fossil fuels and thereby providing a higher degree of national energy security. The Government of India (GoI) has been actively exploring its biofuel potential since 2001 [20]. The Indian approach to bio-fuels is based solely on non-food feedstocks to be raised on degraded or wastelands that are not suited to agriculture, thus avoiding a possible conflict of fuel vs. food security. The biofuel policy adopted in 2009, an important milestone of India's biofuels initiatives, envisages 20% blending of both biodiesel and bioethanol by 2017 [21]. It also hopes to increase energy security by launching one of the world's biggest nonedible oilseed-based biodiesel industries [20].

The salient features of the National Policy on Bio-fuels are [22]:

- Bio-fuel production from non-edible oil seeds grown in waste /degraded / marginal lands.
- An indicative target of 20% blending of bio-fuels, both for bio-diesel and bio-ethanol, by 2017.
- Minimum Support Price (MSP) for non-edible oil seeds would be announced with periodic revision to provide fair price to the growers.
- Minimum Purchase Price (MPP) for purchase of bio-ethanol and bio-diesel would be announced with periodic revision.
- Major thrust will be given to research, development and demonstration with focus on plantations, processing and production of bio-fuels, including second generation bio-fuels.
- Financial incentives, including subsidies and grants, may be considered for second generation bio-fuels. If it becomes necessary, a National Bio-fuel Fund could be considered.
- Setting up of National Biofuel Steering Committee, headed by the Prime Minister to provide policy guidance and coordination.

Demand of energy is growing rapidly in every sector viz., agriculture, industry, transportation, construction or mining. To meet the ever increasing demand, people are inclined towards using biofuels, which refers to liquid or gaseous fuels derived from biomass. The GoI is encouraging production of biofuels for blending with diesel and petrol, respectively. But biofuel production in India is very less comprising only 1% of world production [22]. A National policy on bio-fuels has been drafted to answer the national energy security.

Importance has been given to non-edible sources of biofuels so that energy generation is not hampered at times of declined production. Moreover, maximum portion can be utilized for the same. Wastelands, land not suitable for agriculture are given priority for plantation of energy crops so that no conflict is created between fuel and food security. For this reason several non-edible oilseed tree species e.g., *Jatropha*, *Pongamia*, *Mesua ferrea* etc. are being targeted for experimentation for biofuel production.

A target of 20% blending of biofuels with diesel and petrol in place of government's current 5% ethanol blending with petrol is estimated by 2017. Encouragement of non-edible oil seeds production by announcing MSP with timely revisions will help the growers to provide a fair price. It is proposed that MPP will be utilized by oil companies which will depend mainly on actual cost of production and import price of ethanol.

The GoI is more focussed towards second generation feedstocks. A national biofuel fund is on the line for consideration for providing financial incentives which will help to develop advanced technologies, conversion processes and production unit based on newer feedstocks. Developing bio-based second generation fuels will also generate employment in the otherwise unemployed areas together with answering the energy needs in an eco-friendly manner as less carbon emissions occur from biofuels. Projects and technologies based on biofuel for domestic use will be allowed 100% FDI. Policy guidance and coordination will be provided by a National Biofuel Coordination Committee, headed by the Prime Minister.

A Biofuel Steering Committee will supervise and scrutiny the functioning of the committee.

1.3 Various pathways of biomass conversion

Various processes can be used to convert biomass to energy. The biomass can be burned, transformed into a fuel gas through partial combustion, transformed into a biogas through fermentation, converted to bio-alcohol through biochemical processes, converted to biodiesel, pyrolyzed into a bio-oil or transformed into a syngas from which chemicals and fuels can be synthesized. Fig.1.3 illustrates the various processes to transform variety of biomass feedstock into liquid hydrocarbons. While biological processing is usually very selective and produces a small number of discrete products in high yield using biological catalysts, thermal conversion often gives multiple and often complex products, in very short reaction times with inorganic catalysts often used to improve the product quality or spectrum. Pyrolysis has been applied for thousands of years for charcoal production but it is only in the last 30 years that fast pyrolysis at moderate temperatures of around 500°C and very short reaction times of up to 2 s has become of considerable interest. This is because the process directly gives high yields of liquids of up to 75 wt.% which can be stored and transported, and used for energy and chemicals in a variety of applications [23].

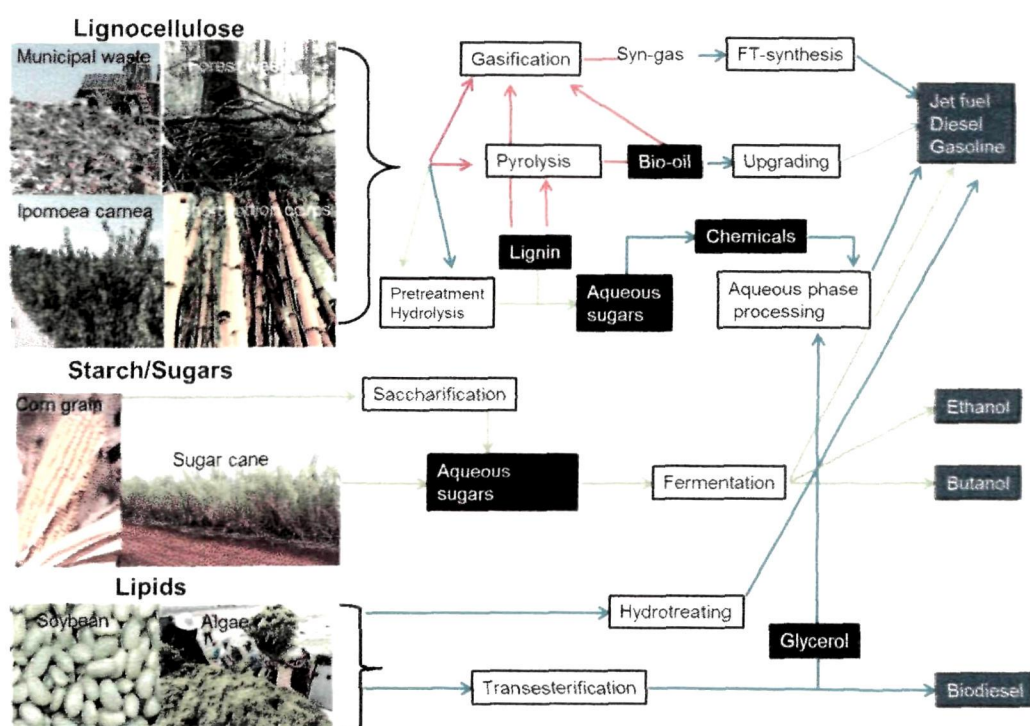


Figure 1.3: A schematic of various processes to transform a variety of biomass into liquid hydrocarbon.

1.4 Pyrolysis process

Pyrolysis is a thermochemical decomposition of biomass at moderate temperature (400-800°C) into a range of useful products, either in the total absence of oxidizing agents or with a limited supply that does not permit gasification to an appreciable extent. It is one of several reaction steps or zones observed in a gasifier. During pyrolysis, large biopolymers (20,000 to 400,000 a.m.u.) break down into smaller molecules (less than 200 a.m.u.) (Figure 1.4) with higher energy content and improved transportability [24]. Pyrolysis, the pioneer in the production of charcoal and the first transportable clean liquid fuel kerosene, produces liquid fuels from biomass. Interest in the production of pyrolysis liquids from biomass has grown rapidly in recent years, due to a number of possibilities [25]:

- Decoupling liquid fuel production (scale, time and location) from its

utilization

- Minerals separation on the site of liquid fuel production (to be recycled to the soil as a nutrient)
- Producing a renewable fuel for boilers, engines and turbines, power stations, and gasifiers
- Secondary conversion to motor fuels, additives or special chemicals (biomass refinery)
- Primary separation of the sugar and lignin fractions in biomass (biomass refinery)

1.5 Historical background

The art of pyrolysis is as old as our natural habitat. The process has been at work since the early days of vegetation on this planet. Flame leaping from forest fires is an example of “flaming pyrolysis” [26]. However human beings learned to harness energy from pyrolysis process much later. The purpose of pyrolysis is not just for energy conversion; production of value added chemicals is also an important application of this process. In fact the first application of pyrolysis of wood into charcoal around 4000 B.C.E. was not used for heating but utilized for iron ore reduction.

1.6 Mechanism of pyrolysis

The structural components of biomass i.e. cellulose, hemicellulose and lignin pyrolyze at different rates and by different mechanisms and pathways. The rate and extent of degradation of each of these components depend on the process parameters of the reactor types i.e. temperature, heating rate, particle size and pressure. It is believed that as the reaction progresses the carbon becomes less reactive and forms stable chemical structure [27]. Dehydration, cracking, isomerization, dehydrogenation, aromatization, coking and condensation reactions and rearrangement occur during the

pyrolysis process. The biomass pyrolysis is a very complex process and the complexity of this process is illustrated in Figure 1.5.

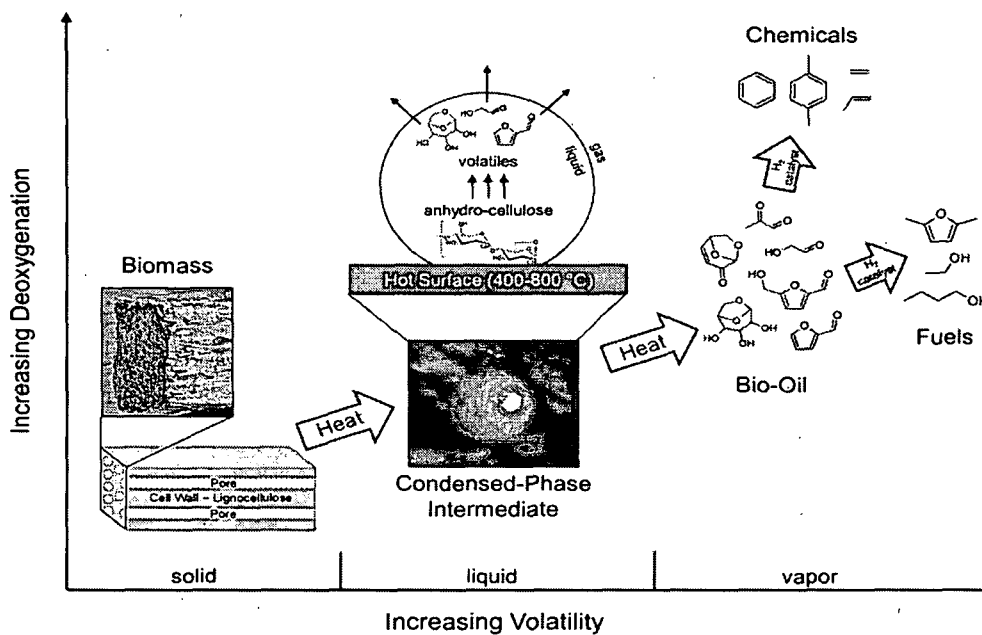


Figure 1.4: Biomass pyrolysis process adopted from reference [24] with due permission from RSC publishing.

As shown in Figure 1.4 the biomass pyrolysis process is initiated with a network of largely unidentified solid-phase reactions which results to a short-lived intermediate liquid droplet before further decomposing and boiling completely to volatile species [28].

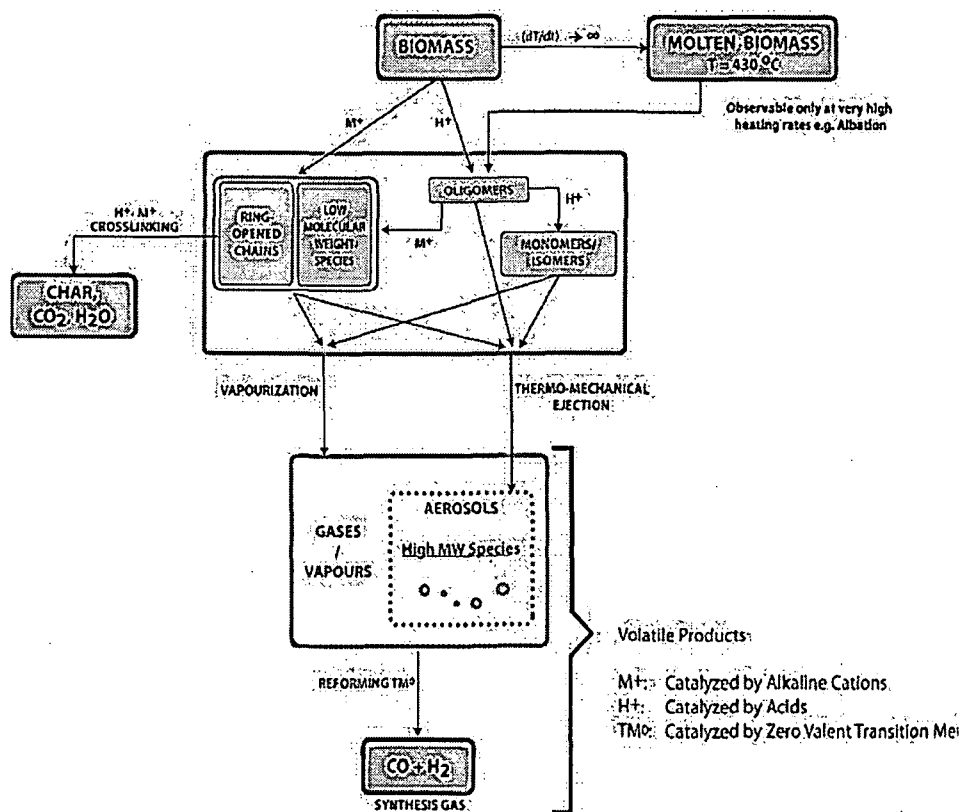


Figure 1.5: Mechanism of pyrolysis adopted from reference [27] with due permission from Wiley publishing.

1.7 Pyrolysis products

Three products, i.e. solid, liquid and gas can be obtained following biomass pyrolysis. The yield of various fractions of biomass pyrolysis product varies depending upon conditions of conversion process. The product distribution of different types of pyrolysis process is tabulated in Table 1.1.

Table 1.1 Product yield from different modes of pyrolysis process [29]

	Liquid	Char	Gas
Fast pyrolysis	75%	12%	13%
Moderate temperature and short residence time, particularly vapour			
Carbonization	30%	35%	35%
Low temperature and long residence time			

1.7.1 Liquid product (Bio-oil)

The liquid fraction of biomass pyrolysis is termed as bio-oil, bio-crude etc. It is a multi-component mixture of water and different size molecules derived from depolymerization and fragmentation of the three main building blocks of biomass: cellulose, hemicellulose and lignin. As depicted in figure 1.6, various compounds are formed from cellulose, hemicellulose and lignin during pyrolysis. For example, guaiacols and syringols are formed from the lignin fraction, whereas the miscellaneous oxygenates, sugars, and furans form from the cellulose and hemicellulose biomass fraction. The esters, acids, alcohols, ketones and aldehydes probably form from decomposition of the miscellaneous oxygenates, sugars and furans [30]. Therefore, the elemental composition of bio-oil and petroleum derived fuel is different. The physico-chemical properties of bio-oil are very well documented in literature [31, 32] and are tabulated in Table 1.2.

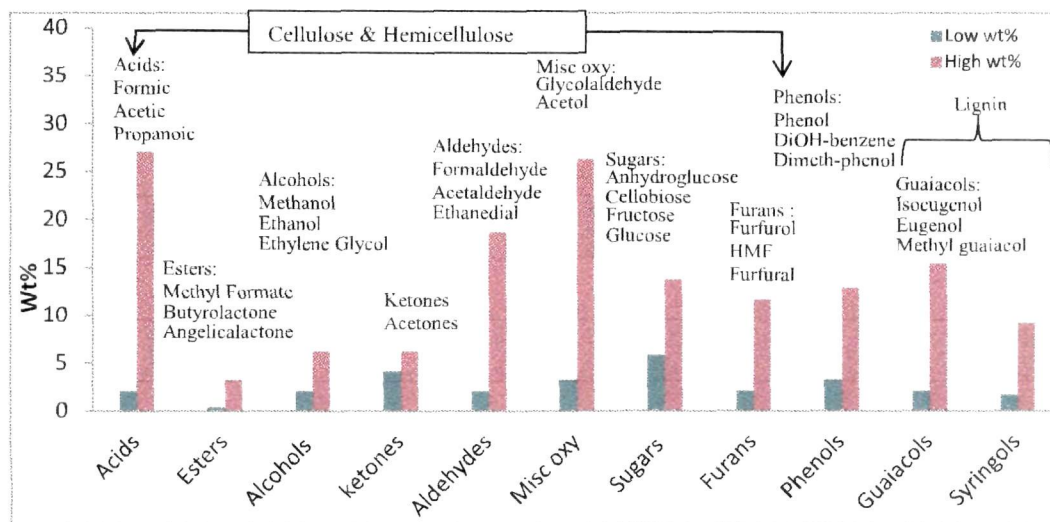


Figure 1.6: Chemical composition of bio-oils adopted from reference [30] with due permission from ACS publishing.

Table 1.2 Typical properties of wood pyrolysis bio-oil and heavy fuel-oil^a [33]

Physical Property	Bio-oil	Heavy fuel oil
Moisture content (wt.%)	15-30	0.1
pH	2.5	-
Specific gravity	1.2	0.94
Elemental composition (wt.%)		
C	54-58	85
H	5.5-7.0	11
O	35-40	1.0
N	0-0.2	0.3
Ash	0-0.2	0.1
HHV(MJ/kg)	16-19	40
Viscosity(at 50°C) (cP)	40-100	180
Solids (wt.%)	0.2-1.0	1
Distillation residue (wt.%)	Up to 50	1

^a Data taken from ref [33] with due permission from ACS

1.7.2 Gases

Thermal decomposition of biomass produces both condensable and non-condensable gases (primary gas). The vapours which are made of heavier molecules, condense upon cooling, produces the liquid part of pyrolysis. The non-condensable gas mixture contains lower molecular weight gases e.g. carbon dioxide, carbon monoxide, methane, hydrogen, ethane, ethylene, minor amounts of higher gaseous organics and water vapor [26, 27]. It is reported in the literature that CO₂ releasing is mainly caused by primary pyrolysis, while CO and CH₄ released during secondary pyrolysis. The hemicellulose shows higher CO and CO₂ while higher CH₄ release is from lignin [34].

1.7.3 Solid product (Char)

The solid product of pyrolysis is termed as char. It is another important product of pyrolysis process. The char can be used within the process to provide the process heat requirements by combustion. The fresh char is pyrophoric i.e. it spontaneously combusts when exposed to air so careful handling and storage is required. This property deteriorates with time due to oxidation of active sites on the char surface.

1.8 Feedstock suitability and justification of the work

A feedstock is defined as any renewable, biological material that can be used directly as a fuel or converted to another form of fuel or energy product. Biomass feedstocks are marked by their tremendous diversity. The pyrolysis process uses the entire content of biomass unlike biochemical and biological processes where individual conversion technologies favor specific biomass types and pretreatment requirement before processing [35]. As of now, the existent available bio-energy feedstock cannot suffice for the petro crude reservoirs; consequently new feedstock for the same will serve as a cumulative step for addressing the long documented problem of energy production and supply. The successful utilization of any biofuel fundamentally depends on the availability of feedstock. The greatest share of production costs of biofuel is linked with the feedstock. Consequently, availability of

low-cost and good quality non-edible feedstock is critical to large-scale commercial production of biofuels [36, 37]. For an agriculture based economy like India, the vista of utilization of feedstocks like agricultural residues to various forms of fuel as supplement for conventional fossil based fuel is attractive, as it has numerous advantages suitable for achieving energy and benefiting in environmental, agricultural and trade policies. This is also important as these resources are otherwise low-value perishable products. Deoiled seed cake is a processing waste obtained from processing of edible oil yielding seeds for human consumption and non-edible oil yielding seeds for energy and other industrial processes. Edible deoiled seed cakes have been used for feed application to poultry, fish and swine industry due to their protein rich nature (ranging from 15-50%) [38]. Biodiesel production by transesterification of oil also generates deoiled seed cakes. As Indian Biofuel policy favours use of non-edible oils for biodiesel production, non-edible deoiled seed cakes will be available in huge quantities. But due to the toxic nature, non-edible deoiled seed cakes cannot be considered for food supplementation like edible deoiled seed cakes. However, these deoiled seed cakes are studied for a number of non-energy applications including synthesis of chemicals, anti-microbial properties, anti-oxidative properties and organic manure and limited energy application. For example, non-edible oil cakes such as castor cake, karanja cake, neem cake are used as organic nitrogenous fertilizers, due to their N P K content [38]. Energy application includes biogas production from jatropha cake [39], bio-oil production from cotton seed cake [40], polanga seed cake [41] etc. Moreover, Government of India's recent biofuel policy targets bringing more and more waste/unused lands under cultivation for biofuel crops and trees for producing commercial grade biodiesel [42]. It can, therefore, be expected that massive amounts of bioenergy byproducts like deoiled seed cakes will be produced as well. Table 1.3 indicates the potential availability of some non-edible oil seeds and residues in India.

Table 1.3: Production of non-edible seeds and residues in India [43]

Species	Oil fraction (%)	Seed estimate (10 ⁶ tons/year)	Residues (10 ⁶ tons/year)
Castor	45-50	0.25	0.13 – 0.14
Jatropha	30-40	0.20	0.12 – 0.14
Mahua	35-40	0.20	0.12 – 0.13
Sal	10-12	0.20	0.17 – 0.18
Linseed	35-45	0.15	0.08 – 0.09
Neem	20-30	0.10	0.07 – 0.08
Pongamia	30-40	0.06	0.03 – 0.04
Others (including <i>M. ferrea</i>)	10-50	0.50	0.25 – 0.45

Conversion of deoiled seed cakes to liquid fuel has been established as one of the promising route of value addition of these resources [44-50]. Presently, the non-edible deoiled seed cakes have been utilized for low value applications (heat/solid fuel etc.). The non-edible deoiled seed cake is a rich source of hydrocarbons due to the presence of lignin, cellulose and hemicellulose. By weight, the quantity of lipid present in the non-edible seed (less than 5 wt.% of plant) is very low while the total lignocellulosic portion in non-edible seed is very high (more than 90%). Under these circumstances, the thermo-chemical processes makes worthy in effective utilization of organic carbon present in these biowastes. As there is an ever increasing demand for renewable biofuels, exploration of new, cheaper and abundantly available feedstock for bio-energy generation is both critical and indispensable. In this regard, the present study aims to explore new, cheaper and renewable feedstock for bio-energy generation. This doctoral research study was undertaken to highlight new feedstocks (*Pongamia glabra* and *Mesua ferrea* deoiled cakes) in the futuristic energy scenario. It is also worth mentioning here that India being an agricultural economy generates enormous quantum of agricultural residues and *Pongamia glabra* and *Mesua ferrea* deoiled seed cake which is a bioenergy-byproduct are no exceptions in this regard.

1.9 Research objectives

The Specific objectives of this study were:

1. To determine the composition of the biomass samples and their thermal degradation behaviour.
2. To investigate the feasibility of thermal decomposition of the biomass through pyrolysis at different thermal regimes via both catalytic and non-catalytic routes.
3. To characterize the products of thermal decomposition.
4. To study the prospect of utilization of pyrolytic products.

References:

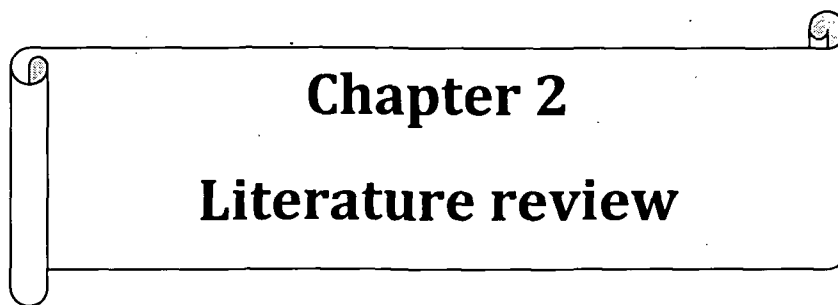
- [1] Hall, C., et al. Hydrocarbons and the evolution of human culture. *Nature*, **426** (6964), 318-322, 2003.
- [2] Crocker, M., *Thermochemical Conversion of Biomass to Liquid Fuels and Chemicals*, Royal Society of Chemistry, 2010.
- [3] U.S. Energy information administration. International Energy outlook 2013. [http://www.eia.gov/forecasts/ieo/pdf/0484\(2013\).pdf](http://www.eia.gov/forecasts/ieo/pdf/0484(2013).pdf), 22/12/2014.
- [4] REN21. Renewables 2012 Global status report. <http://www.map.ren21.net/GSR/GSR2012.pdf>, 2012.
- [5] van Aardenne, J.A., et al. A 1°×1° resolution data set of historical anthropogenic trace gas emissions for the period 1890–1990. *Global Biogeochemical Cycles*, **15** (4), 909-928, 2001.
- [6] Sorensen, B., et al., *Renewable Energy Focus Handbook*, Elsevier Science, 2008.
- [7] Agarwal, A.K. Biofuels (alcohols and biodiesel) applications as fuels for internal combustion engines. *Progress in Energy and Combustion Science*, **33** (3), 233-271, 2007.
- [8] Eissen, M., et al. 10 Years after Rio—Concepts on the Contribution of Chemistry to a Sustainable Development. *Angewandte Chemie International Edition*, **41** (3), 414-436, 2002.
- [9] Nigam, P.S. & Singh, A. Production of liquid biofuels from renewable resources. *Progress in Energy and Combustion Science*, **37** (1), 52-68, 2011.
- [10] Prasad, S., Singh, A., & Joshi, H.C. Ethanol as an alternative fuel from agricultural, industrial and urban residues. *Resources, Conservation and Recycling*, **50** (1), 1-39, 2007.
- [11] Demirbaş, A. Global Renewable Energy Resources. *Energy Sources, Part A: Recovery, Utilization, and Environmental Effects*, **28** (8), 779-792, 2006.
- [12] Searle, S. & Malins, C. A reassessment of global bioenergy potential in 2050. *GCB Bioenergy*, Article in press, 2014.

- [13] World Energy Council. India Energy Book 2012. www.indiaenvironmentportal.org.in/files/file/ieb2012.pdf, 12/09/2014.
- [14] Demirbas, A., *Biodiesel: A Realistic Fuel Alternative for Diesel Engines*, Springer, London, 2008.
- [15] PSI Media Inc. 2011 India Energy Handbook. http://www.psimedia.info/handbook/India_Energy_Handbook.pdf, November 2013.
- [16] Kumar, U. & Jain, V.K. Time series models (Grey-Markov, Grey Model with rolling mechanism and singular spectrum analysis) to forecast energy consumption in India. *Energy*, **35** (4), 1709-1716, 2010.
- [17] Ministry of petroleum & Natural Gas. Indian Petroleum and Natural Gas Statistics 2012-13. <http://petroleum.nic.in/pngstat.pdf>, 10/09/2014.
- [18] Ministry of Statistics and Programme Implementation. Energy Statistics 2013. http://mospi.nic.in/Mospi_New/upload/Energy_Statistics_2013.pdf, 13/09/2014.
- [19] Ministry of New & Renewable Energy. Annual report 2013-14. <http://mnre.gov.in/file-manager/annual-report/2013-2014/EN/overview.html>, 13/09/2014.
- [20] Gunatilake, H., Roland-Holst, D., & Sugiyarto, G. Energy security for India: Biofuels, energy efficiency and food productivity. *Energy Policy*, **65** (0), 761-767, 2014.
- [21] Ministry of New & Renewable Energy. National Policy on Bio-fuels. http://mnre.gov.in/file-manager/UserFiles/biofuel_policy.pdf, 13/09/2014.
- [22] Tiwari, A.K. Ethanol-Blending: Problems, future prospects and economic analysis. *Akshay Urja*, **7** (6), 37-39, 2014.
- [23] Meier, D., et al. State-of-the-art of fast pyrolysis in IEA bioenergy member countries. *Renewable & Sustainable Energy Reviews*, **20** (0), 619-641, 2013.

- [24] Mettler, M.S., et al. Revealing pyrolysis chemistry for biofuels production: Conversion of cellulose to furans and small oxygenates. *Energy & Environmental Science*, **5** (1), 5414, 2012.
- [25] Harmsen, J. & Powell, J.B., *Sustainable Development in the Process Industries: Cases and Impact*, John Wiley & Sons, 2011.
- [26] Basu, P., *Biomass Gasification and Pyrolysis: Practical Design and Theory*, Academic press, 2010.
- [27] Vamvuka, D. Bio-oil, solid and gaseous biofuels from biomass pyrolysis processes-An overview. *International Journal of Energy Research*, **35** (10), 835-862, 2011.
- [28] Dauenhauer, P.J., et al. Reactive boiling of cellulose for integrated catalysis through an intermediate liquid. *Green Chemistry*, **11** (10), 1555-1561, 2009.
- [29] Bridgwater, A.V. Renewable fuels and chemicals by thermal processing of biomass. *Chemical Engineering Journal*, **91** (2-3), 87-102, 2003.
- [30] Huber, G.W., Iborra, S., & Corma, A. Synthesis of transportation fuels from biomass: chemistry, catalysts, and engineering. *Chemical Reviews*, **106** (9), 4044-98, 2006.
- [31] Mohan, D., Pittman, C.U., & Steele, P.H. Pyrolysis of wood/biomass for bio-oil: A critical review. *Energy & Fuels*, **20** (3), 848-889, 2006.
- [32] Zhang, Q., et al. Review of biomass pyrolysis oil properties and upgrading research. *Energy Conversion and Management*, **48** (1), 87-92, 2007.
- [33] Czernik, S. & Bridgwater, A.V. Overview of Applications of Biomass Fast Pyrolysis Oil. *Energy & Fuels*, **18** (2), 590-598, 2004.
- [34] Yang, H.P., et al. Characteristics of hemicellulose, cellulose and lignin pyrolysis. *Fuel*, **86** (12-13), 1781-1788, 2007.
- [35] Mosier, N.S., et al. Industrial scale-up of pH-controlled liquid hot water pretreatment of corn fiber for fuel ethanol production. *Applied Biochemistry and Biotechnology*, **125** (2), 77-97, 2005.

- [36] Kondamudi, N., Mohapatra, S.K., & Misra, M. Spent Coffee Grounds as a Versatile Source of Green Energy. *Journal of Agricultural and Food Chemistry* **56** (24), 11757-11760, 2008.
- [37] Tao, L. & Aden, A. The economics of current and future biofuels. *In Vitro Cellular & Developmental Biology-Plant*, **45** (3), 199-217, 2009.
- [38] Ramachandran, S., et al. Oil cakes and their biotechnological applications – A review. *Bioresource Technology*, **98** (10), 2000-2009, 2007.
- [39] Singh, R.N., et al. SPRERI experience on holistic approach to utilize all parts of *Jatropha curcas* fruit for energy. *Renewable Energy*, **33** (8), 1868-1873, 2008.
- [40] Özbay, N., Pütün, A.E., & Pütün, E. Structural analysis of bio-oils from pyrolysis and steam pyrolysis of cottonseed cake. *Journal of Analytical and Applied Pyrolysis*, **60** (1), 89-101, 2001.
- [41] Shadangi, K.P. & Singh, R.K. Thermolysis of polanga seed cake to bio-oil using semi batch reactor. *Fuel*, **97** 450-456, 2012.
- [42] Planning commission, Govt. of India. Report of the committee on developement of biofuel.
http://planningcommission.nic.in/reports/genrep/cmtt_bio.pdf, 23/05/2010.
- [43] Department of Science and Technology. Byproducts of Biodiesel Manufacture.
http://www.inspirenetwork.org/Dst/Report_5.pdf, 12/09/2014.
- [44] Pütün, A.E., Apaydin, E., & Pütün, E. Bio-oil production from pyrolysis and steam pyrolysis of soybean-cake: product yields and composition. *Energy*, **27** (7), 703-713, 2002.
- [45] Putun, E., Uzun, B.B., & Putun, A.E. Fixed-bed catalytic pyrolysis of cottonseed cake: effects of pyrolysis temperature, natural zeolite content and sweeping gas flow rate. *Bioresource Technology*, **97** (5), 701-10, 2006.
- [46] Şensöz, S., Demiral, İ., & Ferdi Gerçel, H. Olive bagasse (*Olea europea* L.) pyrolysis. *Bioresource Technology*, **97** (3), 429-436, 2006.

- [47] Agrawalla, A., Kumar, S., & Singh, R.K. Pyrolysis of groundnut de-oiled cake and characterization of the liquid product. *Bioresource Technology*, **102** (22), 10711-10716, 2011.
- [48] Şen, N. & Kar, Y. Pyrolysis of black cumin seed cake in a fixed-bed reactor. *Biomass and Bioenergy*, **35** (10), 4297-4304, 2011.
- [49] Volli, V. & Singh, R.K. Production of bio-oil from de-oiled cakes by thermal pyrolysis. *Fuel*, **96** (0), 579-585, 2012.
- [50] Jourabchi, S.A., Gan, S., & Ng, H.K. Pyrolysis of *Jatropha curcas* pressed cake for bio-oil production in a fixed-bed system. *Energy Conversion and Management*, **78** (0), 518-526, 2014.



Chapter 2
Literature review

2.1 Biomass for energy production

Biomass, from antiquity, has been serving human civilization as a primary source of energy either in the form of wood and dung for cooking and heating, charcoal for metallurgy and animal feed, food and transportation. With increasing concerns regarding anthropogenic activity on environment, civilization is once again looking forward for a biobased society where biomass resources will meet a significant portion of our energy and chemical needs. The energy consumption of the world has been steadily increasing day by day for a variety of reasons, which include enhancement in quality of life, population outgrowth, industrialization, rapid economic growth of developing countries, increased transportation of people and goods etc. As a result of which, the demand for energy and its resources is also increasing continuously. Many studies indicate that there will likely be a doubling of the world's energy demand by 2050, perhaps sooner [1]. The major energy demand is fulfilled from the conventional energy resources like coal, petroleum and natural gas but they may not be sufficient to overcome today's increasing energy needs. Also these resources are finite and are the major source of CO₂ emission, a potent GHG. Due to these facts, scientists and researchers around the globe are making serious efforts to explore alternate sources of energy which are renewable, safe and non-polluting. In this regard, biomass can be considered as one of the promising environment friendly renewable energy options. Wood and other forms of biomass are one of the main renewable energy resources available. In contrast to other renewable sources, which provide heat and power, biomass is the only source which can be converted to liquid, solid and gaseous fuels by applying suitable conversion technologies. Wood and other biomass can be treated in a number of different ways to provide such fuels. Basically such methods are divided into

biological (anaerobic digestion and fermentation) and thermal. The different thermo-chemical routes of conversion of biomass and their products are shown in Figure 2.1.

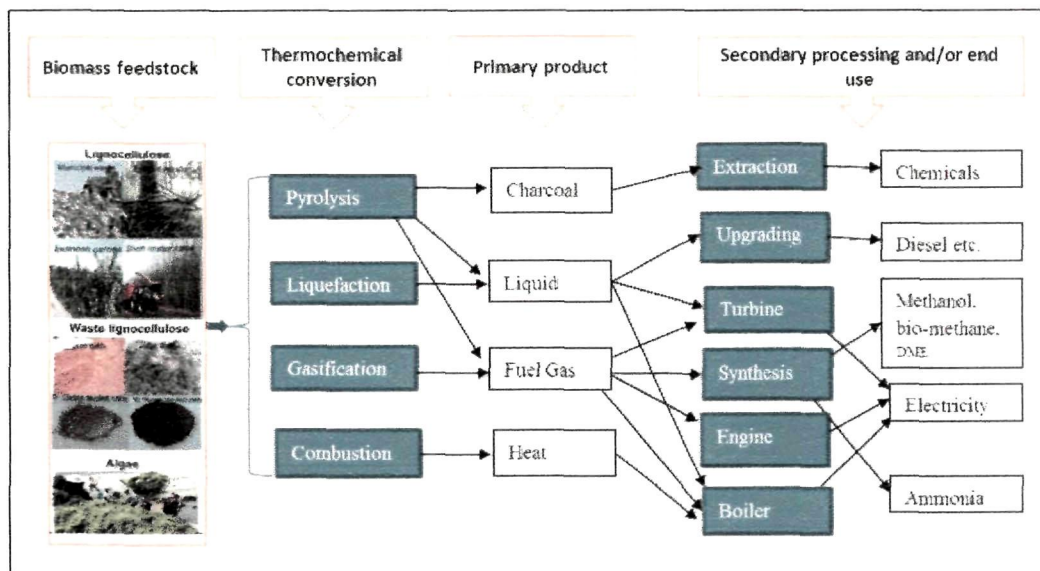


Figure 2.1: Thermo-chemical conversion processes and end products.

As shown in Figure 2.1, direct combustion of biomass provide heat, for steam production and hence electricity can be generated. Gasification also provides a fuel gas that can also be combusted to generate heat or used in an engine or turbine for electricity generation. The third alternative is fast pyrolysis, which provides a liquid fuel that can substitute for fuel oil in any static heating or electricity generation application. The advantage of fast pyrolysis is that it can directly produce a liquid fuel, which can be readily stored and transported and it is beneficial in situations where biomass resources are remotely located for production of heat and bio-power. Also the pyrolysis process is the only renewable energy conversion technique which can convert wide ranging biomass types into solid, liquid and gaseous products with several value added products with end use as shown in Figure 2.2. Recently, pyrolysis process is gaining importance for production of hydrogen from bio-oil and bio-methane production from syngas produced during pyrolysis [2-4]. Although slow pyrolysis is well known and is an established process for making charcoal, the fast pyrolysis process is still under development.

2.2 Liquid fuel/hydrocarbon production from biomass pyrolysis

The history of human culture can be viewed as the progressive development of new energy sources and their associated conversion technologies. These developments have increased the comfort, longevity and affluence of humans, as well as their numbers. Most of these energy technologies rely on chemical bonds of hydrocarbons. Nature has favored the storage of solar energy in the hydrocarbon bonds of plants and animals, and human cultural evolution has exploited this hydrocarbon energy profitably.

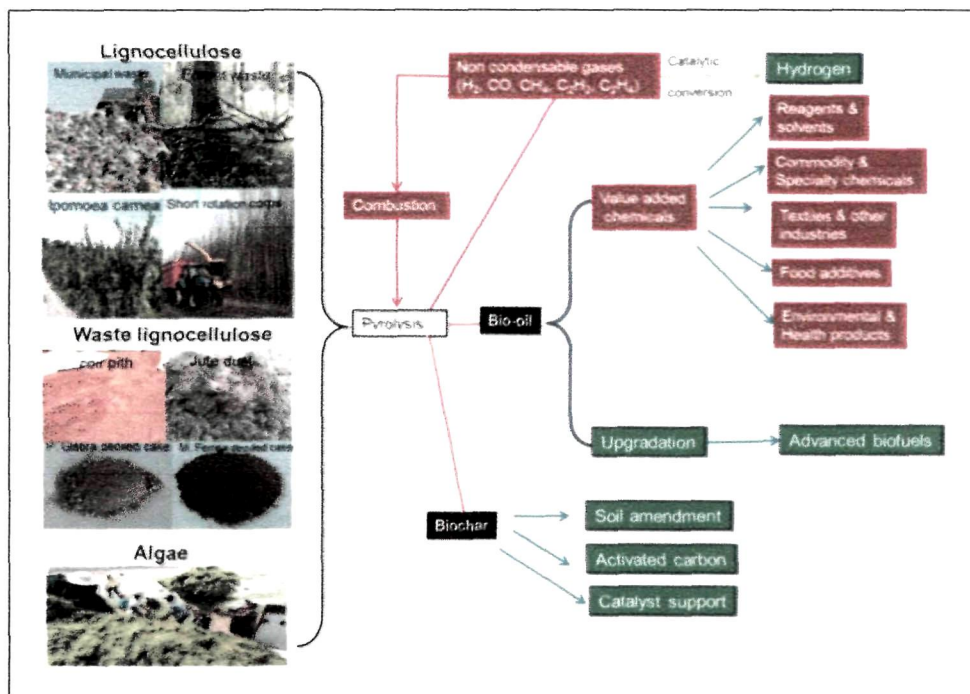


Figure 2.2: A schematic of pyrolysis process to transform a variety of biomass feedstocks.

The art of pyrolysis is a very old thermochemical conversion technology and is as old as our natural habitat. Pyrolysis process dates back to at least ancient Egyptian time, when tar from pyrolysis was used for caulking boats and certain embalming agents. From then, pyrolysis process has been improved and now it is being widely used for coke and charcoal production. In the 1980's researcher have found that the liquid yield from pyrolysis process could be increased by changing certain conditions applied in traditional pyrolysis, known as fast pyrolysis. Here, a biomass feedstock is heated at a rapid rate and

also the produced vapours are condensed rapidly [5]. Recently, this thermochemical conversion technology is gaining interest among various renewable energy conversion technologies due to its wide range of potential for conversion of diverse biomass feedstocks into solid, liquid and gaseous fuel and also value added chemicals. Slow pyrolysis or carbonization primarily targets in the production of solid, i.e. charcoal production, while favouring fast pyrolysis, liquid, i.e. bio-oil maximization in the final product distribution is the major agenda of current research among thermo-chemical community globally. Though, research has achieved desired target but successful commercial application is still a far cry due to several reasons. One of the non-process parameters and a major factor affecting its commercialization is availability of feedstocks, their varied composition and other logistic issues associated with it.

2.3 Types of feedstock

The thermo-chemical conversion process like pyrolysis uses the complete biomass unlike biochemical or biological processes where individual conversion technologies favour specific biomass types and pretreatment requirement before processing [6]. Pyrolysis uses a variety of feedstocks such as forests, agricultural, aquatic plant, algae and industrial waste biomass to produce bio-oil and are listed in Table 2.1. In other words, pyrolysis process is almost non-selective in biomass feedstock processing like combustion. However, feedstock restrictions for pyrolytic conversion process mostly pertain to particle size, moisture and ash content. The thermo-chemical platform aims to efficiently produce bio-based fuels and co-products via liquefaction and pyrolysis, followed by upgrading of bio-oils and gaseous intermediates, respectively. Different physico-chemical and biochemical properties of various biomasses investigated for pyrolysis process are listed in Table 2.1. The following section examines the work of various researchers on different types of feedstock to produce bio-oil using non-catalytic as well as catalytic pyrolysis.

Table 2.1: The diversity of the feedstock types used for pyrolysis along with their compositional analysis

Sl.No	Biomass feedstock	Volatile matter	Fixed carbon	Ash	Moisture	Cellulose	Hemicellulose	Lignin	C	H	N	O	S	References
1. Wood and Wood waste														
1	Alfalfa stems (at early bud)	69.6	16.9	8.3	5.3	-	-	-	39.9	5.5	2.3	38.8	0.2	[7]
2	Aspens	80.4	11.0	0.4	8.2	60.7	19.1	14.8	45.8	5.2	0.4	39.9	0.01	[8]
3	Australian oil mallee wood	81.9	17.6	0.5	-	-	-	-	48.4	6.3	0.1	45.2	-	[9]
4	Beech wood	82.5	17.0	0.5	0.5	50.5	28.4	20.6	52.3	6.1	0.5	41.0	-	[10]
5	Birch	74.4	13.5	0.8	11.4	56.5	24.8	12.2	44.4	3.5	0.3	36.7	-	[8]
6	Holm oak	80.8	7.4	2.3	9.5	37.9	25.9	27.8	48.0	5.9	0.5	45.6	0.02	[11]
7	Mallee bark	69.5	24.1	6.4	-	26.3	18.6	24.7	48.5	5.5	0.3	45.4	0.1	[12, 13]
8	Mallee leaf	74.6	21.7	3.7	-	15.4	17.3	25.1	59.3	6.8	1.3	32.4	0.2	[12]
9	Oak wood	76.8	14.2	0.2	8.8	53.9	28.9	9.4	45.4	5.0	0.3	41.3	0.01	[8]
10	Pine wood	71.5	15.3	0.3	12.9	52.1	15.4	27.5	41.9	4.5	0.2	40.2	-	[8]
11	Pine cone	77.8	-	0.9	9.6	32.7	37.6	24.9	42.6	5.6	0.8	51.0	0.1	[14]
12	Pine sawdust	77.7	16.9	0.3	5.0	43.8	25.2	26.4	50.3	6.7	0.2	42.7	0.2	[15, 16]
13	Pyrenean oak	80.5	6.0	2.4	11.1	33.9	25.5	31.2	48.5	5.9	0.5	45.1	0.01	[11]
14	Silver fir	78.7	6.5	0.4	14.4	52.1	15.0	29.9	51.2	6.4	0.2	42.2	-	[11]
15	Softwood	-	-	0.5	13.5	51.6	9.2	30.6	48.8	5.6	0.0	45.6	-	[17]
16	Stone pine	82.1	7.4	0.7	9.8	41.0	21.0	31.2	50.4	6.0	0.3	43.3	0.01	[11]
17	Subabul wood	85.6	-	0.9	-	39.8	24.0	24.7	48.2	5.9	0.0	45.1	-	[18]

2. Agro-industrial waste															
18	Apricot pulp	71.9	13.0	4.7	10.3	-	-	-	51.4	5.7	2.5	40.2	-	[19]	
19	Coffee ground	77.5	19.8	1.4	1.3	-	-	33.3	54.6	6.6	3.9	34.8	0	[20]	
20	Cotton gin residue	88.0	5.4	-	-	82.8	17.1	0.1	42.7	6.0	0.1	49.5	-	[18, 21]	
21	Empty palm fruit bunches	76.4	11.6	4.6	7.4	59.7	22.1	18.2	51.8	7.0	0.7	40.3	0.2	[22]	
22	Exhausted coffee residue	79.5	8.2	0.7	11.5	-	-	47.2	39.4	52.5	6.9	3.5	34.8	0.1	[23]
23	Grape waste	62.5	20.7	5.3	11.5	-	-	-	47.2	6.3	2.4	38.6	0.1	[24]	
24	Jatropha seed shell cake	79.8	14.1	3.4	2.7	36.6	4.8	39.6	50.5	6.2	2.3	39.4	-	[22]	
25	Palm fibre	75.9	12.4	5.3	6.6	-	-	-	50.3	7.1	0.4	36.3	0.6	[25]	
26	Palm kernel shell	71.3	17.8	4.9	5.9	30.6	30.6	20.4	44.6	6.5	2.9	40.2	<0.1	[22]	
27	Peach pulp	70.2	18.0	2.4	9.3	-	-	-	45.6	6.9	0.9	46.5	-	[19]	
28	Wet distiller grain	24.6	-	1.9	68.3	-	-	-	49.9	7.3	5.3	36.5	1.0	[26]	
3. Agricultural wastes															
3.1. Husk															
29	Millet husks	80.7	-	18.1	-	33.3	26.9	14.0	42.7	6.0	0.1	33.0	-	[18]	
30	Olive husk	64.8	15.9	7.2	-	25.0	24.6	50.4	47.2	5.6	0.8	35.4	0.2	[21, 24]	
31	Rice husk	60.6	15.0	12.4	12.1	43.8	31.6	24.6	45.5	4.5	0.5	36.1	0.1	[27]	
32	Soaked rice husk	70.5	14.3	13.2	2.0	-	-	-	41.3	5.1	0.4	38.0	0.02	[27]	
3.2. Stalk & Straw															
33	Barley straw	80.3	4.8	9.8	6.9	-	-	-	41.4	6.2	0.6	51.7	0.01	[28]	
34	Corn straw	75.0	9.7	6.1	9.2	4.8	24.4	9.0	42.7	5.6	1.5	49.2	<0.1	[29]	
35	Flax straw	80.3	8.8	3.0	7.9	-	-	-	45.2	6.3	1.0	-	1.2	[30]	
36	Lagume straw	73.7	14.8	1.6	9.8	28.1	34.1	34.0	43.3	5.6	0.6	50.4	0.1	[31]	
37	Maize stalk	71.9	12.1	8.3	7.6	-	-	-	49.1	6.1	0.7	43.7	-	[32]	
38	Oat straw	75.9	0.1	17.3	6.7	31.6	49.6	16.6	48.5	6.0	0.4	45.1	-	[33]	
39	Rice straw	62.4	14.9	15.4	7.2	60.3	20.4	14.1	44.8	5.1	0.9	49.2	0.6	[29, 34]	
40	Sunflower stalks	-	-	14.4	12.4	33.0	18.0	23.0	49.9	6.3	0.9	42.9	-	[17]	
41	Tobacco stalk	65.5	16.0	9.9	8.5	21.3	32.9	30.2	39.6	4.9	3.2	52.3	0.1	[16]	
42	Wheat straw	74.2	13.0	6.9	5.9	31.2	45.2	18.1	52.9	6.3	0.4	40.4	-	[33]	

3.3 Bagasse														
43	Grape bagasse	68.4	20.7	4.7	6.2	28.6	-	41.9	46.6	6.3	1.7	45.5	-	[35]
44	Hazelnut bagasse	68.2	15.3	6.7	-	-	-	-	43.8	6.3	7.9	41.9	-	[36]
45	Laurel extraction residues	69.2	10.3	10.5	9.9	22.8	44.0	27.6	48.9	6.4	3.0	41.6	-	[37]
46	Olive bagasse	67.2	21.6	4.4	6.8	-	-	-	53.4	7.5	1.7	37.4	-	[36]
47	Parthenium bagasse	79.1	14.8	3.2	3.1	23.0	25.8	30.0	53.5	6.2	0.6	33.4	0.2	[38]
48	Sugarcane bagasse	79.6	8.1	4.3	16.1	42.7	33.1	24.2	58.1	6.1	0.7	34.5	0.2	[21, 29, 39]
49	Sunflower-extracted bagasse	78.4	10.5	6.1	5.0	-	-	-	53.2	7.1	8.0	31.7	-	[40]
3.4 Shell														
50	Cashew nut shell	69.3	19.3	1.0	10.4	41.3	18.6	40.1	48.7	6.9	0.4	42.9	-	[41]
51	Cherry seed shells	76.1	17.0	0.8	6.1	27.2	31.9	36.9	48.9	6.3	3.1	41.6	0.1	[42]
52	Coconut shells	80.2	22.0	0.7	4.4	40.3	27.8	31.9	50.2	5.7	0.0	43.4	0.1	[18, 43]
53	Parinari fruit shell	78.2	14.5	4.7	2.7	45.4	6.4	30.1	48.0	5.8	2.1	43.5	0.1	[29]
54	Palm shell	73.7	18.4	2.2	5.7	-	-	-	53.8	7.2	0.0	36.3	0.5	[25]
4. Seed and seed cakes														
55	Black cumin seed cake	70.9	19.2	4.8	-	37.1	10.4	26.7	51.2	7.9	5.3	35.1	0.5	[44]
56	Cherry seed (kernel + shell)	77.6	15.7	1.2	5.5	32.1	28.6	29.1	52.5	7.6	4.5	35.3	0.1	[42]
57	Cotton seed cake	79.3	9.7	5.2	5.8	27.6	-	-	52.0	5.9	1.3	40.8	-	[45]
58	Jatropha cake	72.5	10.9	6.5	10.0	-	-	-	44.4	6.2	4.3	44.5	0.5	[29]
59	Jatropha seed cake	43.6	4.4	-	8.1	-	-	-	49.3	6.1	3.4	-	-	[46]
60	Linseed seed	77.0	10.7	5.6	6.7	14.1	-	-	61.0	8.5	2.3	28.2	-	[47]
61	Moringa cakes	75.1	8.3	6.3	10.4	17.9	1.9	24.9	45.6	6.5	6.5	41.5	-	[29]
62	Neem seed	71.0	8.1	4.9	16.0	-	-	-	38.4	8.3	7.5	45.1	0.7	[48]
63	Pomegranate seed	78.7	14.1	1.8	5.4	26.9	25.5	39.7	49.7	7.5	4.0	38.1	0.7	[49]
64	Rapeseed residue	81.7	7.9	5.5	4.9	-	-	-	62.1	9.1	3.9	24.9	-	[50]
65	Safflower seed	80.8	11.3	2.2	5.7	27.2	18.6	28.9	60.5	9.1	3.1	27.4	-	[51]
66	Safflower seed cake	83.0	14.0	3.0	6.0	40.0	16.0	26.7	49.5	6.9	3.0	40.6	-	[52]
67	Soybean cake	71.6	14.4	5.6	8.4	-	-	-	55.9	6.6	9.3	28.3	-	[53]

5. Oil crop and other Agricultural wastes														
68	Cocoa pod	68.5	10.4	10.8	10.3	-	-	-	43.9	4.9	2.2	47.3	0.8	[29]
69	Coconut coirs	82.8	-	0.9	-	52.2	28.4	19.4	47.6	5.7	0.0	43.4	-	[18, 21]
70	Coconut coir pith	73.3	-	7.1	-	38.1	20.3	41.6	44.0	4.7	0.7	40.4	-	[18, 21]
71	Corn stover	64.5	-	7.3	9.4	40.7	26.6	26.0	51.9	5.5	0.8	41.5	0.3	[21, 26]
72	Corn cob	80.7	7.6	2.1	6.3	31.7	31.7	3.4	42.9	6.4	0.6	45.5	0.3	[29]
73	Olive-oil residuc	68.8	17.3	5.1	8.8	23.2	35.6	34.9	49.1	5.6	1.1	44.2	-	[54]
74	Olive residue/waste	70.4	15.3	3.7	10.6	56.0	-	-	44.8	5.1	0.9	49.2	-	[55]
75	Palm empty fruit bunch	79.7	8.7	3.0	8.8	-	-	-	48.8	7.3	0	40.2	-	[22]
6. Non woody/Grass														
76	Bermuda grass	-	-	-	-	37.3	53.2	9.5	-	-	-	-	-	[21]
77	Elephant grass	-	-	-	-	31.5	34.3	34.2	-	-	-	-	-	[21]
78	Reed canary grass	74.9	15.8	3.6	5.7	42.9	28.3	9.4	44.9	6.1	<0.04	39.1	-	[56]
79	Switchgrass	72.6	16.4	3.1	7.9	39.0	31.9	10.2	44.8	5.7	0.2	38.2	-	[56]
80	Timothy grass	77.9	16.0	1.1	5.0	38.0	33.1	28.9	42.4	6.0	1.0	50.4	0.2	[21, 28]
7. Aquatic plants and algae														
81	Microalgae chlorella	72.2	15.1	5.9	6.8	-	9.5	-	47.5	7.1	6.7	38.6	-	[57]
82	S. patens (marine brown algae)	55.5	12.4	17.8	14.4	-	-	-	40.2	5.2	2.0	33.9	0.9	[58]
8. Animal waste														
83	Cattle manure	53.1	4.6	42.3	24.6	32.7	24.5	42.8	21.9	3.6	2.3	20.8	1.1	[21, 26]
9. Municipal solid waste														
84	Kitchen garbage	63.5	8.8	27.8	-	-	-	-	-	4.4	2.3	5.3	0.6	[59]
85	Paper	-	-	-	-	92.5	0.0	7.5	-	-	-	-	-	[21]
86	Paper (newspaper)	-	-	-	-	45.6	31.3	23.1	-	-	-	-	-	[21]
87	Paper (waste pulps)	-	-	-	-	74.3	17.1	8.6	-	-	-	-	-	[21]
88	Plastic	100	0	0	-	-	-	-	-	86.1	13.0	-	0.9	[59]
89	Refuse-derived fuel	-	-	-	-	60.0	20.0	20.0	-	-	-	-	-	[21]
10. Shrub species														
90	Parthenium argentatum	72.7	12.2	12.5	2.6	-	-	-	45.9	5.1	1.3	32.0	0.6	[38]

2.4 Biomass pyrolysis kinetics

Pyrolysis can be used as an independent process for the production of fuels and/or value added chemicals. It also occurs as the first step in a gasification or combustion process. The development of thermochemical processes for biomass conversion and suitable reactor design necessitates the knowledge of several process parameters which include a profound understanding of the mechanism of reactions governing pyrolysis process, the determination of the most significant pyrolysis parameters and of their effect on the process and knowledge of the kinetics [60]. The kinetic modeling of the decomposition is crucial for an accurate prediction of the material's behavior under different working conditions [61]. Also a precise conception of solid state pyrolysis kinetics is very crucial in designing and operating large scale biomass conversion systems. Thermogravimetric analysis (TGA) is an extensively used technique to study the reaction kinetics for pyrolysis process because of its simplicity and retrieval of a host of valuable information from a thermogram and it has gained widespread attention in thermal studies of biomass pyrolysis [62]. The precision and accuracy of the kinetic expression governing the reaction mechanism and the kinetic parameters inferred from kinetic analysis have a profound dependence on the reliability of the evaluation methods used to study the decomposition behavior of biomass under different conditions of temperature and/or atmosphere. Various model fitting approaches such as Kissinger, Friedman, Flynn-Wall-Ozawa, multi-linear regression analysis and Modified Coats-Redfern have been widely used to estimate the kinetic parameters by several authors [63-68]. Di Blasi presented a comprehensive review of the different classes of mechanisms proposed for the pyrolysis of wood and other cellulosic materials [69]. Varhegyi *et al.* [70] used the independent reaction model of three pseudo-components. This model ensures the possibility of simultaneous decomposition of pseudo components. The biomass decomposition results reported in the literature [71-73] show that this model provides consistent parameter values with low fitting errors. Yao *et al.* [63] studied the degradation properties and kinetic parameters of hard wood using all of the above described methods and reported that most of the natural fibers degrades in the temperature range between 215 and 310°C with apparent activation energy of 160 – 170

kJ mol^{-1} . Açıklan [74] observed average activation energies of the second and third stages pistachio shell pyrolysis calculated from model-fitting methods were in the range of 121 – 187 and 320 – 353 kJ mol^{-1} , respectively. The FWO method yielded a compatible result (153 kJ mol^{-1}) for the second stage but a lower result (187 kJ mol^{-1}) for the third stage. Sasmal *et al.* [65] observed that activation energy of all the biomass materials irrespective of degradation zone, lies within the range 116 – 348 kJ mol^{-1} under nitrogen and 91.2 – 175.7 kJ mol^{-1} under air atmosphere, respectively. The macroscopic kinetics of biomass pyrolysis is complex as it includes information about simultaneously occurring multiple steps. Unraveling the macroscopic kinetics presents a certain challenge that can only be met by the computational methods that allow for detecting and treating multi-step processes [75]. According to the results of the International Confederation for Thermal Analysis and Calorimetry (ICTAC) kinetics Project [76], isoconversional methods are among a few methods that are up to this challenge.

2.5 Factors affecting pyrolysis liquid product

Pyrolysis of biomass is a complex thermochemical conversion process during which biomass decomposes through primary and secondary reactions involving heat and mass transfer mechanism. During pyrolysis many factors affect the nature of products obtained. These factors can be divided as the processing parameters and non-processing parameters. The processing parameters include reactor temperature, vapour residence time, heating rate, particle size etc. The non-processing parameters include lignocellulosic composition and presence of inorganic element in biomass feedstock.

2.5.1 Processing parameters

2.5.1.1 Temperature

The temperature in a pyrolysis process is the most significant operating parameter [77]. Pyrolysis is generally conducted in the temperature range 400 – 600°C, where the liquid phase (condensed product vapours) makes out the main product yielding between 60 to 70% on a dry basis [5, 78, 79]. As the reaction temperature increases the liquid product yield increases but further increase in temperature (~ above 500°C) [80, 81] decreases the liquid yield. The reason for the lower bio-oil yield at a lower reaction

temperature may be due to the fact that the reaction temperature becomes too low to complete pyrolysis process. On the other hand, upon increasing the temperature, secondary reactions of the heavy molecular weight compounds in the pyrolysis vapours or between the vapour and solid phases dominated, resulting in a decrease of the bio-oil yield and an increase of the gas yield [81]. The pyrolysis temperature has a remarkable effect on bio-oil composition [82]. Xiao *et al.* [83] reported that the organic functional groups in biomass char decreased greatly with the increase in the final temperature, which were stable in the liquid part but the transmittance of these groups decreased with the increase in temperature.

2.5.1.2 Particle size

Particle size is known to influence pyrolysis product yield. It is generally assumed that an increase in particle size causes greater temperature gradients inside the particle so that at a given time, the core temperature is lower than that of the surface of the biomass particle, and this could possibly give rise to an increase in char yield; hence, gas and oil yields may be expected to be low [84, 85]. Larger particles require high apparent activation energies which can again be attributed to heat transfer limitations. Also, small particles have enough surface area to interact with the pyrolysis medium to form volatile products that leaves the biomass matrix without undergoing secondary reactions [86]. However, in case of slow pyrolysis, particle size does not show any significant influence on product yield [87]. Considering the poor thermal conductivity of biomass, biomass particles have to be very small preferably to provide rapid heating to achieve high bio-oil yield. Although, high heating rates may be achieved in a pyrolysis reactor, the low thermal conductivity of biomass prevents such temperature gradients throughout the whole particle. It is also reported in the literature that the water content of bio-oil increased with increasing biomass particle size [88].

2.5.1.3 Heating rate

Biomass heating rate in a pyrolysis reactor is the most important and significant parameter on bio-oil yield. The effect of heating rate can be visualized in fast pyrolysis mode where the liquid product yields much higher than the conventional pyrolysis

process. This is because of quick fragmentation of biomass due to high heating rates which enhances the yield of volatiles. Enhancement of volatiles could be attributed to the extra tar decomposition at high heating rates [89]. Rapid heating rate reduces the heat and mass transfer limitations and also enhances the abundance of volatiles by fast endothermic decomposition of biomass, thus limiting the time available for secondary reactions: tar cracking and repolymerization [90, 91].

2.5.1.4 Inert gas flow rate

The vapour residence time inside a reactor in pyrolysis process can influence the type and composition of all products in a pyrolysis process. The interaction of the escaping nascent, hot pyrolysis vapours with surrounding solid environment lead to the formation of char which is exothermic in nature. This effect of char formation could be minimized by setting the process parameters of a pyrolysis reaction that support rapid mass transfer such as vacuum pyrolysis, fast removal of pyrolytic vapour and small particle size of feedstock [84]. For this reason, the use of inert gas flow like N₂, Ar and water vapour is of common practice. Flowing of inert gas reduces the residence time for hot pyrolytic vapour inside the reactor and thus minimizes the secondary reactions like thermal cracking, repolymerization and recondensation to maximize the liquid product yield [53]. However, it is to be mentioned that inert gas flow only removes the hot pyrolytic vapour from the reaction zone. Rapid quenching is then needed to stop the secondary chemical reactions occurring in hot vapours before the valuable initial reaction products can be degraded [92].

It is also observed from the literature that pyrolytic liquid yield is not significantly influenced by inert gas flow rates. Putun *et al.* [34] observed ~ 3% more liquid yield (from 27.8% to 30.2%) by increasing the N₂ gas flow from 50 to 200 ml/min. However further increase in sweeping gas flow rate to 400 ml/min slightly decreased the pyrolytic oil yield. Similarly Acıkgöz *et al.* [93] and Demiral and Şensöz [94] observed 3% and 3.3% more pyrolytic oil production by increasing the nitrogen flow rate within the interval of 50-100 ml/min and 50-150 ml/min respectively. Sensoz and Angin [95] also observed that bio-oil yield of 33.8% without any sweeping gas flow increased to 36.1%

with the sweep gas at a flow rate of 100 ml/min. However, further increasing the gas flow rate to 200 ml/min reduced the oil yield from 36.1% to 33%. Usually, low gas velocity is sufficient to attain maximum liquid product yield which could be attributed to the fact that at high gas velocities, the volatiles leave the system without effective condensation, resulting in maximum gas formation [96].

2.5.1.5 Initial moisture content of biomass feedstock

Green biomass contains about 50 – 60% moisture, and therefore, it is necessary to reduce the moisture because pyrolysis process can handle biomass containing moisture content upto 30% effectively. Composition and physical properties of pyrolytic oil are also dependent on initial moisture content. During pyrolysis, almost all of the initial moisture contents appear in the aqueous product fraction. At least 15% of pyrolysis oil consists of water. When the feed moisture content is less than 10%, the water content in bio-oil is reduced to 15-25%, which otherwise ranges from 18-28% [97].

2.5.2 Non-processing parameters

2.5.2.1 Biomass composition

The composition of product of pyrolysis depends very much on the compositional variations of biomass feedstocks. Figure 1.5 depicts the composition of pyrolytic oil depending upon the composition of biomass. Pyrolysis of cellulose and hemicellulose produces more liquid yield than lignin [96, 98]. Yang *et al.* [99] found that the pyrolysis of hemicellulose and cellulose occurred quickly, with the weight loss of hemicellulose mainly occurred at 220 – 315°C and that of cellulose at 315 – 400°C. However, lignin was more difficult to decompose, as its weight loss occurred in a wide temperature range (from 160 to 900°C) and only 54.3% of lignin was volatilized at 900°C. In a very recent study conducted by Burhenne *et al.* [100] it is reported that the lignin content of any biomass feedstock is the main controlling factor in pyrolysis process for industrial application. They observed that the highest liquid product yield (i.e. 48%) and the lowest solid product yield of 32% was obtained from rape straw with a lignin content of 24% while the lowest liquid product yield of 41% and the highest solid product yield of 43% was produced by spruce wood pyrolysis that had a lignin content of 26%. It is therefore,

clear from the literature that final temperature to obtain maximum liquid product yield depends upon biomass components and that lignin contributes to the major portion of solid residues during lignocellulosic biomass pyrolysis process.

2.5.2.2 Mineral matter/metal ions in biomass feedstock

The composition of mineral matter in biomass feedstock is an another important parameter in biomass pyrolysis process as the mineral matter decreases the oil yield and tends to increase the char and gas yield which is evident from the various studies [18, 101, 102]. Moreover the inorganic constituents of biomass can cause fouling and corrosion of pyrolysis reactor. The low melting point constituents can induce agglomeration of reactor bed materials. Raveendran *et al.* [18] developed a correlation to predict the effect of mineral matter (K, Zn) and amount of lignin on the volatiles yield of biomass pyrolysis (Eq. 2.1).

$$\Delta V = -0.964(L^{1.095} \times X_k^{1.3727} \times X_z^{0.0996}) + 7.192 \quad (2.1)$$

Where ΔV = change in percentage yield of volatiles due to demineralization

L = lignin content (wt %) of biomass

X_k = fraction of potassium in silica-free ash and

X_z = fraction of zinc in silica-free ash

Various studies showed that the effect of inorganic constituents in biomass pyrolysis could be minimized by demineralization of mineral matter except for biomass types, which have high amounts of lignin and K metal. To prevent the negative effect of minerals during pyrolysis process, washing of biomass is one of the suitable options [103-105]. More extensive removal of these constituents can be performed by treating the biomass with acid medium. However, if the acid treating conditions are too severe, this could lead to the loss of solid biomass, i.e. the main chemical composition of biomass can change. For example, if very high concentration of acid and/or elevated temperature is applied, some degradation of hemicellulose can occur and thereby, the cellulose and lignin contents become higher in biomass feedstock [103].

2.6 Effect of parameters on pyrolysis solid product (biochar)

2.6.1 Structural and chemical composition

The solid product i.e. char is an important product of pyrolysis process. The fresh char is pyrophoric, so careful handling and storage is required. This property deteriorates with time due to oxidation of active sites on the char surface [79]. It is reported that with increase in pyrolysis reactor temperature, the carbon structure becomes increasingly ordered until, at very high temperatures (>2000°C), the biomass is eventually converted to graphite, with ring-layers systematically stacked on top of each other, however, some feedstocks graphitize at the highest treatment temperature of less than 2000°C [106].

It was observed by various researcher that the total carbon content of biochar varies considerably depending on the feedstock and may range from 400 g/kg up to 900 g/kg. The highest C contents are obtained from hard-wood feedstock pyrolysed at high temperatures, while manures generate biochars with low C contents. In comparison to woody biomasses, nutrient-rich manures contain more minerals, which end up in the biochar, and thus results in low C proportion [107-109]. Besides the large C component, the elemental composition of biochar consist of H and O, as well as different minerals (e.g. N, P, S) depending on the feedstock [110]. It was observed that concentration of inorganic elements increase with increase in the pyrolysis temperature.

2.6.2 Biochar porosity and surface area

The heating rate applied in the pyrolysis process is an important process parameter exerting decisive influence on the size of the surface area. Lua *et al.* [111] obtained the highest surface areas (778 m²/g) in pistachio nut shells at a heating rate of 10°C/min, while further increment of the heating rate up to 40°C/min continuously decreased the surface area. Downie *et al.* [106] suggested that pore size and volume is dependent on the biomass feedstock and pyrolysis settings. During pyrolysis, loss of feedstock mass in the form of volatile organic compounds leaves voids, which creates an extensive pore network consisting of pores and cracks. By increasing the

pyrolysis temperature and by using reactive agents the volatilization of the biomass material increases and leaves a more porous biochar with a larger surface area.

It has been hypothesized that inorganic materials of high-ash feedstocks may partially fill or block access to micropores, thereby reducing the surface area. Lee *et al.* [112] found that the removal of inorganic materials by wet sieving of biochars leads to high surface area.

2.6.3 pH of biochar

Biochar pH, which is a preliminary key property is greatly affected by pyrolysis temperature. Angin [113] reported that with the increase in the pyrolysis temperature the pH values of the biochar also increased. However, he did not notice any significant effect of heating rate on pH values of biochar. Similar result were also observed by Inyang *et al.* [114]; Jindarom *et al.* [115] and Yao *et al.* [116]. Yuan *et al.* [117] suggested that the increases in pH values may be attributed to the separating of alkali salts from organic materials due to increase in pyrolysis temperature.

2.7 Catalytic pyrolysis

The biomass pyrolytic liquid (bio-oil) can be utilized as an energy carrier, source for many commodity chemicals, or can be upgraded as a transportation fuel (Figure 2.3). In biomass catalytic pyrolysis process, ideally, the heavy oxygenated volatiles from the decomposition of biomass are deoxygenated and converted to lighter fuels and chemicals by coming in contact with a suitable catalyst. The decrease of oxygenated, bio-oil component species can increase bio-oil's heating value and result in a product with improved physical and chemical properties. Improving the quality of bio-oil using heterogeneous catalysis has received extreme attention from several research groups.

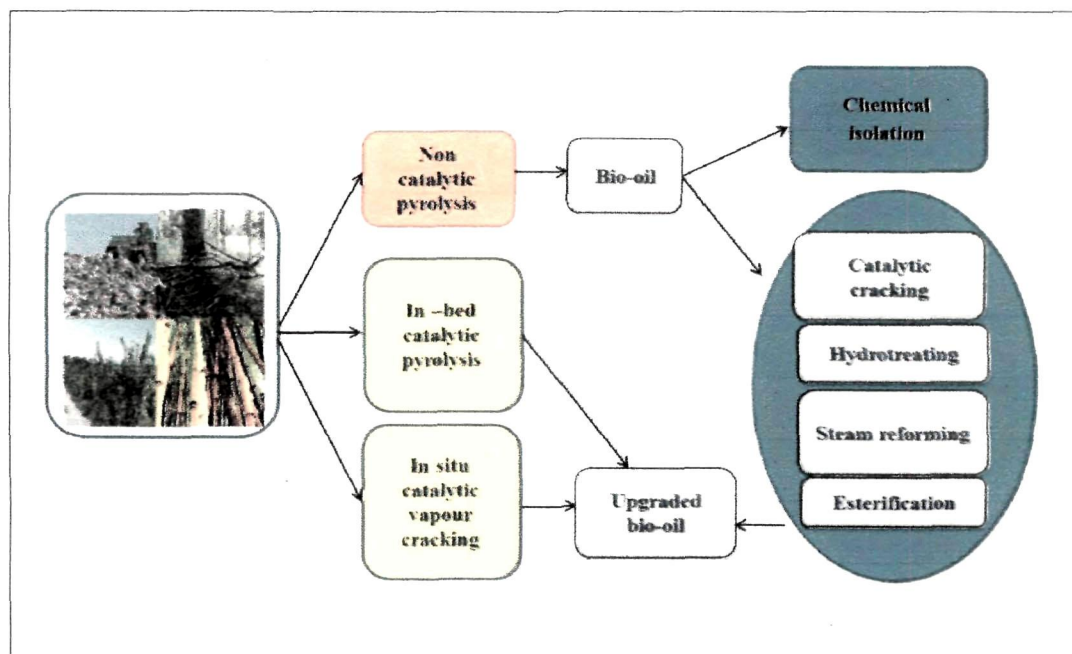


Figure 2.3: Catalytic upgrading of biomass.

2.8 Chemistry of catalytic pyrolysis

Biomass catalytic pyrolysis with molecular sieve mainly aims to produce aromatic hydrocarbons, as they are highly desirable products since they have high octane numbers and can be used in gasoline as octane enhancer. Furthermore, aromatics can be used for production of several high value added chemicals and polymers [118]. As depicted in Figure 2.4, solid biomass (e.g., cellulose) first undergoes thermal decomposition resulting in the production of volatile organics, gases and solid coke followed by dehydration reaction of organic volatiles to produce water and dehydrated species in the process of catalytic pyrolysis. Bridgewater [119] pointed out that aromatization is an important step in the reactions of hydrocarbon over zeolite. Huber and Corma [120] also noticed that this aromatization reaction proceed via Diels-Alder reaction in which olefins obtained through thermal biomass cracking combine each other to form cyclic and aromatic compounds. However, for the production of selective aromatics is to minimize the

production of undesired coke formation inside the catalyst which in turn deactivate the catalyst activity. The coke can form from the biomass feedstock, volatile oxygenates, dehydrated species or the aromatics through homogeneous gas phase thermal decomposition reactions and from heterogeneous reactions on the catalyst [121].

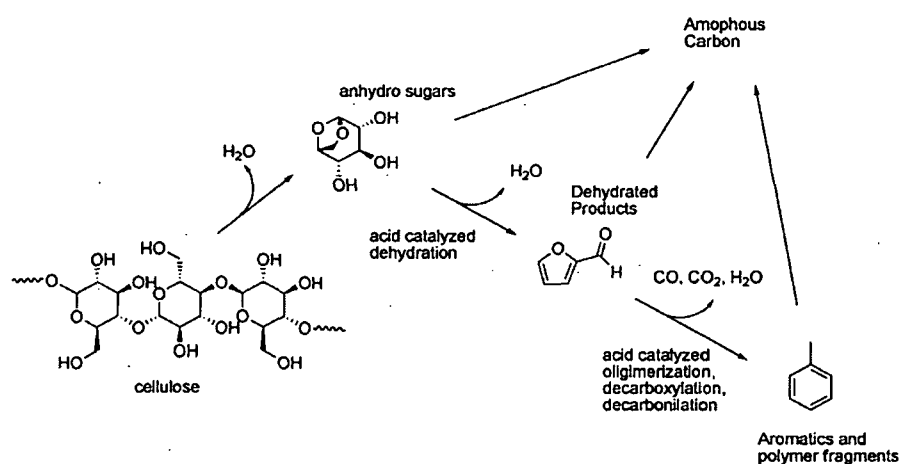


Figure 2.4: Reaction chemistry for the catalytic fast pyrolysis of cellulose on solid acid catalyst [adapted from reference [121] with due permission from springer].

2.9 Factors affecting biomass catalytic pyrolysis

2.9.1 Porosity and acidity of catalyst

Porosity and acidity both affect activity of catalyst for conversion of biomass derived oxygenated product to aromatics. Influence of zeolite pore size and shape selectivity in glucose to aromatic conversion was studied by Jae *et al.* [122] and revealed that aromatic yield was a function of catalyst pore size.

Aho *et al.* [123] observed that increasing the acidity of β -zeolite catalyst (i.e., decreasing Si/Al ratio) resulted in a decrease of organic fraction of the pyrolytic liquid and conversely increase in water and polyaromatic hydrocarbons. The increased concentration of polyaromatic hydrocarbons (mainly naphthalene, phenanthrene, fluorene and their alkylated homologues) in catalytically upgraded bio-oil was also observed by

Williams and Horne [124], some of which are known carcinogen and/or mutagen and may consequently represent significant health hazards. In catalytic pyrolysis of empty fruit branch using Al-MCM-41 and HZSM-5, it was observed that using Al-MCM-41 produced more phenols than HZSM-5 [125]. This could be attributed to the higher porosity of Al-MCM-41 than HZSM-5 encouraging the performance of producing phenols as the catalytic activity is directly related to structural and active sites characteristics [126]. Ma *et al.* [127] compared aromatic yields of non-catalytic and catalytic pyrolysis of lignin using porous catalyst silicate and HZSM-5. They observed that apart from porosity, acid sites are needed in catalyst in order to produce high yield of aromatics. Lignin is an attractive compound to be studied as model compound for biomass catalytic pyrolysis. Though lignin is the most difficult biomass component to be decomposed resulting in the highest solid residue production [128-130], the pyrolytic lignin has high theoretical potential to be converted to aromatics [131]. In catalytic cracking of pyrolytic lignin separated from rice husk derived bio-oil, it was suggested that microporous zeolites favour more aromatic production [131]. It was also observed that, phenols were significantly deoxygenated and converted to aromatics such as toluene, naphthlene and benzene were most abundant aromatic species produced over ZSM-5 catalyst. However, it is to be mentioned that number of acid sites present in a proper porous structure as well as their strength distribution should be simultaneously modified for enhanced aromatic production [103].

Catalyst pore-opening size plays a decisive role to enhance the aromatic production. Pore-opening size affects mass transfer and can restrict diffusion of large molecule into the catalyst pore reaction zone [132]. In catalytic fast pyrolysis of alkaline lignin studied by Ma *et al.* [127], it was observed that catalysts with larger pore size produced more liquid product and less coke in an order of H-USY (7.4 Å) > H-beta (6.6 Å) > HZSM-5 (5.5 Å). Therefore yield of liquid and product selectivity could be controlled by tuning pore size of the catalyst.

2.9.2 Hydrogen to carbon effective ratio

Use of zeolite in biomass conversion to aromatics faces problems due to the production of large amount of coke resulting in rapid deactivation of catalyst [133]. Chen

et al. [134, 135] introduced the hydrogen to carbon effective ratio (H/C_{eff}) as shown in equation 2.2, to describe whether a feed can be efficiently converted into hydrocarbons according to the amount of carbon, hydrogen and oxygen in the feedstock. Feedstocks with same (H/C_{eff}) will have similar theoretical yield of aromatics [121, 136].

$$H/C_{eff} = \frac{H-2O}{C} \quad (2.2)$$

Where H, C, and O correspond to number of atoms of hydrogen, carbon and oxygen in the feedstocks, respectively.

The H/C_{eff} ratio for petroleum derived product ranges from 1 (for benzene) to slightly higher than 2. However the H/C_{eff} for lignocellulosic biomass ranges from 0-0.3. However, biomass is made of hydrogen deficient molecules and so one should must take care the ratio for conversion of biomass and biomass-derived products. Carlson *et al.* [121] studied xylitol, glucose, cellobiose and cellulose with ZSM-5 catalyst and found that xylitol had a higher yield of aromatics than other feedstock which could be attributed to the higher H/C_{eff} ratio (0.4) of xylitol. However no olefins were detected in their study while Lappas *et al.* [137] observed presence of olefins when glycerol and sugars were passed over ZSM-5 catalyst. H/C_{eff} ratio of feedstock can be increased through co-feeding of hydrogen and hydrogen compounds like alcohol. Zhang *et al.* [138] increased the pine wood H/C_{eff} ratio of 0.11 by changing the relative amount of alcohols (methanol, 1-propanol, 1-butanol and 2-butanol) and biomass feedstock and observed enhanced yield of aromatic compounds. Enhancement of H/C_{eff} ratio and aromatics yield could also be achieved by hydrogenation using hydrogen gas [139].

2.9.3 Reaction temperature and heating rate

Reaction temperature and heating rate also play a vital role in product selectivity towards aromatics in biomass catalytic pyrolysis. Carlson *et al.*[140] studied catalytic fast pyrolysis of pinewood in a fluidized bed reactor to observe the effect of temperature on yield and product distribution of pyrolytic products. The result indicated that the catalytic pyrolysis chemistry shifted towards gasification like reactions at higher temperature as the yield of coke and unidentified oxygenates decreased, while CO and CH₄ yield increased with increase in temperature. The aromatic yield was slightly higher and reached a maximum of 11% carbon at 600°C, but further increase in the temperature decreased the yield of aromatics. They also reported that temperature had little effect on total olefin yield. However, product selectivity for olefin such as propylene, butane, ethylene showed an interesting trend. For example, propylene selectivity was maximum at low temperature and decreased to zero at the highest temperature. Butene selectivity also decreased as the temperature was increased to a maximum level. Carlson *et al.*[141] observed significant effect of reaction temperature on aromatics yield in conversion of glucose to aromatics over HZSM-5 catalyst. They observed that increase in temperature from 400 to 600°C increased the carbon yield of aromatics from 10% to 30%, whereas coke formation was remarkably reduced.

2.9.4 Catalyst-to-feed ratio

In addition to other parameters, catalyst-to-feed ratio is also an important factor for product formation and product selectivity in biomass catalytic pyrolysis. Carlson *et al.*[121] showed that the product selectivity for catalytic fast pyrolysis of glucose with ZSM5 is a function of the catalyst-to-glucose weight ratio. The coke yield increases and the aromatic yield decreases as the catalyst-to-glucose ratio decreases. These thermally stable oxygenates are intermediates in the production of aromatics. Thermally stable oxygenates are formed as the catalyst-to-glucose ratio decreases. The increased yield of aromatic hydrocarbon from 54.3% to 56.7% due to the increase of catalyst-to-feed ratio was reported by Zhao *et al.*[142]. The same parameter was also studied by Du *et al.*[143] in catalytic pyrolysis of microalgae *Chlorella* and observed that the aromatics yield increased significantly as the catalyst to feed ratio increased from 1:1 to 5:1. The

of aromatics yield could be attributed to the enough surface contact area provided by the increase of catalyst-to-feed ratio [135]. It was also shown by Carlson *et al.* [144] that increasing ZSM-5 to glucose weight ratio 1.5 to 19, carbon yield of aromatics increased from 13 to 31%, whereas carbon yield of coke decreased from 44 to 33%.

2.9.5 Catalyst surface area

Along with the other influencing parameter, catalyst surface area also has a dominating effect on product distribution and selectivity of the product. Lappas *et al.* [145] observed that more active the catalyst i.e., higher surface area, the less liquid was produced. However, the effect of catalyst on bio-oil yield was not linear. The effect of total surface area on gas yield was also found to be logarithmic, and therefore using a low active catalyst, the gas yield increased considerably in comparison with zero surface area silica sand. However, further use of higher surface area catalyst had a minor effect on gas yield. The total surface area of catalyst had a dominant effect on char yield. The char yield increases with the use of higher surface area catalyst as compared with silica sand. The presence of catalyst also significantly affects the bio-oil composition. The bio-oil produced with silica and sand contained mainly phenolic and carboxylic compounds. Furans, acids and hydrocarbons were also present in small quantities. However, using zeolite catalyst, the concentration of hydrocarbons increased with increase in catalyst surface area. It was also observed that, using the most active catalyst i.e. catalyst with the highest surface area, the hydrocarbon concentration was almost double as compared to that of non-active catalyst.

2.9.6 Incorporation of metal to catalyst

Recently, works on bi-functional catalyst such as zeolites doped with noble metal is gaining popularity. Incorporation of metals into catalyst could control both aromatics and olefin formation in catalytic biomass pyrolysis. Iliopoulou *et al.* [146] observed impregnation of 1 – 10 wt.% transition metals like nickel and cobalt into ZSM-5 catalyst increased the production of aromatics from biomass feedstock which could be attributed to the effect of these transition metals in promoting dehydrogenation reactions. Lanthanum (La) modified HZSM-5 (Si/Al = 25) catalyst was used by Gong *et al.* [147] in

catalytic cracking of bio-oil and observed that addition of La into zeolite efficiently changed the acid distribution among the strong, medium and weak acid sites and found that high percentage of medium acid sites is suitable for selective production of light olefins. Huang *et al.* [148] observed that biomass containing higher content of cellulose or hemicellulose produced more olefins than feedstock with higher content of lignin in an order of cellulose > hemicellulose > sugarcane bagasse > rice husk > sawdust > lignin when pyrolyzed with HZSM-5 impregnated with lanthanum. Increasing the percentage of lanthanum from 2.9 to 6.0 wt.%, increased the production of olefins from rice husk by 15.6% to 26.5%, respectively.

In a very recent study by Du *et al.* [149], a series of zeolites including HZSM-5, H-Beta and H-Y were evaluated for their influence on aromatic production performance of pyrolysis of *Chlorella* and egg whites. Among the zeolites, HZSM-5 showed the highest aromatics yield of 18.1% for *Chlorella* and 11.1% for egg whites with Si/Al ratio of 80. They also studied the effect of metal incorporation (Co, Cu, Fe, Ga, Mo, and Ni) on H-ZSM-5 on the aromatic yields and observed that, among the catalysts, Cu and Ga enhanced the aromatics yields significantly from 16.7% for normal HZSM-5 (30) to 21.2% and 18% respectively, indicating that some transition metals can promote the aromatization function of HZSM-5.

Pyrolysis of biomass has recently gained interest due to its wide ranging potential to produce solid, liquid and gaseous product in a single step conversion technology. The above discussion points towards the fact that pyrolysis could convert almost all types of biomass feedstock (Table 2.1). It is well known that successful utilization of any biofuel fundamentally depends on the availability of feedstock. The greatest share of production costs of large scale commercial use of biofuel is linked with the availability of low cost and good quality non-edible feedstock. Therefore, introduction of such kind of feedstock for pyrolytic conversion is necessary and will be beneficial for pyrolysis process to become a viable one. However, various parameters affect the product yield, properties and composition of pyrolysis product. These parameters can be divided into highly influencing and moderately and/or low influencing parameter. Highly influencing

parameters include temperature, rate of biomass heating, vapour residence time and biomass composition whereas moderately and/or low influencing parameters include size of feed particles, sweeping gas flow rates, mineral contents and initial moisture content. The biomass pyrolytic liquid can be utilized as an energy carrier and source for many commodity chemicals. However, despite of its various potential, bio-oil has some negative properties such as high density, acidity, water content and oxygen content together with low heating value. To overcome these negative attributes, the bio-oil must be upgraded through catalytic processes where a heterogeneous catalyst is used as a heat carrier in the pyrolysis reactor for the in situ upgrading of the quality of the pyrolysis oil. For this reason a plethora of catalytic materials such as zeolites, mesoporous materials with uniform pore size distribution (MCM-41, MSU and SBA-15), microporous or mesoporous hybrid materials doped with noble and transition metals, and base catalysts which act as bifunctional catalysts have been investigated. Among the various catalyst, zeolites seems to be very promising since they crack biomass pyrolytic vapours or oil, producing a better quality product albeit with lower yield. Therefore, research is necessary on biomass catalytic pyrolysis to improve and find optimum catalysts, which would be also beneficial for downstream bio-oil upgrading process.

References:

- [1] World energy outlook. 2007 Survey of Energy Resources. http://www.worldenergy.org/documents/ser2007_final_online_version_1.pdf, 2007.
- [2] Chattanathan, S.A., Adhikari, S., & Abdoulmoumine, N. A review on current status of hydrogen production from bio-oil. *Renewable and Sustainable Energy Reviews*, **16** (5), 2366-2372, 2012.
- [3] Görling, M., Larsson, M., & Alvfors, P. Bio-methane via fast pyrolysis of biomass. *Applied Energy*, **112** (0), 440-447, 2013.
- [4] Larsson, M., et al. Bio-methane upgrading of pyrolysis gas from charcoal production. *Sustainable Energy Technologies and Assessments*, **3** (0), 66-73, 2013.
- [5] Mohan, D., Pittman, C.U., & Steele, P.H. Pyrolysis of wood/biomass for bio-oil: A critical review. *Energy & Fuels*, **20** (3), 848-889, 2006.
- [6] Mosier, N.S., et al. Industrial scale-up of pH-controlled liquid hot water pretreatment of corn fiber for fuel ethanol production. *Applied Biochemistry and Biotechnology*, **125** (2), 77-97, 2005.
- [7] Boateng, A.A., et al. Production of Bio-oil from Alfalfa Stems by Fluidized-Bed Fast Pyrolysis. *Industrial & Engineering Chemistry Research*, **47** (12), 4115-4122, 2008.
- [8] Shen, D.K., et al. Kinetic study on thermal decomposition of woods in oxidative environment. *Fuel*, **88** (6), 1024-1030, 2009.
- [9] Garcia-Perez, M., et al. Fast pyrolysis of oil mallee woody biomass: effect of temperature on the yield and quality of pyrolysis products. *Industrial & Engineering Chemistry Research*, **47** (6), 1846-1854, 2008.
- [10] Demirbas, A. The influence of temperature on the yields of compounds existing in bio-oils obtained from biomass samples via pyrolysis. *Fuel Processing Technology*, **88** (6), 591-597, 2007.

-
- [11] López, F.A., et al. Textural and fuel characteristics of the chars produced by the pyrolysis of waste wood, and the properties of activated carbons prepared from them. *Journal of Analytical and Applied Pyrolysis*, **104** (0), 551-558, 2013.
- [12] Min, Z., et al. Catalytic reforming of tar during gasification. Part III. Effects of feedstock on tar reforming using ilmenite as a catalyst. *Fuel*, **103** (0), 950-955, 2013.
- [13] Mourant, D., et al. Effects of temperature on the yields and properties of bio-oil from the fast pyrolysis of mallee bark. *Fuel*, **108** (0), 400-408, 2013.
- [14] Brebu, M., et al. Co-pyrolysis of pine cone with synthetic polymers. *Fuel*, **89** (8), 1911-1918, 2010.
- [15] DeSisto, W.J., et al. Fast Pyrolysis of Pine Sawdust in a Fluidized-Bed Reactor. *Energy & Fuels*, **24** (4), 2642-2651, 2010.
- [16] Wei, L., et al. Characteristics of fast pyrolysis of biomass in a free fall reactor. *Fuel Processing Technology*, **87** (10), 863-871, 2006.
- [17] Tröger, N., Richter, D., & Stahl, R. Effect of feedstock composition on product yields and energy recovery rates of fast pyrolysis products from different straw types. *Journal of Analytical and Applied Pyrolysis*, **100** (0), 158-165, 2013.
- [18] Raveendran, K., Ganesh, A., & Khilar, K.C. Influence of mineral matter on biomass pyrolysis characteristics. *Fuel*, **74** (12), 1812-1822, 1995.
- [19] Özbay, N., et al. Characterization of bio-oil obtained from fruit pulp pyrolysis. *Energy*, **33** (8), 1233-1240, 2008.
- [20] Bok, J.P., et al. Fast pyrolysis of coffee grounds: Characteristics of product yields and biocrude oil quality. *Energy*, **47** (1), 17-24, 2012.
- [21] Vassilev, S.V., et al. An overview of the organic and inorganic phase composition of biomass. *Fuel*, **94** (0), 1-33, 2012.
- [22] Kim, S.W., et al. Bio-oil from the pyrolysis of palm and *Jatropha* wastes in a fluidized bed. *Fuel Processing Technology*, **108** (0), 118-124, 2013.
- [23] Tsai, W.-T., Liu, S.-C., & Hsieh, C.-H. Preparation and fuel properties of biochars from the pyrolysis of exhausted coffee residue. *Journal of Analytical and Applied Pyrolysis*, **93** (0), 63-67, 2012.

-
- [24] Celma, A.R., Rojas, S., & Lopez-Rodriguez, F. Waste-to-energy possibilities for industrial olive and grape by-products in Extremadura. *Biomass & Bioenergy*, **31** (7), 522-534, 2007.
- [25] Yang, H.P., et al. Thermogravimetric analysis-Fourier transform infrared analysis of palm oil waste pyrolysis. *Energy & Fuels*, **18** (6), 1814-1821, 2004.
- [26] Wang, L., Shahbazi, A., & Hanna, M.A. Characterization of corn stover, distiller grains and cattle manure for thermochemical conversion. *Biomass and Bioenergy*, **35** (1), 171-178, 2011.
- [27] Gu, S., et al. A detailed study of the effects of pyrolysis temperature and feedstock particle size on the preparation of nanosilica from rice husk. *Industrial Crops and Products*, **50** (0), 540-549, 2013.
- [28] Naik, S., et al. Characterization of Canadian biomass for alternative renewable biofuel. *Renewable Energy*, **35** (8), 1624-1631, 2010.
- [29] Titiloye, J.O., Abu Bakar, M.S., & Odetoye, T.E. Thermochemical characterisation of agricultural wastes from West Africa. *Industrial Crops and Products*, **47** (0), 199-203, 2013.
- [30] Tushar, M.S.H.K., et al. Analysis of gaseous and liquid products from pressurized pyrolysis of flax straw in a fixed bed reactor. *Industrial & Engineering Chemistry Research*, **49** (10), 4627-4632, 2010.
- [31] Li, S., et al. Fast pyrolysis of biomass in free-fall reactor for hydrogen-rich gas. *Fuel Processing Technology*, **85** (8-10), 1201-1211, 2004.
- [32] Zheng, J.L. Pyrolysis oil from fast pyrolysis of maize stalk. *Journal of Analytical and Applied Pyrolysis*, **83** (2), 205-212, 2008.
- [33] Ates, F. & Isakdag, M.A. Evaluation of the role of the pyrolysis temperature in straw biomass samples and characterization of the oils by GC/MS. *Energy & Fuels*, **22** (3), 1936-1943, 2008.
- [34] Putun, A.E., Apaydin, E., & Putun, E. Rice straw as a bio-oil source via pyrolysis and steam pyrolysis. *Energy*, **29** (12-15), 2171-2180, 2004.

-
- [35] Demiral, İ. & Ayan, E.A. Pyrolysis of grape bagasse: Effect of pyrolysis conditions on the product yields and characterization of the liquid product. *Bioresource Technology*, **102** (4), 3946-3951, 2011.
- [36] Demiral, İ. & Şensöz, S. The effects of different catalysts on the pyrolysis of industrial wastes (olive and hazelnut bagasse). *Bioresource Technology*, **99** (17), 8002-8007, 2008.
- [37] Ertaş, M. & Hakkı Alma, M. Pyrolysis of laurel (*Laurus nobilis* L.) extraction residues in a fixed-bed reactor: Characterization of bio-oil and bio-char. *Journal of Analytical and Applied Pyrolysis*, **88** (1), 22-29, 2010.
- [38] Boateng, A.A., et al. Energy-dense liquid fuel intermediates by pyrolysis of guayule (*Parthenium argentatum*) shrub and bagasse. *Fuel*, **88** (11), 2207-2215, 2009.
- [39] Tsai, W.T., Lee, M.K., & Chang, Y.M. Fast pyrolysis of rice straw, sugarcane bagasse and coconut shell in an induction-heating reactor. *Journal of Analytical and Applied Pyrolysis*, **76** (1-2), 230-237, 2006.
- [40] Yorgun, S., Sensoz, S., & Kockar, O.M. Characterization of the pyrolysis oil produced in the slow pyrolysis of sunflower-extracted bagasse. *Biomass & Bioenergy*, **20** (2), 141-148, 2001.
- [41] Das, P. & Ganesh, A. Bio-oil from pyrolysis of cashew nut shell—a near fuel. *Biomass and Bioenergy*, **25** (1), 113-117, 2003.
- [42] Duman, G., et al. The slow and fast pyrolysis of cherry seed. *Bioresource Technology*, **102** (2), 1869-1878, 2011.
- [43] Werther, J., et al. Combustion of agricultural residues. *Progress in Energy and Combustion Science*, **26** (1), 1-27, 2000.
- [44] Şen, N. & Kar, Y. Pyrolysis of black cumin seed cake in a fixed-bed reactor. *Biomass and Bioenergy*, **35** (10), 4297-4304, 2011.
- [45] Putun, E., Uzun, B.B., & Putun, A.E. Fixed-bed catalytic pyrolysis of cotton-seed cake: effects of pyrolysis temperature, natural zeolite content and sweeping gas flow rate. *Bioresource Technology*, **97** (5), 701-10, 2006.

-
- [46] Murata, K., et al. Analyses of liquid products from catalytic pyrolysis of jatropha seed cakes. *Energy & Fuels*, **25** (11), 5429-5437, 2011.
- [47] Acikgoz, C. & Kockar, O.M. Characterization of slow pyrolysis oil obtained from linseed (*Linum usitatissimum* L.). *Journal of Analytical and Applied Pyrolysis*, **85** (1-2), 151-154, 2009.
- [48] Nayan, N.K., Kumar, S., & Singh, R.K. Production of the liquid fuel by thermal pyrolysis of neem seed. *Fuel*, **103** (0), 437-443, 2013.
- [49] Uçar, S. & Karagöz, S. The slow pyrolysis of pomegranate seeds: The effect of temperature on the product yields and bio-oil properties. *Journal of Analytical and Applied Pyrolysis*, **84** (2), 151-156, 2009.
- [50] Onay, O. & Koçkar, O.M. Pyrolysis of rapeseed in a free fall reactor for production of bio-oil. *Fuel*, **85** (12-13), 1921-1928, 2006.
- [51] Onay, O. Influence of pyrolysis temperature and heating rate on the production of bio-oil and char from safflower seed by pyrolysis, using a well-swept fixed-bed reactor. *Fuel Processing Technology*, **88** (5), 523-531, 2007.
- [52] Sensoz, S. & Angin, D. Pyrolysis of safflower (*Charthamus tinctorius* L.) seed press cake in a fixed-bed reactor: part 2. Structural characterization of pyrolysis bio-oils. *Bioresource Technology*, **99** (13), 5498-504, 2008.
- [53] Uzun, B.B., Putun, A.E., & Putun, E. Fast pyrolysis of soybean cake: product yields and compositions. *Bioresource Technology*, **97** (4), 569-76, 2006.
- [54] Uzun, B.B., Pütün, A.E., & Pütün, E. Composition of products obtained via fast pyrolysis of olive-oil residue: Effect of pyrolysis temperature. *Journal of Analytical and Applied Pyrolysis*, **79** (1-2), 147-153, 2007.
- [55] Pütün, A.E., et al. Bio-oil from olive oil industry wastes: Pyrolysis of olive residue under different conditions. *Fuel Processing Technology*, **87** (1), 25-32, 2005.
- [56] Bridgeman, T.G., et al. Influence of particle size on the analytical and chemical properties of two energy crops. *Fuel*, **86** (1-2), 60-72, 2007.
- [57] Phukan, M.M., et al. Microalgae *Chlorella* as a potential bio-energy feedstock. *Applied Energy*, **88** (10), 3307-3312, 2011.
-

- [58] Li, D., et al. Preparation and characteristics of bio-oil from the marine brown alga *Sargassum patens* C. Agardh. *Bioresource Technology*, **104** 737-42, 2012.
- [59] Luo, S., et al. Effect of particle size on pyrolysis of single-component municipal solid waste in fixed bed reactor. *International Journal of Hydrogen Energy*, **35** (1), 93-97, 2010.
- [60] Koufopoulos, C.A., Lucchesi, A., & Maschio, G. Kinetic modelling of the pyrolysis of biomass and biomass components. *The Canadian Journal of Chemical Engineering*, **67** (1), 75-84, 1989.
- [61] Sánchez-Jiménez, P.E., et al. A new model for the kinetic analysis of thermal degradation of polymers driven by random scission. *Polymer Degradation and Stability*, **95** (5), 733-739, 2010.
- [62] Hujuri, U., Ghoshal, A.K., & Gumma, S. Modeling pyrolysis kinetics of plastic mixtures. *Polymer Degradation and Stability*, **93** (10), 1832-1837, 2008.
- [63] Yao, F., et al. Thermal decomposition kinetics of natural fibers: Activation energy with dynamic thermogravimetric analysis. *Polymer Degradation and Stability*, **93** (1), 90-98, 2008.
- [64] Jiang, G., Nowakowski, D.J., & Bridgwater, A.V. A systematic study of the kinetics of lignin pyrolysis. *Thermochimica Acta*, **498** (1-2), 61-66, 2010.
- [65] Sasmal, S., Goud, V., & Mohanty, K. Determination of salutary parameters to facilitate bio-energy production from three uncommon biomasses using thermogravimetric analysis. *Journal of Thermal Analysis and Calorimetry*, **111** (3), 1649-1655, 2013.
- [66] Li, D., et al. Pyrolytic characteristics and kinetics of two brown algae and sodium alginate. *Bioresource Technology*, **101** (18), 7131-7136, 2010.
- [67] Li, D., et al. Pyrolytic characteristics and kinetic studies of three kinds of red algae. *Biomass & Bioenergy*, **35** (5), 1765-1772, 2011.
- [68] Chouchene, A., et al. Thermal degradation of olive solid waste: Influence of particle size and oxygen concentration. *Resources, Conservation and Recycling*, **54** (5), 271-277, 2010.

- [69] Di Blasi, C. Modeling and simulation of combustion processes of charring and non-charring solid fuels. *Progress in Energy and Combustion Science*, **19** (1), 71-104, 1993.
- [70] Varhegyi, G., et al. Kinetics of the thermal decomposition of cellulose, hemicellulose, and sugarcane bagasse. *Energy & Fuels*, **3** (3), 329-335, 1989.
- [71] Várhegyi, G., et al. Kinetic modeling of biomass pyrolysis. *Journal of Analytical and Applied Pyrolysis*, **42** (1), 73-87, 1997.
- [72] Orfão, J.J.M., Antunes, F.J.A., & Figueiredo, J.L. Pyrolysis kinetics of lignocellulosic materials—three independent reactions model. *Fuel*, **78** (3), 349-358, 1999.
- [73] Grønli, M.G., Várhegyi, G., & Di Blasi, C. Thermogravimetric Analysis and Devolatilization Kinetics of Wood. *Industrial & Engineering Chemistry Research*, **41** (17), 4201-4208, 2002.
- [74] Açıkalın, K. Pyrolytic characteristics and kinetics of pistachio shell by thermogravimetric analysis. *Journal of Thermal Analysis and Calorimetry*, **109** (1), 227-235, 2011.
- [75] Vyazovkin, S. & Sbirrazzuoli, N. Isoconversional Kinetic Analysis of Thermally Stimulated Processes in Polymers. *Macromolecular Rapid Communications*, **27** (18), 1515-1532, 2006.
- [76] Brown, M. Computational aspects of kinetic analysis Part A: The ICTAC kinetics project-data, methods and results. *Thermochimica Acta*, **355** (1-2), 125-143, 2000.
- [77] Salehi, E., Abedi, J., & Harding, T. Bio-oil from Sawdust: Effect of Operating Parameters on the Yield and Quality of Pyrolysis Products. *Energy & Fuels*, **25** 4145-4154, 2011.
- [78] Van de Velden, M., et al. Fundamentals, kinetics and endothermicity of the biomass pyrolysis reaction. *Renewable Energy*, **35** (1), 232-242, 2010.
- [79] Bridgwater, A.V. Review of fast pyrolysis of biomass and product upgrading. *Biomass & Bioenergy*, **38** 68-94, 2012.
- [80] Heo, H.S., et al. Bio-oil production from fast pyrolysis of waste furniture sawdust in a fluidized bed. *Bioresource Technology*, **101** (1), S91-S96, 2010.

- [81] Park, H.J., et al. Pyrolysis characteristics of Oriental white oak: Kinetic study and fast pyrolysis in a fluidized bed with an improved reaction system. *Fuel Processing Technology*, **90** (2), 186-195, 2009.
- [82] Horne, P.A. & Williams, P.T. Influence of temperature on the products from the flash pyrolysis of biomass. *Fuel*, **75** (9), 1051-1059, 1996.
- [83] Xiao, R. & Yang, W. Influence of temperature on organic structure of biomass pyrolysis products. *Renewable Energy*, **50** (0), 136-141, 2013.
- [84] Encinar, J.M., González, J.F., & González, J. Fixed-bed pyrolysis of *Cynara cardunculus* L. Product yields and compositions. *Fuel Processing Technology*, **68** (3), 209-222, 2000.
- [85] Chan, W.C.R., Kelbon, M., & Krieger-Brockett, B. Single-particle biomass pyrolysis: correlations of reaction products with process conditions. *Industrial & Engineering Chemistry Research*, **27** (12), 2261-2275, 1988.
- [86] Haykiri-Acma, H. The role of particle size in the non-isothermal pyrolysis of hazelnut shell. *Journal of Analytical and Applied Pyrolysis*, **75** (2), 211-216, 2006.
- [87] Beaumont, O. & Schwob, Y. Influence of physical and chemical parameters on wood pyrolysis. *Industrial & Engineering Chemistry Process Design and Development*, **23** (4), 637-641, 1984.
- [88] Shen, J., et al. Effects of particle size on the fast pyrolysis of oil mallee woody biomass. *Fuel*, **88** (10), 1810-1817, 2009.
- [89] Gibbins-Matham, J. & Kandiyoti, R. Coal pyrolysis yields from fast and slow heating in a wire-mesh apparatus with a gas sweep. *Energy & Fuels*, **2** (4), 505-511, 1988.
- [90] Seebauer, V., Petek, J., & Staudinger, G. Effects of particle size, heating rate and pressure on measurement of pyrolysis kinetics by thermogravimetric analysis. *Fuel*, **76** (13), 1277-1282, 1997.
- [91] Strezov, V., Moghtaderi, B., & Lucas, J.A. Thermal study of decomposition of selected biomass samples. *Journal of Thermal Analysis and Calorimetry*, **72** (3), 1041-1048, 2003.

- [92] Maggi, R. & Delmon, B. Comparison between 'slow' and 'flash' pyrolysis oils from biomass. *Fuel*, **73** (5), 671-677, 1994.
- [93] Acikgoz, C., Onay, O., & Kockar, O.M. Fast pyrolysis of linseed: product yields and compositions. *Journal of Analytical and Applied Pyrolysis*, **71** (2), 417-429, 2004.
- [94] Demiral, İ. & Şensöz, S. Fixed-bed pyrolysis of hazelnut (*Corylus Avellana* L.) bagasse: influence of pyrolysis parameters on product yields. *Energy Sources, Part A: Recovery, Utilization, and Environmental Effects*, **28** (12), 1149-1158, 2006.
- [95] Sensoz, S. & Angin, D. Pyrolysis of safflower (*Charthamus tinctorius* L.) seed press cake: part 1. The effects of pyrolysis parameters on the product yields. *Bioresource Technology*, **99** (13), 5492-7, 2008.
- [96] Akhtar, J. & Saidina Amin, N. A review on operating parameters for optimum liquid oil yield in biomass pyrolysis. *Renewable and Sustainable Energy Reviews*, **16** (7), 5101-5109, 2012.
- [97] Scott, D.S., et al. A second look at fast pyrolysis of biomass—the RTI process. *Journal of Analytical and Applied Pyrolysis*, **51** (1–2), 23-37, 1999.
- [98] Venderbosch, R.H. & Prins, W. Fast pyrolysis technology development. *Biofuels, Bioproducts and Biorefining*, **4** (2), 178-208, 2010.
- [99] Yang, H.P., et al. Characteristics of hemicellulose, cellulose and lignin pyrolysis. *Fuel*, **86** (12-13), 1781-1788, 2007.
- [100] Burhenne, L., et al. The effect of the biomass components lignin, cellulose and hemicellulose on TGA and fixed bed pyrolysis. *Journal of Analytical and Applied Pyrolysis*, **101** (0), 177-184, 2013.
- [101] Richards, G.N. & Zheng, G. Influence of metal ions and of salts on products from pyrolysis of wood: Applications to thermochemical processing of newsprint and biomass. *Journal of Analytical and Applied Pyrolysis*, **21** (1–2), 133-146, 1991.
- [102] Aho, A., et al. Pyrolysis of pine and gasification of pine chars – Influence of organically bound metals. *Bioresource Technology*, **128** (0), 22-29, 2013.

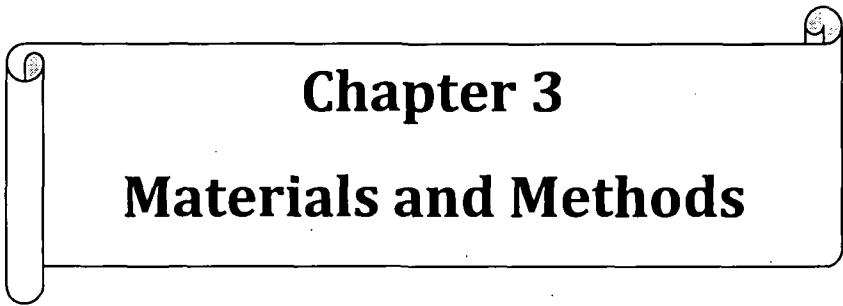
-
- [103] Stephanidis, S., et al. Catalytic upgrading of lignocellulosic biomass pyrolysis vapours: Effect of hydrothermal pre-treatment of biomass. *Catalysis Today*, **167** (1), 37-45, 2011.
- [104] Davidsson, K.O., et al. The effects of fuel washing techniques on alkali release from biomass. *Fuel*, **81** (2), 137-142, 2002.
- [105] Eom, I.-Y., et al. Characterization of primary thermal degradation features of lignocellulosic biomass after removal of inorganic metals by diverse solvents. *Bioresource Technology*, **102** (3), 3437-3444, 2011.
- [106] Downie, A., Crosky, A., & Munroe, P., eds. *Physical properties of biochar*. Biochar for environmental management: Science and technology, ed. J. Lehmann and S. Joseph 2009, Earthscan: London. 13-32.
- [107] Antal, M.J. & Grønli, M. The Art, Science, and Technology of Charcoal Production. *Industrial & Engineering Chemistry Research*, **42** (8), 1619-1640, 2003.
- [108] Chan, K.Y. & Xu, Z. Biochar: nutrient properties and their enhancement. *Biochar for environmental management: science and technology*. Earthscan, London, 67-84, 2009.
- [109] Gaskin, J.W., et al. Effect of Peanut Hull and Pine Chip Biochar on Soil Nutrients, Corn Nutrient Status, and Yield. *Agronomy Journal*, **102** (2), 623, 2010.
- [110] Lehmann, J. & Joseph, S., *Biochar for Environmental Management: Science and Technology*, Earthscan, 2009.
- [111] Lua, A.C., Yang, T., & Guo, J. Effects of pyrolysis conditions on the properties of activated carbons prepared from pistachio-nut shells. *Journal of Analytical and Applied Pyrolysis*, **72** (2), 279-287, 2004.
- [112] Lee, J.W., et al. Characterization of biochars produced from cornstovers for soil amendment. *Environmental Science & Technology*, **44** (20), 7970-7974, 2010.
- [113] Angin, D. Effect of pyrolysis temperature and heating rate on biochar obtained from pyrolysis of safflower seed press cake. *Bioresource Technology*, **128** (0), 593-597, 2013.

- [114] Inyang, M., et al. Biochar from anaerobically digested sugarcane bagasse. *Bioresource Technology*, **101** (22), 8868-8872, 2010.
- [115] Jindarom, C., et al. Surface characterization and dye adsorptive capacities of char obtained from pyrolysis/gasification of sewage sludge. *Chemical Engineering Journal*, **133** (1-3), 239-246, 2007.
- [116] Yao, Y., et al. Biochar derived from anaerobically digested sugar beet tailings: Characterization and phosphate removal potential. *Bioresource Technology*, **102** (10), 6273-6278, 2011.
- [117] Yuan, J.-H., Xu, R.-K., & Zhang, H. The forms of alkalis in the biochar produced from crop residues at different temperatures. *Bioresource Technology*, **102** (3), 3488-3497, 2011.
- [118] Thring, R.W., Katikaneni, S.P.R., & Bakhshi, N.N. The production of gasoline range hydrocarbons from Alcell® lignin using HZSM-5 catalyst. *Fuel Processing Technology*, **62** (1), 17-30, 2000.
- [119] Bridgwater, A.V. Catalysis in thermal biomass conversion. *Applied Catalysis A: General*, **116** (1-2), 5-47, 1994.
- [120] Huber, G.W. & Corma, A. Synergies between bio- and oil refineries for the production of fuels from biomass. *Angew Chem Int Ed Engl*, **46** (38), 7184-201, 2007.
- [121] Carlson, T.R., et al. Aromatic production from catalytic fast pyrolysis of biomass-derived feedstocks. *Topics in Catalysis*, **52** (3), 241-252, 2009.
- [122] Jae, J., et al. Investigation into the shape selectivity of zeolite catalysts for biomass conversion. *Journal of Catalysis*, **279** (2), 257-268, 2011.
- [123] Aho, A., et al. Catalytic pyrolysis of biomass in a fluidized bed reactor: influence of the acidity of H-Beta zeolite. *Process Safety and Environmental Protection*, **85** (5), 473-480, 2007.
- [124] Williams, P.T. & Horne, P.A. Analysis of aromatic hydrocarbons in pyrolytic oil derived from biomass. *Journal of Analytical and Applied Pyrolysis*, **31** (0), 15-37, 1995.

- [125] Misson, M., et al. Pretreatment of empty palm fruit bunch for production of chemicals via catalytic pyrolysis. *Bioresour Technol*, **100** (11), 2867-73, 2009.
- [126] Aguado, J., et al. Feedstock recycling in a two-step thermo-catalytic reaction system. *Journal of Analytical and Applied Pyrolysis* **79** 415–423, 2006.
- [127] Ma, Z., Troussard, E., & van Bokhoven, J.A. Controlling the selectivity to chemicals from lignin via catalytic fast pyrolysis. *Applied Catalysis A: General*, **423–424** (0), 130-136, 2012.
- [128] Ben, H. & Ragauskas, A.J. Pyrolysis of kraft lignin with additives. *Energy & Fuels*, **25** (10), 4662-4668, 2011.
- [129] Li, X., et al. Catalytic fast pyrolysis of Kraft lignin with HZSM-5 zeolite for producing aromatic hydrocarbons. *Frontiers of Environmental Science & Engineering*, **6** (3), 295-303, 2012.
- [130] Mullen, C.A. & Boateng, A.A. Catalytic pyrolysis-GC/MS of lignin from several sources. *Fuel Processing Technology*, **91** (11), 1446-1458, 2010.
- [131] Zhao, Y., et al. Aromatics production via catalytic pyrolysis of pyrolytic lignins from bio-oil. *Energy & Fuels*, **24** (10), 5735-5740, 2010.
- [132] Rezaei, P.S., Shafaghat, H., & Daud, W.M.A.W. Production of green aromatics and olefins by catalytic cracking of oxygenate compounds derived from biomass pyrolysis: A review. *Applied Catalysis A: General*, (0), 2013.
- [133] Lin, Y.-C. & Huber, G.W. The critical role of heterogeneous catalysis in lignocellulosic biomass conversion. *Energy & Environmental Science*, **2** (1), 68-80, 2009.
- [134] Chen, N., Degnan, T., & Koenig, L. Liquid fuel from carbohydrates. *Chemtech*, **16** (8), 506-511, 1986.
- [135] Chen, N.Y., Walsh, D.E., & Koenig, L.R. Fluidized-bed upgrading of wood pyrolysis liquids and related compounds, in *Pyrolysis Oils from Biomass*, eds., American Chemical Society, 1988, 277-289
- [136] Zhang, H., et al. Catalytic conversion of biomass-derived feedstocks into olefins and aromatics with ZSM-5: the hydrogen to carbon effective ratio. *Energy & Environmental Science*, **4** (6), 2297-2307, 2011.

- [137] Lappas, A.A., et al. Biomass pyrolysis in a circulating fluid bed reactor for the production of fuels and chemicals. *Fuel*, **81** (16), 2087-2095, 2002.
- [138] Zhang, H.Y., et al. Catalytic fast pyrolysis of wood and alcohol mixtures in a fluidized bed reactor. *Green Chemistry*, **14** (1), 98-110, 2012.
- [139] Vispute, T.P., et al. Renewable chemical commodity feedstocks from integrated catalytic processing of pyrolysis oils. *Science*, **330** (6008), 1222-7, 2010.
- [140] Carlson, T.R., et al. Production of green aromatics and olefins by catalytic fast pyrolysis of wood sawdust. *Energy & Environmental Science*, **4** (1), 145, 2011.
- [141] Carlson, T.R., et al. Catalytic fast pyrolysis of glucose with HZSM-5: The combined homogeneous and heterogeneous reactions. *Journal of Catalysis*, **270** (1), 110-124, 2010.
- [142] Zhao, Y., Fu, Y., & Guo, Q.-X. Production of aromatic hydrocarbons through catalytic pyrolysis of γ -valerolactone from biomass. *Bioresource Technology*, **114** (0), 740-744, 2012.
- [143] Du, Z., et al. Catalytic pyrolysis of microalgae and their three major components: Carbohydrates, proteins, and lipids. *Bioresource Technology*, **130** (0), 777-782, 2013.
- [144] Carlson, T.R., Vispute, T.P., & Huber, G.W. Green gasoline by catalytic fast pyrolysis of solid biomass derived compounds. *ChemSusChem*, **1** (5), 397-400, 2008.
- [145] Lappas, A.A., Iliopoulou, E.F., & Kalogiannis, K. Catalysts in Biomass Pyrolysis, in *Thermochemical Conversion of Biomass to Liquid Fuels and Chemicals*, M. Crocker, eds., The Royal Society of Chemistry, UK, 2010, 263-287
- [146] Iliopoulou, E.F., et al. Catalytic upgrading of biomass pyrolysis vapors using transition metal-modified ZSM-5 zeolite. *Applied Catalysis B: Environmental*, **127** (0), 281-290, 2012.
- [147] Gong, F., et al. Selective conversion of bio-oil to light olefins: controlling catalytic cracking for maximum olefins. *Bioresour Technol*, **102** (19), 9247-54, 2011.

- [148] Huang, W., et al. Production of light olefins by catalytic conversion of lignocellulosic biomass with HZSM-5 zeolite impregnated with 6 wt.% lanthanum. *Bioresource Technology*, **121** (0), 248-255, 2012.
- [149] Du, Z., et al. Production of aromatic hydrocarbons by catalytic pyrolysis of microalgae with zeolites: Catalyst screening in a pyroprobe. *Bioresource Technology*, **139** (0), 397-401, 2013.



Chapter 3
Materials and Methods

Chapter 3 : Materials and Methods

3.1 Methodology flow diagram

The methodology adopted in this study for conducting the proposed research is shown in the form of a flow chart (Figure 3.1).

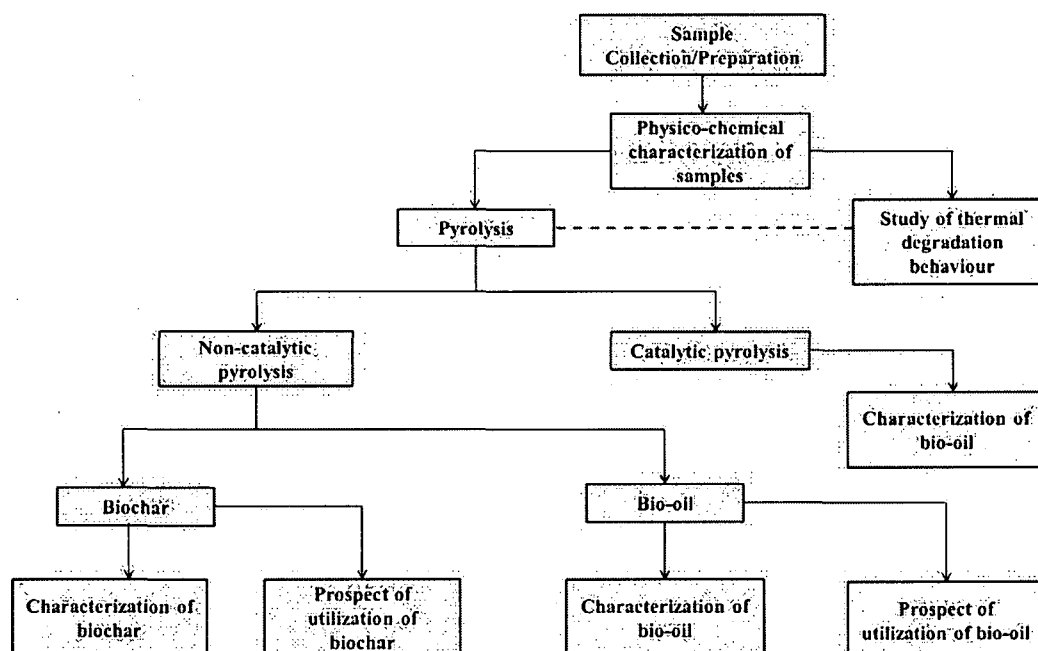
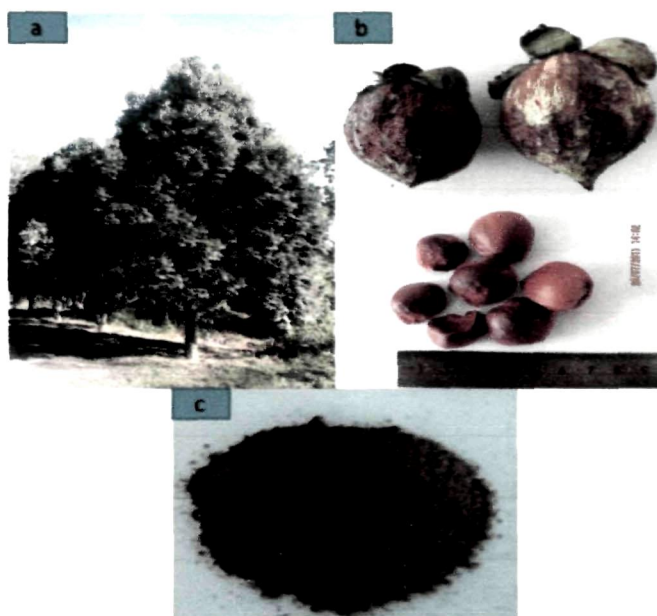


Figure 3.1: Flow diagram of methodology adopted in the study.

3.2 Description of tree species

3.2.1 *Mesua ferrea*



**Figure 3.2: (a) *Mesua ferrea* tree (b) *Mesua ferrea* seed
(c) *Mesua ferrea* deoiled cake.**

Mesua ferrea deoiled seed cake (MFDC) [Figure 3.2(c)] is one of the feedstock opted for the present study. MFDC is produced after oil extraction from *M. ferrea* seed [Figure 3.2(b)]. *M. ferrea* is a plant [Figure 3.2(a)] with one of the highest oil containing seeds [1].

Botanical Name : *Mesua ferrea* L.

English Name : Iron wood tree

Vernacular Name : Nahar (Assamese); Nageswar (Hindi)

Family : Guttiferae

It is a middle-size tree that grows mostly in the mountains of the Eastern Himalayas, Eastern Bengal, Eastern and Western Peninsulas and Andaman Islands. In

Assam it is found particularly in upper Assam, lower Nagaland, Darrang district and the North Cashar Hills. Its seeds contain 75% percent of oil on the basis of shelled kernel weight [1]. Flowering starts in April-May and seeds become mature in August-October. A fully mature tree yields 30-60 kg of seeds annually and yields per hectare ranges from 6122 to 12245 kg (assuming a spacing of $7 \times 7 \text{ m}^2$). *M. ferrea* is one of the hardest trees of north-east India. Its timbers are used in railway sleepers, construction of houses, furniture and cart wheels etc. In early days when kerosene and electricity were not available the rural people of this region used its seeds for illumination at night. Flowers and leaves have snake repellent properties.

3.2.2 *Pongamia glabra*



Figure 3.3: (a) *Pongamia* tree (b) *Pongamia* seed (c) *Pongamia glabra* deoiled cake.

The *Pongamia glabra* deoiled seed cake (PGDC) [Figure 3.3(c)] taken for the present study is a byproduct of biodiesel production from oil of *P. glabra* seed [Figure 3.3(b)].

Botanical Name	: <i>Pongamia glabra</i> V.
English Name	: Indian Beech, Pongam, Hongay
Vernacular Name	: Koroch (Assamese); Karanja (Hindi)
Family	: Leguminosae

P. glabra is an arboreal legume, is a member of the subfamily Papilionoideae, more specifically the Millettieae tribe. This medium-size tree [Fig. 3.3(a)] is indigenous to the Indian subcontinent and also found in the humid tropical regions of the world as well as some parts of Australia, New Zealand, China and the USA [2]. The seeds or nuts of the tree are its most useful product. The non-edible oil extracted from seeds has traditionally been used as fuel and lubricant and in soap making [3, 4]. More importantly, India's biofuel policy screened *P. glabra* as a viable source of oil for the escalating biofuel industry [5]. The main features which support *Pongamia* a potential biofuel crop are-

- It is a fast growing leguminous trees and it improve the soil where it grows [2],
- High seed yielding tree and maximum oil production (900–9000 kg seed/ha/year. The oil content of the seeds varies from 30-35 %) [6, 7],
- The tree has the ability to grow on marginal land with a high productive life,
- The seed is non-edible (contains several unsaponifiable and toxic components) [8], so it alleviates today's major competitive situation that exists with food crops as biofuels and engrossing arable land and water use

Some important features of *P. glabra* and *M. ferrea* seed oil are presented in Table 3.1.

Table 3.1: Important features of *P. glabra* and *M. ferrea* seed oil

<i>Properties</i>	<i>P. glabra</i> [9]	<i>M. ferrea</i> [7, 10]
<i>Density at 15°C (kg/m³)</i>	931.0	935.0
<i>Viscosity at 40°C (mm²/s)</i>	26.06	26.00
<i>Calorific value (MJ/kg)</i>	40.51	39.84
<i>Acid value (mgKOH/g)</i>	7.51	16.40
<i>Ash (wt.%)</i>	0.001	0.02
<i>Carbon residue (wt.%)</i>	1.21	1.60
<i>Saturated fatty acids (wt.%)</i>	26	25.40
<i>Unsaturated fatty acids (wt.%)</i>	73	74.60

3.3 Materials and analytical methods

3.3.1 Sample preparation

MFDC and PGDC were collected from Biomass Conversion & Gasification Laboratory, Department of Energy, Tezpur University, India, after lipid extraction with mechanical oil expeller [Malnad type oil expeller (Indus)]. MFDC were ground using a Wiley mill to pass through 0.2mm (70 mesh) and 0.4mm (40 mesh) screen (as per TAPPI T257 Om-85 methods) to fine particles of 210 and 420 μ respectively in order to eliminate heat transfer effects during pyrolysis and then samples were oven dried and kept in a desiccator.

3.3.2 Determination of moisture content

Moisture content of both the samples was determined according to the ASTM D 3173. The collected samples were weighed initially and then the samples were taken in an aluminum container and dried in an oven at $105 \pm 3^\circ\text{C}$. The samples were kept in the oven until a constant weighed was reached. The weight of the samples at this point is considered as the direct measurement of the dry weight of the sample which is subtracted from the initial weight of the sample to obtain the weight of moisture content present in the sample. For each sample, the experiment was conducted in triplicate and the mean value was reported. The moisture content was determined using the following equation:

$$\text{Moisture content (\%)} = \frac{\text{Initial weight} - \text{Oven dry weight}}{\text{Initial weight}} \times 100$$

3.3.3 Determination of ash content

For determination of ash content, ASTM D 3174 was followed. At first, an empty 25 ml silica crucible was heated in a muffle furnace at $575 \pm 25^\circ\text{C}$ for 15 min. and allowed to cool in desiccators for 45 min. and then weighed accurately. Oven dried biomass samples under investigation were weighed and transferred into the

crucible and kept in a muffle furnace at $575 \pm 25^\circ\text{C}$ to ignite for a period of 3 hours or longer to burn away the carbon, completion of which was indicated by the absence of black particles. Crucible was then removed from the furnace and kept in desiccators and weighed accurately. For each sample, the estimation was done in triplicate and the mean value was reported. The percentage of ash content was calculated as follows:

$$\text{Ash content (\%)} = \frac{\text{Weight of ash}}{\text{Weight of sample}} \times 100$$

3.3.4 Determination of volatile matter

Volatile matter of MFDC and PGDC samples were determined using the method described in ASTM 3175. A platinum crucible of 10 ml capacity was taken and its surface was cleaned by rubbing with fine steel wool. After that it was heated in a preheated furnace at 950°C for 2 min and then cooled in a desiccator for 15 min. The weight of the platinum crucible was taken. The crucible was filled up to $1/2$ to $3/8$ inch with the ground oven dried samples and gross weight was taken. It was then heated again in the preheated furnace at 950°C for 2 min. After that the crucible was removed from the furnace and cooled in air for 2 to 5 min and then cooled in desiccators for 15 min. For each sample, the estimation was done in triplicate and the mean value was reported. The percentage of weight loss of the samples was reported as volatile matter and calculated as follows:

$$\text{Volatile matter (\%)} = \frac{\text{Weight loss of dry sample}}{\text{Net weight of dry sample}} \times 100$$

3.3.5 Determination of fixed carbon

Fixed carbon content of MFDC and PGDC was determined by simple calculation as given in ASTM Test No. D-271-48. Fixed carbon was calculated as follows:

$$\text{Fixed carbon (on dry basis)(\%)} = 100 - [\text{volatile matter (\%)} + \text{ash (\%)}]$$

3.3.6 Higher heating value (HHV)

Gross calorific value (GCV) or Higher heating value (HHV) was determined using an auto bomb calorimeter (Changsha Kaiyuan Instruments Co, 5E-1AC/ML). About 1 g. of oven dried sample tablet was completely combusted in an adiabatic bomb containing 3.4 MPa pure oxygen under pressure.

3.3.7 Determination of net calorific value (NCV)

The NCV was calculated from the following equation [11]:

$$NCV = GCV \times \left(1 - \frac{w}{100}\right) - 2.444 \times \left(\frac{w}{100}\right) - 2.444 \times \left(\frac{H}{100}\right) \times 8.936 \times \left(1 - \frac{w}{100}\right); \left[\frac{MJ}{kg}\right]$$

Where 2.444=Enthalpy difference between gaseous and liquid water at 25°C.

$$8.936 = \frac{M_{H_2O}}{M_{H_2}}; \text{ i.e the molecular mass relation between } H_2O \text{ and } H_2$$

Where, NCV= Net calorific value

GCV= Gross calorific value

H= Concentration of hydrogen in biomass sample (wt.%)

w= Moisture content of biomass sample (wt.%)

3.3.8 Biochemical analysis of biomass samples

Cellulose, hemicellulose and lignin were determined by using the Fibertec I and M Systems (Foss AB, Denmark) as described by Van Soest [12]. This method is based on subsequent steps of chemical treatments to solubilise “non-fiber” components and final determination of the residue obtained. Before the determination of biochemical constituents, ground samples were extracted with acetone (100%) at 5°C and water at 60 – 70°C. Extractions were repeated several times. The residues were dried and used for the determination of acid detergent fiber (ADF), neutral detergent fiber (NDF) and acid detergent lignin (ADL).

As the first step, NDF was determined after treatment with a neutral detergent solution (sodium lauryl sulphate and EDTA), and the residue consisted of cellulose, hemicellulose and lignin. The next step was to determine ADF after treatment of the residue with an acid detergent solution (cetyltrimethylammonium bromide in sulphuric acid solution), the residue was cellulose and lignin. Finally, ADL was determined after initial treatment for ADF measurement followed by removal of the cellulose fraction through extraction using 72% H₂SO₄. This residue contains only lignin. A fraction of acid-soluble lignin and cellulose could be lost during this procedure. Acid-resistant residue was recovered by filtration on a glass crucible with an asbestos filter, carefully washed and dried at 70°C for 24 hours to constant weight. This acid insoluble residue is insoluble lignin (hereafter called 'lignin'). After weighing, the residue was ashed at 525 ± 25°C for at least 5 hours and lignin was calculated after correcting for mineral elements.

Simple subtraction rules were used to calculate cellulose and hemicelluloses: ADF – ADL = cellulose and NDF – ADF = hemicelluloses. The results for lignin, cellulose and hemicellulose were expressed as percentage of dry mass of biomass species (% dw). For each sample, the estimation was done in triplicate and the mean value was reported.

3.3.9 Determination of pH of biochar

pH of MFDC biochar was measured by method described by Kim *et al.* [13]. 10 g of biochar was mixed in 200 ml of deionized water followed by stirring (180 rpm) for 24 h. The supernatant was taken for measurement of pH by a digital pH meter (Inolab pH level 1, WTW, Germany).

3.3.10 Determination of acid sites

The Brønsted-acid sites in the zeolite catalysts were determined by the titration method described by Onda *et al.* [14]. Sodium hydroxide aqueous solution (0.01 mol/l, 20 ml) was added to a catalyst (0.040 g). The mixture was stirred for 2 hours at room

temperature. After centrifugal separation, the supernatant solution was titrated by a hydrochloric acid (0.01 mol L^{-1}) aqueous solution using phenolphthalein.

3.3.11 Total acid number

The total acid number determines the purity of the bio-oil and the presence of acidic and corrosive components in the aqueous sample. It is determined by the amount of potassium hydroxide (KOH) base required to neutralise the acid in 1 g of an oil sample. The standard unit of measure is mg KOH/g. Acid values of the bio-oils were determined as per ASTM D664. 0.2 – 0.5 g of oil was mixed with diethylether and the solution was titrated against 0.1M KOH using phenolphthalein as indicator. The acid value was determined as follows:

$$\text{Acid value} = \frac{\text{ml of } 0.1\text{M KOH consumed by sample} \times \text{Molarity of KOH} \times 56.1}{\text{Weight in grams of the sample}}$$

3.4 Kinetic modeling

The pyrolysis of biomass may be assumed to be represented by the following reaction scheme:

Biomass solid \longrightarrow volatiles + solid residues

The fraction of pyrolyzed biomass (conversion factor), α is defined by the following expression:

$$\alpha = \frac{(m_0 - m_t)}{(m_0 - m_\infty)} \quad (3.1)$$

where m_0 , m_t and m_∞ refer to the values of biomass at the beginning, at time t and at the end of the degradation event of interest, respectively.

The kinetic equation of common type can be written as:

$$\frac{d\alpha}{dt} = kf(\alpha) \quad (3.2)$$

Where $d\alpha/dt$ is degradation rate and it is a linear function of temperature dependent rate constant, k and $f(\alpha)$, a temperature-independent function of conversion which depends on reaction mechanism.

Replacing the rate constant with Arrhenius equation and introducing the non-isothermal condition, heating rate ($\beta = dT/dt$), Eq. 3.2 becomes:

$$\frac{d\alpha}{dt} = \frac{A}{\beta} e^{(E/RT)} f(\alpha) \quad (3.3)$$

where A is the pre-exponential factor, E is the activation energy, R is the gas constant ($8.314 \text{ J mol}^{-1} \text{ K}^{-1}$) and T is the absolute temperature.

Selecting n^{th} order reaction model in the light of a previously accomplished kinetics study in the literature [15] and rearranging, Eq. 3.3, becomes:

$$\frac{d\alpha}{(1-\alpha)^n} = \frac{A}{\beta} e^{(E/RT)} f(\alpha) \quad (3.4)$$

In this study, Eq. 3.4 is the fundamental expression used in model-fitting kinetic calculation methods on the basis of TG data.

3.4.1 Arrhenius method

The final rate equation of Arrhenius method can be obtained by taking the logarithm of Eq. 3.4 and making some rearrangements. It is given as follows:

$$\ln\left(\frac{d\alpha}{dt}\right) - n \ln(1-\alpha) = \ln\left(\frac{A}{\beta}\right) - \frac{E}{RT} \quad (3.5)$$

According to Eq. 3.5, the plot of $\ln(d\alpha/dt) - n \ln(1-\alpha)$ versus $1/T$ should give a straight line for the appropriate value of reaction order n . The activation energy and pre-exponential factor of each of the active pyrolysis stages were calculated from the related slope ($-E/R$) and interception $\ln(A/\beta)$ of final plots, respectively.

3.4.2 Coats–Redfern method

In Coats–Redfern method, the integral of Eq. 3.4 is taken, and the resulting exponential integral, which does not have an exact analytical solution is approximated using a Taylor series expansion. The obtained equation is simplified by considering $2RT/E \ll 1$ [16]. The final form is given as follows:

$$\ln g(\alpha) = -\frac{E}{RT} + \ln\left(\frac{AR}{\beta E}\right)$$

Where $g(\alpha) = -\ln(1-\alpha)/T^2$ if $n=1$; $g(\alpha) = (1-\alpha)^{1-n}/(1-n)T^2$ if $n \neq 1$.

In this method, a straight line should be obtained by plotting $\ln g(\alpha)$ versus $(1/T)$ if n is selected properly. The activation energy and pre-exponential factor of each active pyrolysis stage were determined from the slope $(-E/R)$ and the interception $\ln(AR/\beta E)$ of final plots, respectively.

3.4.3 FWO method

Iso-conversional methods do not require knowledge of reaction mechanism to calculate activation energy and for this reason, they are referred as model-free methods. The FWO method is an integral iso-conversional technique in which activation energy is related to heating rate and temperature at a constant conversion [17]. The equation is as follows:

$$\ln \beta = C_1 - (E/RT), \text{ where } C_1 \text{ is a constant}$$

Activation energy can be calculated from the slope of $\ln \beta$ versus $1/T$. Hence, the temperatures corresponding to the fixed values of conversion were measured at three different heating rates and necessary plots were drawn. Activation energy of active

pyrolysis stages were calculated from the slopes $(-E/R)$ of related plots at 0.1–0.9 conversion interval.

3.4.4 Global independent reactions model (Multilinear regression analysis method)

In this method, the parameters of the reaction kinetics were determined by using the procedure applied by Kumar, Vamvuka and Chouchene *et al.* [18-20]. Global kinetics of the vitalization reaction can be written as:

$$-\frac{dx}{dt} = kx^n \quad (3.6)$$

Where x is the sample weight, k the reaction constant and n , the order of the reaction. Applying the Arrhenius equation,

$$k = Ae^{-E/RT} \quad (3.7)$$

The combined form of the two equations 3.6 and 3.7 can be written in linear form as

$$\ln \left[\frac{-1}{m_0 - m_\infty} \frac{dm}{dt} \right] = \ln(A) - \left(\frac{E}{RT} \right) + n \ln \left(\frac{m - m_\infty}{m_0 - m_\infty} \right) \quad (3.8)$$

The parameters are described above.

Equation 3.8 is of the form

$$y = B + Cx + Dz$$

Where

$$y = \ln \left[\frac{-1}{m_0 - m_\infty} \frac{dm}{dt} \right], x = \frac{1}{T}, z = \ln \left(\frac{m - m_\infty}{m_0 - m_\infty} \right)$$

$$B = \ln(A), C = \left(-\frac{E}{R} \right), D = n$$

The constants B, C and D were estimated by multi-linear regression of the TGA data for each stage using Microsoft excel program.

3.4 Pyrolysis experiment

The pyrolysis experiments were performed on 10 g of the biomass samples in a lab scale fixed-bed tubular reactor with a length of 30 cm and an internal diameter of 2.47 cm equipped with a sweep gas (nitrogen) connection. The reactor was heated externally by an electric furnace, with the temperature being controlled by a Ni-Cr thermocouple which was placed in the center of pyrolysis reactor as shown in Figure 3.4. At the outlet of reactor, a condenser was attached to condense the vapours coming out of it. The condensed liquid was collected in a container at the end of condenser. The other important parts of the system are liquid collecting and condensing unit as shown in Figure 3.5(a). A 600W furnace with an inner volume large enough to contain the whole reactor was employed for heating. The yields of liquid products and char were determined by weighing. The amount of gas was determined by difference. The liquid product consisted of two phases; aqueous phase and organic phase [Fig. 3.5(b)]. The organic phase was extracted with equal quantity of diethyl ether. The obtained ether fraction (organic phase) was dried over anhydrous sodium sulfate, filtered and evaporated in a rotary evaporator at 30°C to remove diethyl ether. Then, this fraction was weighed, bottled and denoted as bio-oil in the present study.

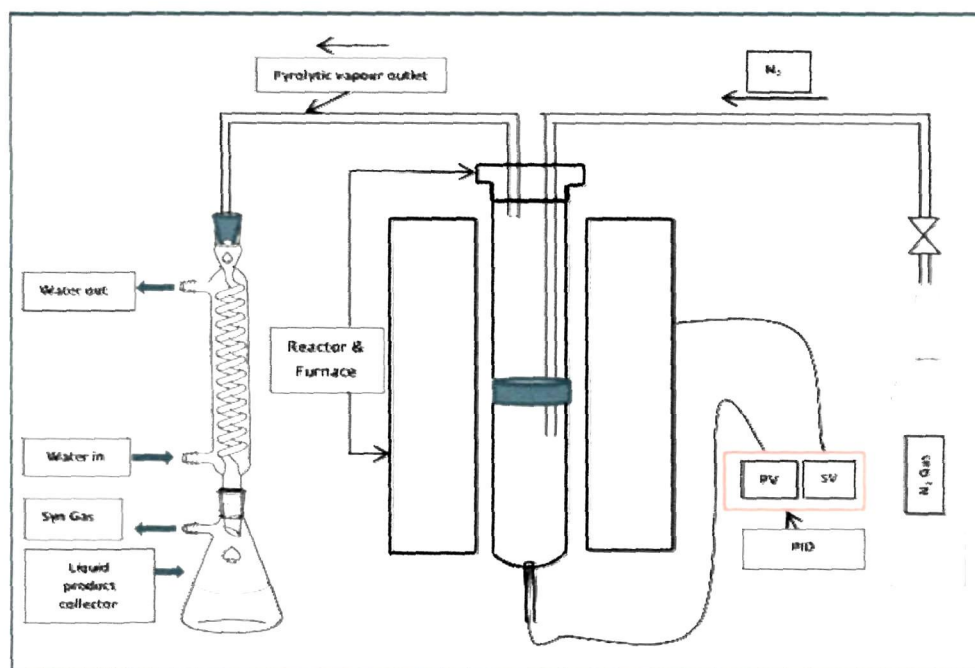


Figure 3.4: Schematic of pyrolysis experimental setup.

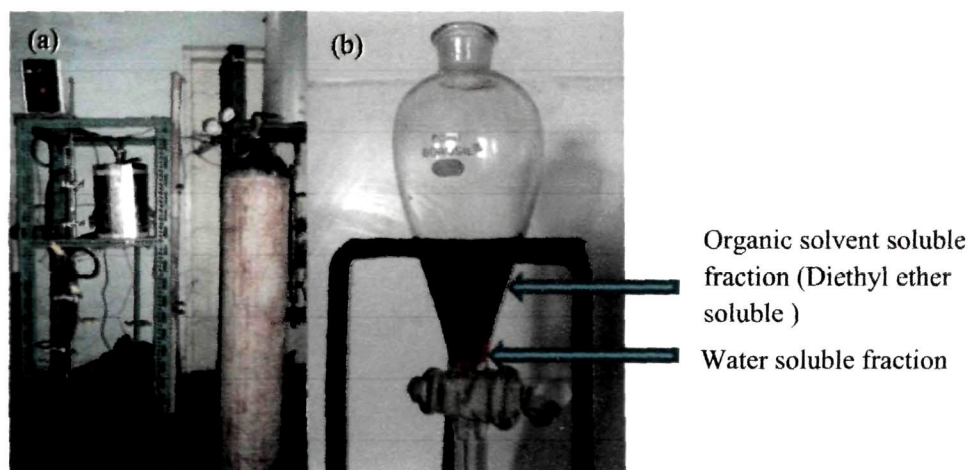


Figure 3.5: (a) Pyrolysis experimental setup (b) separation of pyrolytic liquid.

3.5.1 Non-catalytic pyrolysis

The non-catalytic pyrolysis experiments were performed on 10 g of biomass samples having particle size of 210 μ and 420 μ in the pyrolysis reactor described above. The pyrolysis experiments were carried out at temperature 350, 400, 450, 500 and 600°C with a heating rate of 10, 20 and 40°C/min.

3.5.2 Catalytic pyrolysis

The catalytic pyrolysis experiments were carried out with the conditions obtained from non catalytic pyrolysis experiments i.e. at 500°C and heating rate of 40°C/min. The particle size taken for this study was 420 μ . Three zeolite catalysts viz. HZSM-5, Y-zeolite and Mordenite were used in the experiment, obtained from Biofuels division, CSIR-Indian Institute of Petroleum, Dehradun.

Table 3.2: Catalysts properties

<i>Properties</i>	HZSM-5	Y zeolite	Mordenite
<i>Crystal structure</i>	Orthorhombic crystal Structure	Cubic crystal	Orthorhombic crystal structure
<i>Pore size</i>	Medium pore (10MR)	Large pore (12MR)	Large pore (12MR)
<i>Si/Al ratio</i>	30-40	5-8	10-20
<i>BET surface area</i>	>300 m ² /g	>300 m ² /g	> 300 m ² /g
<i>Acid sites (mmol/g)</i>	0.81	0.74	0.77

3.6 Instrumental characterization

Carbon, hydrogen and nitrogen of the biomass samples were determined by using elemental analyzer (PE 2400 C, H, N analyzer, Perkin Elmer). Chlorine and sulfur were not considered since they are known to be negligible for biomass samples as observed from literature [21]. Oxygen percentage was determined by difference.

The IR spectrum of the sample was recorded on a Nicolet IR spectrometer at room temperature ($26 \pm 2^\circ\text{C}$). A region in the spectral range of 4000 – 400 cm^{-1} was used for analysis.

The TG analysis of MFDC was measured by Pyris Diamond TG/DTA analyzer (PERKIN ELMER). The experiments were conducted non-isothermally at three different heating rates of 10, 20 and 40°C/min. A high purity N₂ gas (99.99%) was used as a carrier gas at a flow rate of 100 ml/min. In each experiment, a sample weighing approximately 4 – 8 mg was used. The tests were carried out from ambient temperature to 900°C.

The bio-oil selected for the NMR characterization was the one obtained at the pyrolysis conditions which gave the maximum bio-oil yield. ¹H and ¹³C NMR spectra were recorded in a 400 MHz NMR spectrophotometer (JEOL, JNM ECS) using deuterated chloroform (CDCl₃) as the internal standard and coupling constants are expressed in Hertz.

The chemical compounds present in the pyrolytic oil were analyzed using Perkin Elmer Clarus 680 GC/600C MS analyzer and details of the analysis conditions are given in Table 3.2.

Table 3.3: GC–MS analyzer details

<i>Instrument: Model</i>	<i>Perkin Elmer Clarus 680 GC/600C MS</i>	
<i>GC conditions:</i>		
<i>Column oven temperature</i>	70°C	
<i>Injection mode</i>	Split	
<i>Injection temperature</i>	200°C	
<i>Split ratio</i>	10:1	
<i>Carrier gas</i>	He	
<i>Column oven temperature progress:</i>		
<i>Heating rate</i>	Temperature	Hold time (min)
-	70°C	2
10°C/min	290°C	7 (31 min total)
<i>Column: DB -5</i>	60.0m x 250µm	
<i>MS condition</i>		
<i>Ion source temperature</i>	180°C	
<i>Interface temperature</i>	200°C	

The Brunauer-Emmett-Teller (BET) surface area and pore sizes were measured by the multipoint liquid N₂ adsorption – desorption method with ASAP® 2020 Accelerated Surface Area and Porosimetry Analyzer, at liquid nitrogen temperature (-196°C). Scanning Electron Microscopy (SEM) images were taken using Scanning Electron Microscope (Jeol 6390LV, Japan) operated at an accelerating voltage of 15kV. Images of MFDC and PGDC char were taken at 3000× magnifications. The powder X-ray were recorded on a Rigakuminiflex diffractometer (Cu-K α radiation, $\lambda = 1.5406 \text{ \AA}$) in 2θ range 10 – 70° at a scanning rate of 2°/min. Inorganic constituents of biochar were determined by using atomic absorption spectrometer (SOLAR, M6, Dual Zeeman, Thermo Electron, UK).

The SimDist analysis was carried out according to ASTM 2887. The capillary column was about 5m length, 530 μ internal diameter. The temperature conditions of the column oven and injector were set initially at either near ambient or sub-ambient (-25°C) and then programmed at a specified linear rate to a final temperature of about 400°C. Sub-ambient initial conditions are generally required to cover a wide boiling range of samples. Helium was used as a carrier gas. The detector signal was recorded as area slices (time intervals) for consecutive increasing retention times. SimDist software was used for data acquisition and results calculations.

3.7 Assessment of antimicrobial activity

3.7.1 Preparation of cultures

Escherichia coli MTCC723 and *Staphylococcus aureus* MTCC96 were collected from CSIR-Institute of Microbial Technology (IMTECH), Chandigarh, India. Fresh bacterial cultures (*S. aureus* and *E. coli*) were prepared by adding a loopful of stock culture to sterilized nutrient broth. The media was incubated at 37°C for 24 hours and used for accessing antibacterial activity. Fresh cultures of *Candida albicans* ATCC 183 and *Sachharomyces cerevisiae* ATCC 4126 were prepared by adding a loopful of stock culture to Potato Dextrose Broth (PDB) and YPD media respectively.

The former culture was incubated at 37°C (24 hours) and the later at 28°C (48 hours) respectively, for evaluating antiyeast and antifungal activity.

3.7.2 Agar well diffusion method

The antimicrobial assay was done by using the agar well diffusion method. The assay was carried out to find out if the thermally converted products (TCP) had any antimicrobial activity. Microbial cultures were adjusted to 0.5 McFarland standards before the tests. The media used for antibacterial assay was Muller Hinton Agar, whereas PDB and YPD media were used to access the antifungal and antiyeast activity. The standard solutions of the samples (MFDC and PGDC bio-oil) were 500 µg/ml DMSO. The sterile liquid culture media (25ml) was poured into petriplates and after solidification were inoculated by spread plate method with an inoculum corresponding to 0.5 McFarland standards. Three (3) wells of 5 mm diameter were punched into the agar with the help of a sterilized well puncturer (5 mm diameter) and 50 µl of the sample was added to the sample well. Chloramphenicol (30µg/ml) was used as the positive control for antibacterial assay, whereas Indofil M-45, a commercial fungicide was used as the positive control for antifungal and antiyeast assay. 1% DMSO was used as the negative control for all the tests. The plates were then sealed with paraffin and kept for incubation at 37°C for 24 hours (for *S. aureus*, *E. coli* and *S. cerevisiae*) and 28°C for 48 hours (for *C. albicans*). The antimicrobial activity was evaluated by measuring the ZOI diameter observed using zone scale (Antibiotic Zone Scale, HIMEDIA). The tests were carried out in triplicates and only the mean values are reported.

3.7.3 Determination of minimum inhibitory concentration (MIC)

MIC was determined following the protocol of Wang *et al.* [22] with slight modification. The MIC activity was determined using a 96-well microtitre plate. The stock solutions for the sample oil were (200 µl/ml DMSO) for BMFR and BPGR, whereas (100 µl/ml DMSO) for BMR. 10 ml culture of *E. coli* and *S.aureus* were

prepared in LB broth, whereas the same amount of culture of *C. albicans* and *S. cerevisiae* were prepared in PDB and YPD broth respectively. Saturated cultures of all the four strains were then diluted to form an approximately 1×10^6 colony forming units (CFU)/ml. In the 1st well, 200 μ l of stock solution was added and serially diluted (8 fold) by adding the respective culture media. Following this 100 μ l of culture was added to the respective wells. Kanamycin (50 mg/ml) was used as the positive control for bacteria, whereas Indofil (50 mg/ml, commercial fungicide) as the positive control for *C. albicans* and *S. cerevisiae*. DMSO (1%) was used as negative control for all the test samples. The plates were covered and incubated overnight at 37°C (for *S. aureus* and *E. coli*), and 28°C for 48 hours (for *C. albicans* and *S. cerevisiae*). At the end of the incubation period, 40 μ L of MTT solution (0.2 mg/ml) was added into each well and then further incubated at 37°C for 45 minutes. The culture absorbance was recorded at 570 nm.

3.7.4 Statistical analysis

The following statistical analysis was performed to investigate the significant difference of antimicrobial activity of MFDC and PGDC bio-oil on different microorganisms. The two-sample t-test is used to determine if two population means are equal [23]. The two-sample t-test for unpaired data:

Test statistics,

$$t = \frac{\bar{x}_1 - \bar{x}_2}{\sqrt{\frac{s_1^2}{n_1} + \frac{s_2^2}{n_2}}}$$

Where n_1 and n_2 are sample size, \bar{x}_1 and \bar{x}_2 are sample mean and s_1 and s_2 are sample variances.

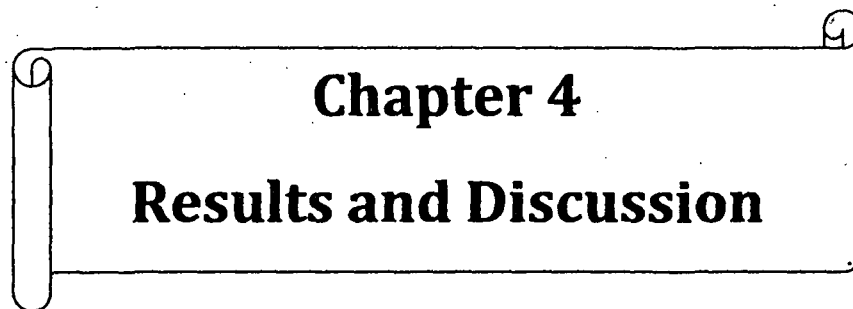
If equal variances are assumed, then the formula reduces to

$$t = \frac{\bar{x}_1 - \bar{x}_2}{s_p \sqrt{\frac{1}{n_1} + \frac{1}{n_2}}} \quad \text{where, } s_p = \sqrt{\frac{(n_1-1)s_1^2 + (n_2-1)s_2^2}{n_1 + n_2 - 2}}$$

References

- [1] Sarma, A.K. & Konwer, D. Feasibility Studies for Conventional Refinery Distillation with a (1:1) w/w of a Biocrude Blend with Petroleum Crude Oil. *Energy & Fuels*, **19** (4), 1755-1758, 2005.
- [2] Scott, P.T., et al. *Pongamia pinnata*: An Untapped Resource for the Biofuels Industry of the Future. *Bioenergy Research*, **1** (1), 2-11, 2008.
- [3] Chopade V.V, et al. *Pongamia pinnata*: phytochemical constituents, traditional uses and pharmacological properties: a review. *International Journal of Green Pharmacy*, **2** 72-75, 2008.
- [4] Kesari, V. & Rangan, L. Development of *Pongamia pinnata* as an alternative biofuel crop — current status and scope of plantations in India. *Journal of Crop Science and Biotechnology*, **13** (3), 127-137, 2010.
- [5] Planning commission, Govt. of India. Report of the committee on development of biofuel. http://planningcommission.nic.in/reports/genrep/cmtt_bio.pdf, 23/05/2010.
- [6] Karmee, S.K. & Chadha, A. Preparation of biodiesel from crude oil of *Pongamia pinnata*. *Bioresource Technology*, **96** (13), 1425-9, 2005.
- [7] Sarma, A.K. *Biodiesel Production from Mesua ferrea L. (Nahor) and Pongamia glabra vent. (Koroch) Seed Oil*, Ph.D Thesis, Tezpur University at Dept. of Energy, India, 2006.
- [8] Naik, M., et al. Production of biodiesel from high free fatty acid Karanja (*Pongamia pinnata*) oil. *Biomass and Bioenergy*, **32** (4), 354-357, 2008.
- [9] Sarma, A.K., Konwer, D., & Bordoloi, P.K. A Comprehensive Analysis of Fuel Properties of Biodiesel from Koroch Seed Oil. *Energy & Fuels*, **19** (2), 656-657, 2005.
- [10] Konwer, D., et al. Liquid fuels from *Mesua ferrea L.* seed oil. *Journal of the American Oil Chemists Society*, **66** (2), 223-226, 1989.
- [11] Koppejan, J. & van van Loo, S., *The Handbook of Biomass Combustion and Co-firing*, Taylor & Francis, 2012.

- [12] Van Soest, P.J., *Nutritional Ecology of the Ruminant*, Comstock Pub., 1994.
- [13] Kim, P., et al. Surface functionality and carbon structures in lignocellulosic-derived biochars produced by fast pyrolysis. *Energy & Fuels*, **25** (10), 4693-4703, 2011.
- [14] Onda, A., Ochi, T., & Yanagisawa, K. Selective hydrolysis of cellulose into glucose over solid acid catalysts. *Green Chemistry*, **10** (10), 1033-1037, 2008.
- [15] Açıkalm, K. Pyrolytic characteristics and kinetics of pistachio shell by thermogravimetric analysis. *Journal of Thermal Analysis and Calorimetry*, **109** (1), 227-235, 2011.
- [16] Vlaev, L.T., Markovska, I.G., & Lyubchev, L.A. Non-isothermal kinetics of pyrolysis of rice husk. *Thermochimica Acta*, **406** (1-2), 1-7, 2003.
- [17] Hu, S., Jess, A., & Xu, M.H. Kinetic study of Chinese biomass slow pyrolysis: Comparison of different kinetic models. *Fuel*, **86** (17-18), 2778-2788, 2007.
- [18] Kumar, A., et al. Thermogravimetric characterization of corn stover as gasification and pyrolysis feedstock. *Biomass and Bioenergy*, **32** (5), 460-467, 2008.
- [19] Vamvuka, D., et al. Pyrolysis characteristics and kinetics of biomass residuals mixtures with lignite. *Fuel*, **82** (15-17), 1949-1960, 2003.
- [20] Chouchene, A., et al. Thermal degradation of olive solid waste: Influence of particle size and oxygen concentration. *Resources, Conservation and Recycling*, **54** (5), 271-277, 2010.
- [21] Vassilev, S.V., et al. An overview of the chemical composition of biomass. *Fuel*, **89** (5), 913-933, 2010.
- [22] Wang, J.L., et al. Nosocomial methicillin-resistant *Staphylococcus aureus* (MRSA) bacteremia in Taiwan: mortality analyses and the impact of vancomycin, MIC = 2 mg/L, by the broth microdilution method. *BMC Infectious Diseases* **10** 159, 2010.
- [23] Snedecor, G.W. & Cochran, W.G., *Statistical Methods*, Wiley, 1991.



Chapter 4
Results and Discussion

4-1.1 Physico-chemical and thermal decomposition studies of MFDC and PGDC

Each type of biomass has specific properties that determine its performance and reactivity during the conversion processes. Therefore, a fundamental characterization of biomass as a feedstock is necessary for bio-fuel and chemical production, which exhibit very different properties with respect to traditional fossil fuels and their derivatives. Particularly, ligno-cellulosic materials are more reactive and have a higher volatility than coals and the volatile matter concentration differs greatly for different types of biomass, even the same type of biomass can have different composition based on the climatic conditions and seasonal variation [1]. Furthermore, characterization of biomass is essential as the composition and properties of biomass affects the conversion process differently. Also, from the information of feedstock composition, thermal behavior in conversion processes can be known, yield can be predicted, and mathematical models can be created to make biomass conversion more efficient, effective and better competitive with fossil fuel production. In this regard, the characterization of MFDC and PGDC as a bioenergy feedstock is taken into consideration in the present investigation.

Table 4.1 shows the biomass properties of MFDC and PGDC with their average characteristic composition. Moisture content of the feedstock has a marked effect on the conversion efficiency of pyrolysis processes, its energy content and the product yield. It has been reported that to ensure rapid heat transfer rates in a pyrolysis reactor, the moisture content should be less than 10 wt.% [2]. In this regard, MFDC and PGDC biomass with moisture content of 4.1% and 6.8% respectively seems to be suitable for thermal conversion. The inorganic component (ash content) of biomass affects both the handling and processing costs of overall biomass energy conversion. The ash content of the deoiled cakes of MFDC and PGDC were found to be 4.8% and 4.2%. Low ash content in both the deoiled

cakes as compared to other feedstocks used for pyrolysis process such as rice husk (12.4%) [3], Oat straw (17.3%) [4] and rice straw (15.4%) [5] is an indicator that both MFDC and PGDC have the potentiality to be a suitable candidate for thermochemical conversion processes. The volatile matter content was found to be 83.6% and 73.6% for MFDC and PGDC respectively. The high amount of volatile matter strongly influences its combustion behavior and thermal decomposition and thus, suggests good potential of the present feedstock for energy production by pyrolysis and gasification [6]. The fixed carbon content was 8.5% for MFDC and 13.3% for PGDC biomass. The elemental content of carbon, hydrogen, oxygen and nitrogen was found to be 48.6, 7.4, 40.3 and 3.7 % and 43.7, 6.6, 46.5 and 3.2 % in MFDC and PGDC respectively. Higher value of hydrogen and oxygen compared with carbon reduces the energy value of MFDC and PGDC as compared to fossil fuel due to lower energy contained in carbon-oxygen and carbon-hydrogen bonds than in carbon-carbon bonds [7]. The GCV and NCV for MFDC were 18.7 and 16.3 MJ/kg and for PGDC the values were 16.9 MJ/kg and 14.3 MJ/kg respectively. The empirical formula of MFDC is $C_{15.58}H_{28.38}NO_{9.69}$ and PGDC is $C_{15.82}H_{28.52}NO_{12.6}$. The H/C and O/C molar ratios were calculated from elemental composition as 1.8 and 0.6 and 1.8 and 0.8 for MFDC and PGDC, respectively. PGDC biomass has less heating value than MFDC biomass and this could be attributed to the higher O/C ratio of PGDC than MFDC biomass. The compositional analysis is very essential for biomass to be used as a feedstock for pyrolysis system because the pyrolytic product distribution entirely depends upon the three major building blocks of biomass i.e., cellulose, hemicellulose and lignin as described in chapter 2. The cellulose, hemicellulose and lignin contents were found to be 56.9, 29.0 and 14.1% for MFDC and 59.3, 28.4 and 12.3% for PGDC biomass (Table 4.1).

Table 4.1: Properties of MFDC and PGDC biomass

Properties	MFDC	PGDC	
Gross calorific value (MJ/Kg)	18.68	16.95	
Net calorific value (MJ/Kg)	16.28	14.29	
Empirical formulae (on ash free basis)	C _{15.58} H _{28.38} NO _{9.69}	C _{15.82} H _{28.52} NO _{12.6}	
H/C molar ratio (on ash free basis)	1.82	1.80	
O/C molar ratio (on ash free basis)	0.62	0.79	
Elemental analysis, wt.%	Carbon	48.63	43.69
	Hydrogen	7.38	6.56
	Nitrogen	3.65	3.23
	Oxygen (by difference)	40.34	46.52
Proximate analysis, wt.%	Moisture	4.08 ± 0.27	6.8 ± 0.35
	Volatile matter	82.63 ± 0.66	73.59 ± 0.40
	Fixed carbon	8.46 ± 0.54	13.29 ± 0.59
	Ash	4.82 ± 0.47	4.16 ± 0.19
Composition analysis, wt.%	Cellulose	56.91 ± 0.67	59.3 ± 0.54
	Hemicellulose	29 ± 0.49	28.4 ± 0.53
	Lignin	14.09 ± 0.51	12.3 ± 0.36

The FTIR spectrum of MFDC and PGDC biomass on the infrared region are shown in the Figure 4.1. The large band in the region of 3600 – 3100 cm⁻¹ is characteristic of polymeric involvement of hydroxyl groups and the bonded O-H stretching vibration present in carbohydrates (hemicellulose + cellulose) and lignin [8]. This peak appeared at 3425 and 3413 cm⁻¹ for MFDC and PGDC respectively. CH₂ stretching vibrations in the range of 3100 – 2800 cm⁻¹ implies the presence of lipid [9]. The absorption at 2921 cm⁻¹ for both MFDC and PGDC biomass implies CH₂ asymmetric stretching in lipid (a small quantum of lipid is traceable in the deoiled cake by FTIR spectroscopy since mechanical expeller was used for lipid extraction). The region between 1800 and 1500 cm⁻¹ demonstrate characteristic bands for proteins, whereas 1700 – 1600 cm⁻¹ is precise for amide-I bands [10], which is mainly due to C=O stretching vibrations of peptide bond [11]. The bands

in the amide I region provide insight into the protein secondary structure, whereas the region from 1600 to 1500 cm^{-1} is specific for amide-II bands, which is due to N-H bending vibrations [12]. The region from 1200 to 900 cm^{-1} are chiefly dominated by a sequence of bands due to C-O, C-C, C-O-C and C-O-P stretching vibrations of polysaccharides [13-15] and CH_3 , CH_2 rocking modes. The absorption at 1638 cm^{-1} implies the presence of C=O of carboxylic acid and derivatives. The O-H stretching band at 3324 cm^{-1} , C-H stretching bands in the region of 1500-1300 cm^{-1} and a C-O stretching band at 1034 cm^{-1} are attributed to the presence of cellulosic structure [9].

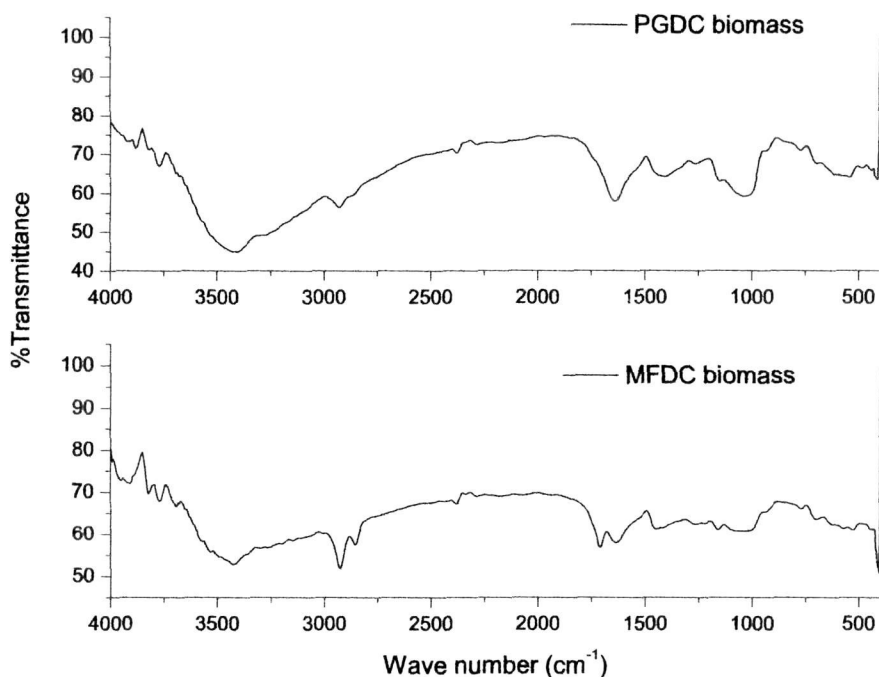


Figure 4.1: FTIR spectra of PGDC and MFDC biomass.

4-1.1.1 Thermal degradation behavior of MFDC biomass

Thermogravimetric analysis (TGA) is an extensively used technique to study the reaction kinetics for pyrolysis process because of its simplicity and retrieval of a host of valuable information from a thermogram [16]. Several methods leading to the determination of the kinetic parameters (E , A , n) are available in the literature [17-19]. These can be classified into three categories: differential, integral and special methods. Differential methods require data for both mass loss and rate of mass loss while integral methods are based on the mass loss data. Special methods are generally based on particular couples of experimental data, e.g. data from different heating rates, or they need data evaluated from graphical plots.

The TG and DTG curves for heating rates of 10, 20 and 40°C/min are shown in Figures 4.2 and 4.3. As shown in Figure 4.3, the entire pyrolysis process can be divided into four stages since every single slope change on a TG curve indicates the beginning of a new stage.

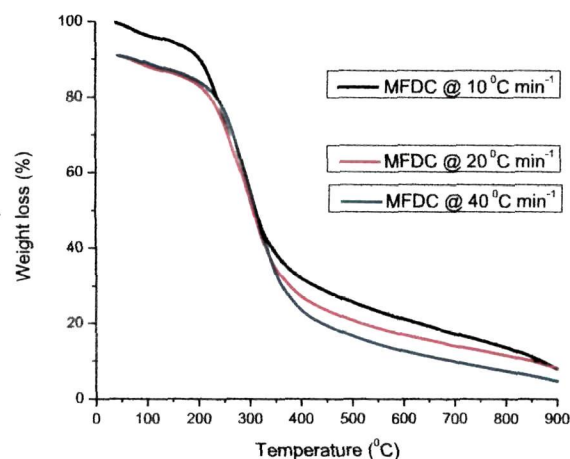


Figure 4.2: TG Profile of MFDC at different heating rates.

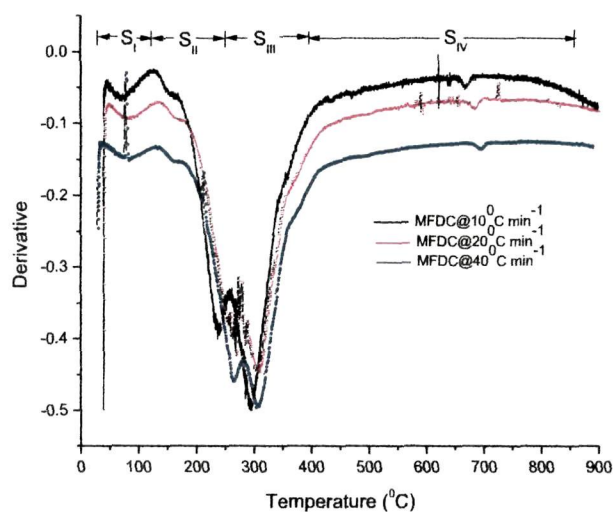


Figure 4.3: DTG Profile of MFDC at different heating rates.

Considering the TG/DTG curves (Figure 4.2, 4.3) obtained at 10°C/min, the following observations (Table 4.2) can be listed:

- (a) The first stage (S_I) starts at 39°C and finishes at 130°C. The weight loss occurred at this stage was 4.6%, and could be attributed to exclusion of

physically absorbed water in the biomass and/or external water. Stage S_I is depicted by the left most weak peak in the DTG curve.

- (b) The second stage (S_{II}) starts at 130°C and finishes at 254°C with a mass loss of 21.7%. From the DTG curve, it is seen that maximum mass loss rate occurred at 238°C. This stage can be referred to as active pyrolysis stage since weight loss rate is high.
- (c) The third stage (S_{III}) begins at 260°C and finishes at 383°C. This stage shows a mass loss of 37.9% with a mass loss rate of 4.1% min⁻¹. In view of its high mass loss rate, this stage can also be referred to as stage of active pyrolysis.
- (d) The fourth stage (S_{IV}) starts at 383°C and continues up to 900°C. Weight loss occurred in this stage was 25.9% and it can be referred to as zone of passive pyrolysis since mass loss rate is much lower compared to S_{II} & S_{III} .

The characteristics temperatures such as starting temperature (T_{onset}), ending temperature (T_{end}), the temperature where maximum mass loss rate occurred (T_{max}) and maximum mass loss rate (W_{max}) related to active pyrolysis stages (S_{II} and S_{III}) were determined for all the heating rates applied, and their values are given in Table 4.2.

Table 4.2 Properties of active pyrolysis stages for MFDC

Heating rate (°C/min)	S_{II}				S_{III}			
	T_{onset} (°C)	T_{max} (°C)	T_{end} (°C)	W_{max} (%/min)	T_{onset} (°C)	T_{max} (°C)	T_{end} (°C)	W_{max} (%/min)
10	130	238	254	1.46	260	291	383	4.05
20	139	261	271	3.18	279	304	409	8.41
40	156	272	288	6.89	291	316	420	19.18

It can be observed from the table that all characteristic temperatures were laterally shifted to higher temperature values with increasing heating rate. This could be due to reduced efficiency of heat transfer at higher heating rate than the efficiency at lower heating rate. At lower heating rates, heating of biomass particles occurs

more gradually leading to an improved and more effective heat transfer to the inner portions and among the particles [20]. The maximum mass loss rates were also shifted to higher temperatures with increasing heating rate as a consequence of the increasing effect of the inertia of the devolatilization process with the decrease in characteristic time of the process [21].

Table 4.3 Kinetic parameters for MFDC calculated by Arrhenius, Coats-Redfern and multilinear regression analysis method

(°C/min)	Stage	E (kJ/mol)	Log A (min ⁻¹)	Plot equation	R ²	n
Arrhenius method						
10	S _{II}	58.70	4.94	y = -7060.4x + 9.08	0.96	1.5
	S _{III}	98.23	8.53	y = -11816x + 17.34	0.99	1.9
20	S _{II}	52.32	4.89	y = -6293.2x + 8.25	0.95	0.5
	S _{III}	158.63	14.30	y = -19080x + 29.95	0.98	1.6
40	S _{II}	51.34	4.88	y = -6175.6x + 7.55	0.93	0.5
	S _{III}	251.79	22.44	y = -30286x + 47.99	0.90	1.9
Average	S _{II}	54.12	4.90			1.32
	S _{III}	169.55	15.09			
Coats & Redfern method						
10	S _{II}	72.04	4.05	y = -8665.2x + 4.86	0.97	1.1
	S _{III}	154.35	10.60	y = -18565x + 19.19	0.93	0.8
20	S _{II}	58.38	2.46	y = -7021.3x + 0.716	0.99	0.6
	S _{III}	274.12	21.80	y = -32971x + 43.72	0.94	0.7
40	S _{II}	61.74	2.93	y = -7435.6x + 1.05	0.97	0.6
	S _{III}	329.20	26.65	y = -39596x + 54.00	0.92	0.6
Average	S _{II}	64.08	3.14			0.73
	S _{III}	252.56	19.68			
Multi-linear regression method						
10	S _{II}	44.18	17.01		0.99	1.01
	S _{III}	212.60	2.37		0.99	0.96
20	S _{II}	40.40	14.98		0.98	0.45
	S _{III}	253.87	16.69		0.99	1.08
40	S _{II}	46.72	15.06		0.95	0.84
	S _{III}	303.98	17.67		0.96	1.46
Average	S _{II}	43.77				0.97
	S _{III}	256.82				

The values of kinetic parameter calculated on the basis of three methods are tabulated in Table 4.3. It is clear from the table that heating rate has a great influence on activation energy in thermogravimetric decomposition process. In active pyrolysis stages, the calculated activation energy values exhibited almost the same behavior with the changes in heating rate. In stage S_{II}, increasing heating rate from 10 to 20°C/min resulted in an increase, but further increase of heating rate to 40°C/min led to a decrease in activation energy values for Coats–Redfern and Global independent reactions model while a gradual decrease for Arrhenius method is observed as the heating rate is increased from 10 to 40°C/min.

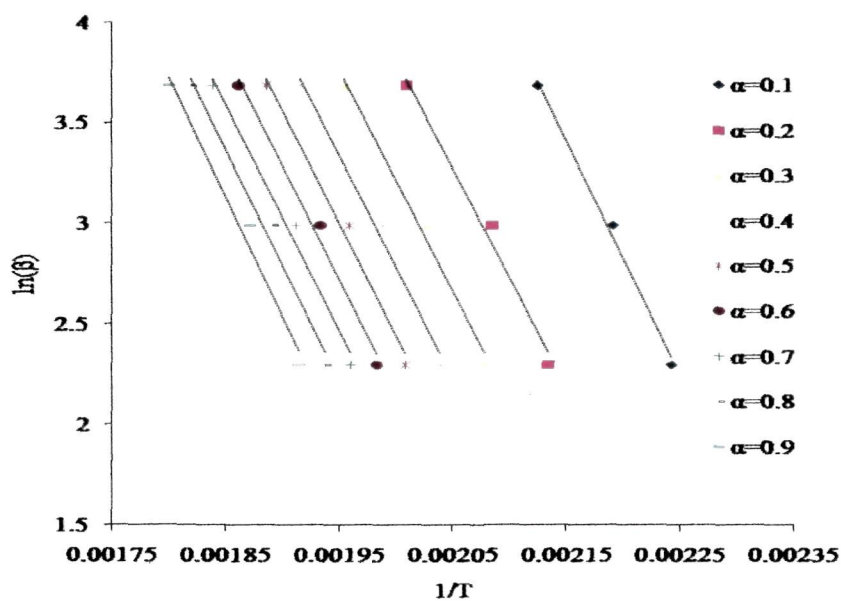


Figure 4.4: Plots obtained by FWO method for determination of activation energy of MFDC at S_{II}.

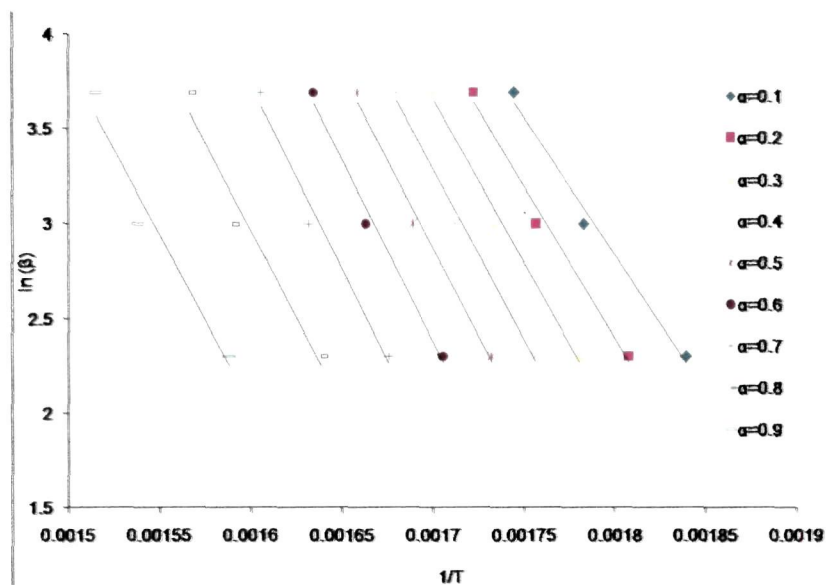


Figure 4.5: Plots obtained by FWO method for determination of activation energy of MFDC at S_{III} .

Table 4.4 Activation energy for MFDC calculated by FWO method (kJ/mol)

Stage	Conversion degree (%)									Average
	10	20	30	40	50	60	70	80	90	
S_{II}	97.47	90.15	91.51	92.48	93.27	94.16	93.49	95.44	98.18	94.02
S_{III}	120.55	132.43	142.62	149.93	154.81	158.79	160.34	153.64	149.79	146.98

On the other hand, in S_{III} , activation energy showed a continuous increase with increasing heating rate from 10 to 40°C/min for all the methods applied. Thus, it would be more convenient to compare the results on average basis (average of the results obtained at different heating rates). The average activation energy of stage S_{II} was calculated as 54.1, 64.1 and 43.8 kJ/mol by Arrhenius, Coats–Redfern and Global independent reactions model, respectively. The results obtained in this study shows a good agreement with the result obtained from the kinetic study of pistachio shell [22]. Figures 4.4 and 4.5 show the plots obtained by FWO method for determination of activation energy of MFDC at S_{II} and S_{III} respectively. The

model-free FWO method yielded 94 kJ/mol in the 0.1 – 0.9 conversion interval (Table 4.4). In this stage, the results were almost closer for all the methods applied for calculation. For S_{III} , the average activation energy was calculated as 169.6, 252.6, 146.9 and 256.8 kJ/mol by Arrhenius, Coats–Redfern, FWO and Global independent reactions model respectively. In S_{III} , results obtained from Coats–Redfern and Global independent reactions model are much closer than the result obtained from Arrhenius and FWO methods. The variation encountered in this study can be generally attributed to the approximations of the method used for determination of kinetic parameters. From this study, it was also observed that the activation energy at S_{III} was always higher than S_{II} as these two stages are characteristic of hemicellulose and cellulose decomposition and it is also well known that cellulose is thermally more stable than hemicellulose. The present findings on kinetic parameters of MFDC mostly agree with the findings of Tonbul [23].

4-1.1.2 Thermal degradation behavior of PGDC biomass

The TG and DTG curves for heating rates of 10, 20 and 40°C/min for PGDC biomass are shown in Figures 4.6 and 4.7. As discussed in the previous section, the entire pyrolysis process can be divided into four stages.

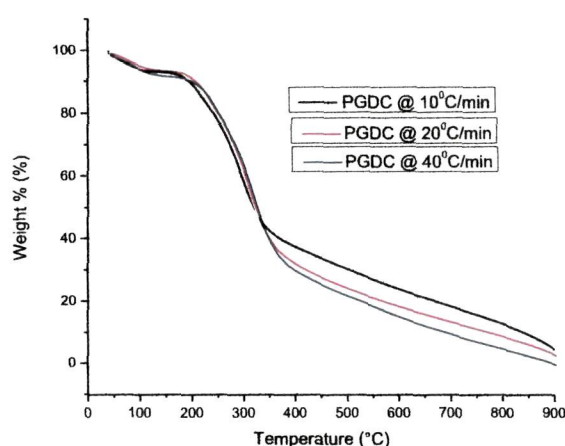


Figure 4.6: TG profile of PGDC at different heating rates.

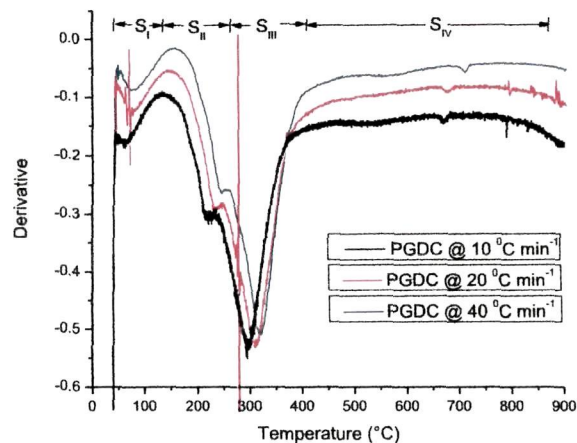


Figure 4.7: DTG profile of PGDC at different heating rates.

The characteristics temperatures as mentioned in the previous section related to active pyrolysis stages (S_{II} and S_{III}) were determined for all the heating rates applied, and their values are given in Table 4.5. It can be observed from the table that all characteristic temperatures were laterally shifted to higher temperature values with increasing heating rate as in the case of thermal degradation of MFDC biomass described in the previous section. The maximum mass loss rates were also shifted to higher temperatures with increasing heating rate as a consequence of the increasing effect of the inertia of the devolatilization process with the decrease in characteristic time of the process [21].

Table 4.5 Properties of active pyrolysis stages for PGDC

Heating rate (°C/min)	S_{II}				S_{III}			
	T_{onset} (°C)	T_{max} (°C)	T_{end} (°C)	W_{max} (%/min)	T_{onset} (°C)	T_{max} (°C)	T_{end} (°C)	W_{max} (%/min)
10	144	212	216	0.94	235	297	368	3.51
20	151	225	228	2.01	250	310	372	7.14
40	160	233	238	4.32	252	314	393	14.36

The kinetic parameter values calculated for PGDC biomass on the basis of three methods are tabulated in Table 4.6. The non-uniformity of rise and fall of

activation energies in response to different heating rates applied makes sense to compare the results on an average basis (average of the results obtained at different heating rates). The average activation energy of stage S_{II} was calculated as 91.7, 127.7 and 76.1 kJ/mol by Arrhenius, Coats–Redfern and Global independent reactions model, respectively. The results from this study are in good agreement with the result obtained elsewhere [22].

The plots obtained by FWO method for PGDC are shown in Figures 4.8 and 4.9. The model-free FWO method yielded 130.8 kJ/mol in the 0.1 – 0.9 conversion interval (Table 4.7). In this stage, the results were almost closer for all the methods applied for calculation. For S_{III}, the average activation energy was calculated as 96.6, 128.7, 76.1 and 193.2 kJ/mol by Arrhenius, Coats–Redfern, Global independent reactions model and FWO methods, respectively.

Table 4.6 Kinetic parameters for PGDC calculated by Arrhenius, Coats-Redfern and multilinear regression analysis method

(°C/min)	Stage	E (kJ/mol)	Log A (min ⁻¹)	Plot equation	R ²	n
Arrhenius method						
10	S _{II}	88.88	8.99	y = -10690x + 18.42	0.99	0.9
	S _{III}	83.56	7.16	y = -10050x + 14.18	0.91	1.2
20	S _{II}	93.55	9.97	y = -11252x + 19.97	0.96	0.5
	S _{III}	111.12	9.90	y = -13366x + 19.81	0.86	1.4
40	S _{II}	92.74	9.99	y = -11155x + 19.31	0.94	0.5
	S _{III}	95.19	8.57	y = -11449x + 16.04	0.89	1.3
Average	S _{II}	91.72	9.65			0.97
	S _{III}	96.62	8.54			
Coats & Redfern method						
10	S _{II}	125.08	10.58	y = -15045x + 19.34	0.96	0.9
	S _{III}	127.00	8.31	y = -15276x + 14.10	0.96	1.7
20	S _{II}	133.82	11.61	y = -16096x + 20.95	0.96	1.3
	S _{III}	132.53	8.84	y = -15940x + 14.59	0.95	1.6
40	S _{II}	124.28	10.46	y = -14948x + 17.70	0.95	0.8
	S _{III}	126.61	8.47	y = -15229x + 13.10	0.96	1.7
Average	S _{II}	127.73	10.88			1.3
	S _{III}	128.71	8.54			

Table contd...

Multi-linear regression method					
10	S _{II}	78.18	17.01	0.97	1.21
	S _{III}	212.60	2.37	0.99	0.93
20	S _{II}	63.40	14.98	0.97	0.67
	S _{III}	253.87	16.69	0.99	1.13
40	S _{II}	86.72	15.06	0.95	0.76
	S _{III}	303.98	17.67	0.98	1.59
Average	S _{II}	76.10	15.68		1.04
	S _{III}	256.82	12.24		

In S_{III}, results obtained from Arrhenius and Coats-Redfern methods are closer than the result obtained from Global Independent Reactions Model and FWO method. The variation encountered in this study can be generally attributed to the approximations of the method used for determination of kinetic parameters as discussed earlier. From this study, it was also observed that the activation energy at S_{III} was always higher than S_{II} as comparatively thermally stable cellulose is degraded in the S_{III} region while S_{II} region marks degradation of hemicellulose. The same observation was also found in MFDC thermal degradation behavior. The present findings on kinetic parameters of PGDC mostly agree with the findings of Tonbul [23].

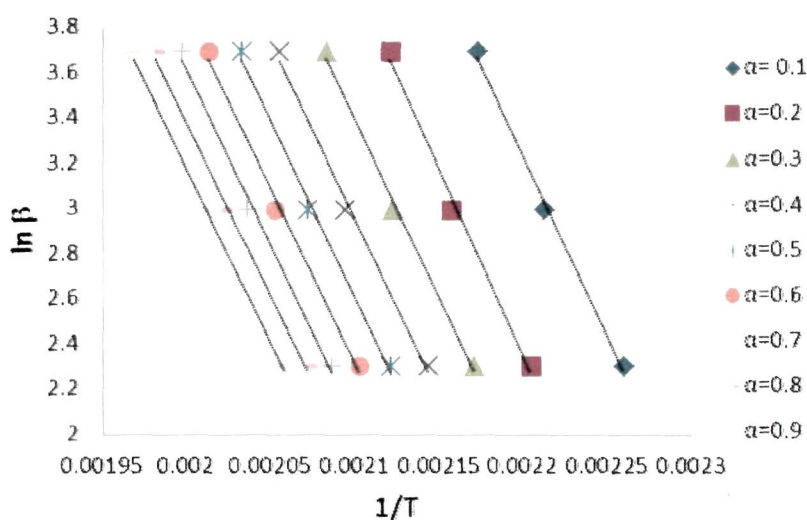


Figure 4.8: Plots obtained by FWO method for determination of activation energy of PGDC at S_{II}.

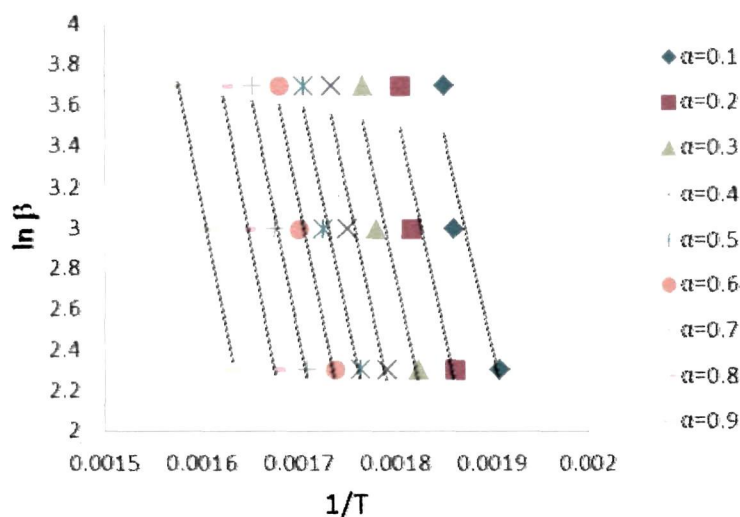


Figure 4.9: Plots obtained by FWO method for determination of activation energy of PGDC at S_{III}.

Table 4.7: Activation energy for PGDC calculated by FWO method (kJ/mol)

Stage	Conversion degree (%)									Average
	10	20	30	40	50	60	70	80	90	
S _{II}	132.37	136.93	131.39	129.76	129.96	129.46	130.18	128.12	128.54	130.75
S _{III}	173.13	183.62	185.39	189.30	189.88	198.18	201.66	212.08	205.31	193.17

4-1.2 Pyrolysis of MFDC and PGDC

Pyrolysis of MFDC and PGDC was carried out in a fixed bed tubular reactor at different terminal temperatures of 350, 400, 450, 500 and 600°C at heating rates of 10, 20 and 40°C/min. The experiments were carried out in order to observe the effect of the pyrolysis temperature, heating rate and particle size on pyrolysis yields with particle sizes of 210 and 420 μ. Experimental apparatus was held at adjusted temperature either for a minimum of 30 min or until no further significant release of gas was observed.

4-1.2.1 Influence of pyrolysis parameters on product yields of MFDC pyrolysis

Different parameters influence pyrolysis process as discussed in chapter 2. In the present study, the effect of temperature, heating rate and particle size on pyrolysis product yield was investigated. Figures 4.10, 4.11 and 4.12 show the influence of pyrolysis temperature and heating rate on the liquid, solid and gaseous product yield of MFDC pyrolysis process.

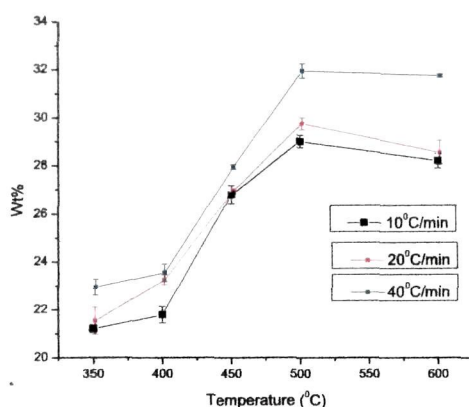


Figure 4.10: Effect of temperature and heating rate on liquid product yield of MFDC pyrolysis.

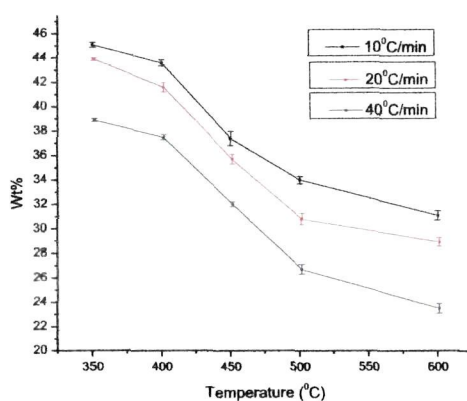


Figure 4.11: Effect of temperature and heating rate on solid product yield of MFDC pyrolysis.

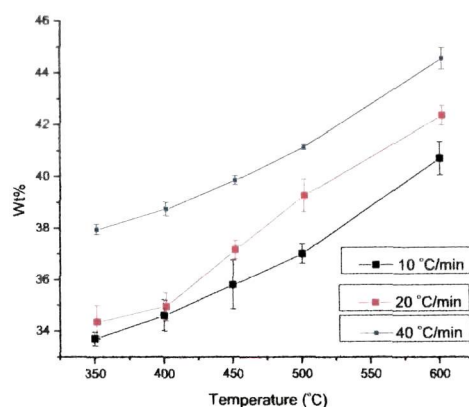


Figure 4.12: Effect of temperature and heating rate on gaseous product yield of MFDC pyrolysis.

Table 4.8: Products distribution of pyrolysis of MFDC

10 °C/min				
Temperature (°C)	Biochar (%)	Bio-oil (organic solvent soluble) (%)	Bio-oil (water soluble fraction) (%)	Gas (%), by difference
350	45.1	12.2	9.0	33.7
400	43.6	12.7	9.1	34.6
450	37.4	16.2	10.6	35.8
500	34.0	18.0	11.0	37.0
600	31.1	17.3	10.9	40.7
20 °C/min				
350	44.0	12.3	9.3	34.4
400	41.7	12.9	10.4	35.0
450	35.8	13.9	13.1	37.2
500	30.9	18.4	11.4	39.3
600	29.0	17.1	11.5	42.4
40 °C/min				
350	39.0	13.0	10.0	38.0
400	37.6	13.3	10.3	38.8
450	32.1	16.1	11.9	39.9
500	26.8	20.0	12.0	41.2
600	23.6	19.1	12.1	44.6

Table 4.8 shows the product yields from the pyrolysis of MFDC in the tubular reactor with heating rates of 10 and 20 and 40°C/min in relation to final pyrolysis temperatures of 350, 400, 450, 500 and 600°C with N₂ gas flow. For the

lower heating rate of 10°C/min, the char yield decreased from 45% to 31% as the pyrolysis temperature increased from 350°C to 600°C. In other words, the pyrolysis conversion yield (condensable + non-condensable) increased from 54% to 64%. For the higher heating rates of 20 and 40°C/min, the char yield decreased from 44 to 29% and 39 to 23% respectively as the pyrolysis temperature increased from 350°C to 500°C. In other words, the pyrolysis conversion yield increased from 56 to 71% and 61 to 76% for heating rate 20 and 40°C/min, respectively. The decrease in the char yield with increasing temperature could be attributed either to the significant loss of volatile matter and indicates the significant loss of CH₄, H₂ and CO, the dehydration of hydroxyl groups, and the thermal degradation of the lignocellulose structure [24] or to secondary decomposition of the char at higher temperature [25]. It was also observed that, char yields for higher heating rates were lower than the yields achieved from lower heating rates, as fast depolymerization of solid biomass to primary volatiles due to rapid heating occurs at higher heating rate while dehydration to more stable anhydrocellulose is limited and slow at lower heating rate [26]. However, by increasing the pyrolysis temperature to 600°C, the bio-oil yield decreased to 28%, 29% and 31% for 10, 20 and 40°C/min heating rates respectively, in comparison to the same at 500°C. The higher pyrolysis temperatures have been associated with secondary cracking reactions of the pyrolysis gases to produce increased gas yields and reduced bio-oil yield [27]. The pyrolysis liquid product is a combination of an aqueous phase and an organic phase. In this study, the organic phase of pyrolysis product was taken for different characterization. The gas product yield was calculated by difference and was observed that gaseous product yield increased with increasing pyrolysis temperature for all the heating rates applied. The gas yield obtained was found to be minimum of 36% at 350°C and maximum of 45% at 600°C for a heating rate of 10°C/min. As the heating rates were increased from 20 to 40°C/min, gaseous product yield were also increased for all the pyrolysis temperature as shown in Table 4.8 and Figure 4.12. The increase in gas products is

thought to be predominantly due to secondary cracking of the pyrolysis vapours at higher temperatures and heating rates. The secondary decomposition of the char at higher temperatures and heating rates may also yield some non-condensable gaseous products, which also contributes to the overall increase in gas yield [28-31].

4-1.2.2 Influence of pyrolysis parameters on product yields of PGDC pyrolysis

Figures 4.13, 4.14 and 4.15 show the product yields from the pyrolysis of PGDC in the tubular reactor with heating rates of 10 and 20 and 40°C/min in relation to final pyrolysis temperatures of 350, 400, 450, 500 and 600°C with N₂ gas flow. For the lower heating rate of 10°C/min, the char yield decreased from 44.9% to 34.9% as the pyrolysis temperature increased from 350°C to 500°C. In other words, the pyrolysis conversion yield (condensable + non-condensable) increased from 55.1% to 65.1%. For the higher heating rates of 20 and 40°C/min the char yield decreased from 44.1% to 32.7% and 41.4 to 26.3% respectively as the pyrolysis temperature increased from 350°C to 500°C.

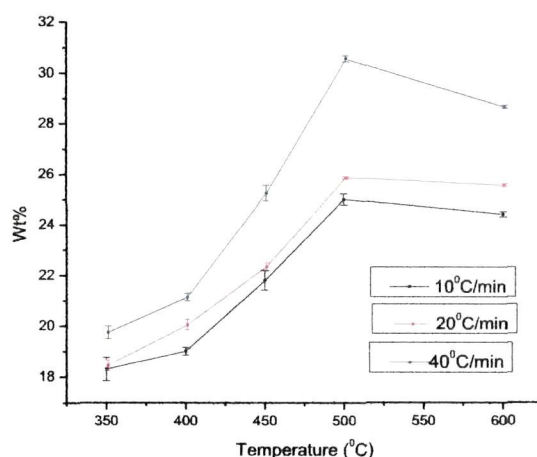


Figure 4.13: Effect of temperature and heating rate on liquid product yield of PGDC pyrolysis.

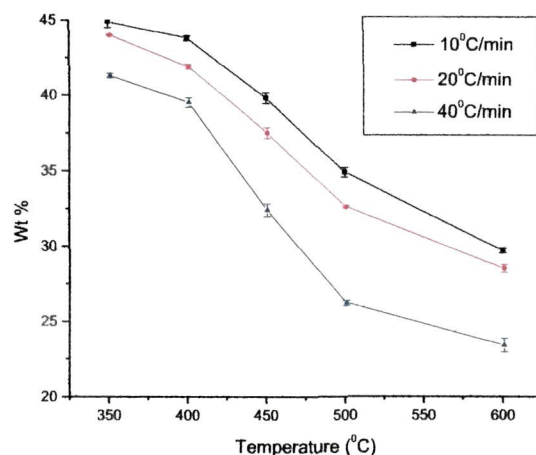


Figure 4.14: Effect of temperature and heating rate on solid product yield of PGDC pyrolysis.

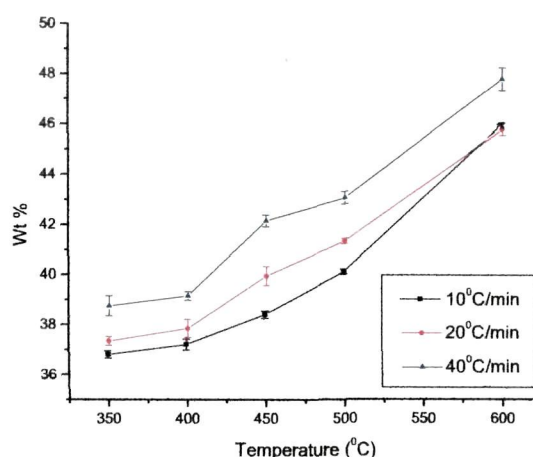


Figure 4.15: Effect of temperature and heating rate on gaseous product yield of PGDC pyrolysis.

In other words, the pyrolysis conversion yield increased from 55.9% to 67.3% and 58.6% to 73.7 % for heating rate 20 and 40°C/min respectively. The decrease in the char yield with increasing temperature could be attributed either to the significant loss of volatile matter and indicates the significant loss of CH₄, H₂ and CO, the dehydration of hydroxyl groups and the thermal degradation of the

lignocellulose structure [24] or to secondary decomposition of the char at higher temperature [25]. It was also observed that, char yields for higher heating rates were lower than the yields achieved from lower heating rates, as fast depolymerization of solid biomass to primary volatiles due to rapid heating occurs at higher heating rate while dehydration to more stable anhydrocellulose is limited and slow at lower heating rate [26]. However, by increasing the pyrolysis temperature to 600°C, the bio-oil yield decreased to 24.4%, 25.6% and 28.7% for 10, 20 and 40°C/min heating rates, in comparison to the same at 500°C. The higher pyrolysis temperatures have been associated with secondary cracking reactions of the pyrolysis gases to produce increased gas yields and reduced bio-oil yield [27]. The pyrolysis liquid product is a combination of an aqueous phase and an organic phase. In this study the organic phase of pyrolysis product was taken for different characterization. The gas product yield was calculated by difference and was observed that gaseous product yield increased with increasing pyrolysis temperature for all the heating rates applied.

Table 4.9: Products distribution of pyrolysis of PGDC

Temperature (°C)/Heating rate	Biochar (%)	Bio-oil (organic solvent soluble) (%)	Bio-oil (water soluble fraction) (%)	Gas (%), by difference
10 °C/min				
350	44.9	10.7	7.6	36.8
400	43.8	12.3	6.7	37.2
450	39.8	15.7	6.1	38.4
500	34.9	17.8	7.2	40.1
600	29.7	16.2	8.2	45.9
20 °C/min				
350	44.1	12.8	5.7	37.4
400	42	13.1	7	37.9
450	37.6	13.6	8.8	40.0
500	32.7	18.2	7.7	41.4
600	28.6	17.5	8.1	45.8
40 °C/min				
350	41.4	12.6	7.2	38.8
400	39.6	13.0	8.2	39.2
450	32.5	15.5	9.8	42.2
500	26.3	19.0	11.6	43.1
600	23.5	18.3	10.4	47.8

The gas yield obtained was found to be minimum 36.8% at 350°C and maximum 45.9% at 600°C for heating rate 10°C/min. As the heating rates were increased from 20 to 40°C/min, gaseous product yield were also increased for all the pyrolysis temperature as shown in Table 4.9 and Figure 4.15. The increase in gas products is thought to be predominantly due to secondary cracking of the pyrolysis vapours at higher temperatures and heating rates. The secondary decomposition of the char at higher temperatures and heating rates may also give some non-condensable gaseous products, which also contributes to the increase in gas yield, which is parallel to the increase in temperature of pyrolysis [28-31].

4-1.2.3 Influence of feedstock particle on liquid product yields of MFDC and PGDC pyrolysis

In order to observe the influence of particle size on pyrolysis yield, two particle sizes of 210 and 420 μ are taken into account. Figures 4.16 and 4.17 show the effect of particle size on liquid product yield at different temperatures at the heating rate of 40°C/min for MFDC and PGDC biomass, respectively. A number of literatures discussed effects of particle size on product yield and composition of products during pyrolysis [31-34]. However, in the present study, no such significant effect of particle size on liquid product yield was observed for both MFDC and PGDC pyrolysis as shown in Figures 4.16 and 4.17. There have been contradictory observations made by a number of researchers in this regard. Though, significant effect of particle size could be observed in case of fast pyrolysis process, but the effect of particle size may vary depending upon the type of biomass and pyrolyzer which is evident from previous studies. For example, Puttun *et al.* [35], Encinar *et al.* [36] and Sensoz *et al.* [37] observed higher liquid yield from sunflower bagasse, grape bagasse and rapeseed in case of intermediate particle size distribution. Onay *et al.* [38] also reported that medium particle size ($0.6 < dp < 0.8$ mm) yielded maximum liquid compared to smaller (< 0.4 mm) and larger (> 1.8 mm) particle size in fixed bed pyrolysis of rapeseed. Bridgewater and

Peacocke [39] suggested general specification for different types of pyrolyzer i.e. <200 mm for rotating cone, <2 mm for fluid bed and <6 mm for circulating fluid bed. As the size reduction of biomass feed is associated with penalty for cost of grinding, higher particle size i.e., 420 μ was opted for pyrolysis to obtain liquid and solid product for characterization in the present study.

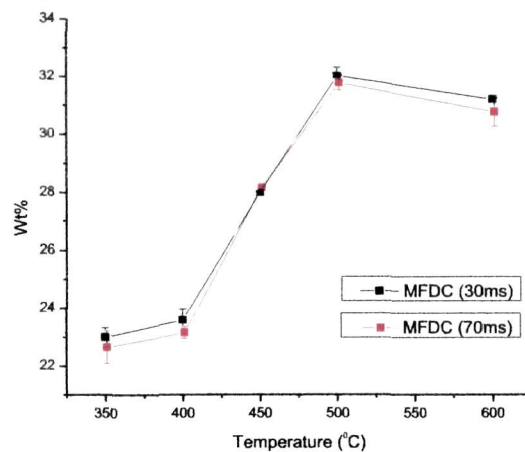


Figure 4.16: Effect of particle size on liquid product yield of MFDC pyrolysis.

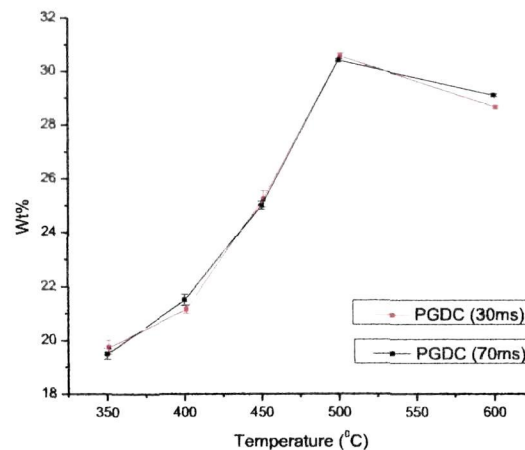


Figure 4.17: Effect of particle size on liquid product yield of PGDC pyrolysis.

4-1.2.4 Influence of catalyst on product yield and elemental composition

Non-catalytic pyrolysis of both MFDC and PGDC yielded highest liquid product at temperature 500°C with a heating rate of 40°C/min as mentioned in the previous sections. To observe the effect of catalyst on product yield of pyrolysis and elemental composition of MFDC and PGDC bio-oil, catalytic pyrolysis was carried out at temperature 500°C and heating rate 40°C/min. As shown in Figures 4.18 and 4.19, the liquid yield decreased with the application of catalyst while the char yield increased for both the feedstocks. According to Carlson *et al.* [40], increase in char yield during catalytic pyrolysis is due to its small pore size and strong acidity.

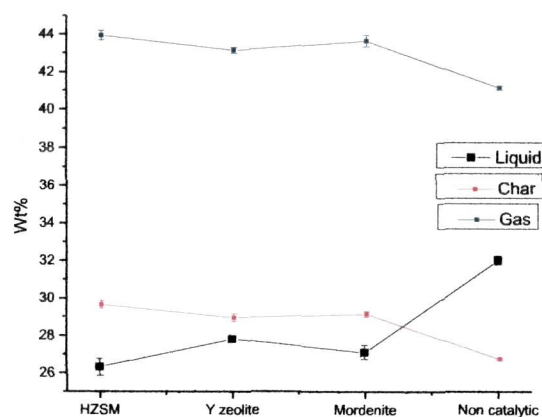


Figure 4.18: Influence of catalysts on product yields of MFDC pyrolysis.

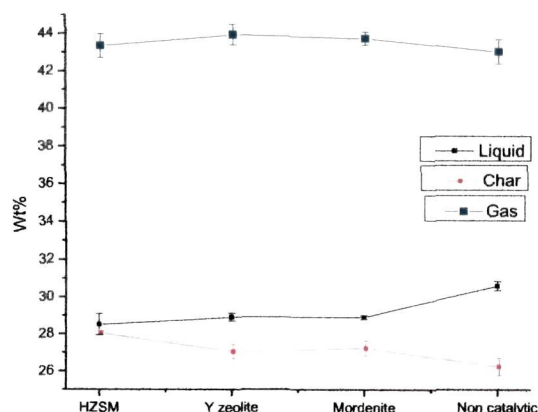


Figure 4.19: Influence of catalysts on product yields of PGDC pyrolysis.

Table 4.10 shows the result of ultimate analysis of bio-oil from catalytic pyrolysis. Compared with non-catalytic pyrolysis experiment, the bio-oils obtained with catalyst, had higher C and H values and lower oxygen content. It can be seen from the table that the extent of removal of oxygen from the bio-oil was different for three different kinds of catalyst used in pyrolysis. The oxygen content of non-catalytic pyrolysis oil for MFDC was 28.10%, which was decreased to 24.3%, 22% and 25.1% with HZSM-5, Mordenite and Y-zeolite respectively while for PGDC bio-oil, the oxygen content of non-catalytic pyrolysis oil was 31.1%, which also decreased to 26.2%, 27.3% and 28.4% during the catalytic pyrolysis using HZSM-5, Mordenite and Y-zeolite. Removal of oxygen content lead to higher CV of catalytic bio-oil than non-catalytic bio-oil as reported by Wang *et al.* [41].

Table 4.10: Elemental composition of bio-oil

	C	H	N	O ^a
MFDC bio-oil				
Non catalytic	57.80	8.20	5.90	28.10
HZSM-5	62.80	8.69	4.23	24.28
Mordenite	63.40	8.77	5.80	22.03
Y zeolite	62.40	8.77	3.70	25.13
PGDC bio-oil				
Non-catalytic	55.40	7.8	5.70	31.10
HZSM-5	59.40	8.3	6.10	26.20
Mordenite	58.60	8.2	5.90	27.30
Y zeolite	57.40	8.0	6.16	28.44

^aby difference

4-1.3 Characterization of bio-oil

Table 4.11 presents the analysis results of MFDC and PGDC bio-oil. The average chemical composition of bio-oil is $C_{11.43}H_{19.46}NO_{4.18}$ and $C_{11.34}H_{19.16}NO_{4.77}$ for MFDC and PGDC bio-oils, respectively. The oil was characterized by lower oxygen content than that of original biomass feedstock. The significant decrease in oxygen content in bio-oil as compared to original feedstock is favorable since high oxygen content is not attractive for the

production of transportation fuel [42]. From the result of the elemental analyses, the carbon and hydrogen content of bio-oils at 500°C are 57.8% and 8.2%, and 55.4% and 7.8% for MFDC and PGDC bio-oil, respectively, and are higher than that of raw materials, indicating that bio-oils have a higher energy density [43]. The H/C ratio of bio-oil was higher than that of original material and comparison of this value with conventional fuels indicates that bio-oil obtained in this study falls between those of light and heavy petroleum products [37]. As can be seen in Table 4.11, the low ash content suggests that bio-oils have obvious advantages as a clean fuel oil.

Table 4.11: Properties of the pyrolysis product

Properties	MFDC bio-oil ^a	PGDC bio-oil ^a
Ultimate analysis		
C	57.8	55.4
H	8.2	7.8
N	4.9	5.7
O ^b	29.1	31.1
Empirical formula	C _{11.43} H _{19.46} NO _{4.18}	C _{11.34} H _{19.16} NO _{4.77}
H/C molar ratio	1.70	1.69
O/C molar ratio	0.36	0.42
Higher heating value (MJ/kg)	30.63	28.19
Ash	0.30	0.39
Density (kg/m ³)	1075	1051
Acid number (mg KOH/g)	42.71	45.20

^a Obtained at 500°C with heating rate 40°C/min

^b By difference

Biomass pyrolysis oils contain a very wide range of complex organic chemicals. The FTIR analysis of PGDC and MFDC bio-oil (Figures. 4.20, 4.21 and 4.22) shows the presence of functional groups in the liquid product at various operating temperature. The functional groups identified from FTIR spectrum of MFDC and PGDC bio-oil are shown in Table 4.12. The absorption peaks at 3270 cm⁻¹ indicate the presence of oxygenated compounds along with moisture [44]. Bio-oil displays strong absorbance band in the position of 2857, 2932 (for MFDC bio-oil) and 2864,

2952, 2932 cm^{-1} (for PGDC bio-oil), indicating a high content of methylene groups. The peak appears at 2213 cm^{-1} (for MFDC bio-oil) and 2220 cm^{-1} (for PGDC bio-oil) which gives indication of presence of alkynes or cyanide group in the bio-oil. Absorbance peaks appears at 1705 cm^{-1} for both the bio-oils that attributes to the presence of carbonyl group of aldehyde and ketone. The presence of C=C stretching vibration at 1637 and 1495 cm^{-1} (for MFDC bio-oil) and 1658 and 1515 cm^{-1} (for PGDC bio-oil) gives evidence of the presence of alkenes as well as aromatic compounds. The presence of aromatic compounds is further confirmed by the C-H in plane bending vibration between 650 – 950 cm^{-1} for both the bio-oils. The bio-oil contains a high amount of oxygenated compounds and part of oxygenated compounds present in the forms of alcohol and ether are confirmed by the FTIR peak at 1109 and 1264 cm^{-1} (for MFDC bio-oil) and 1115 and 1271 cm^{-1} (for PGDC bio-oil). The C-O-C pyranose ring skeletal vibrations from 1076 – 1023 cm^{-1} indicate the presence of levoglucosan which also found to be present in MFDC bio-oil through GC-MS analysis [45]. The details of the functional group determination by the FTIR spectra and class of compounds present in the bio-oil are shown in the Table 4.12.

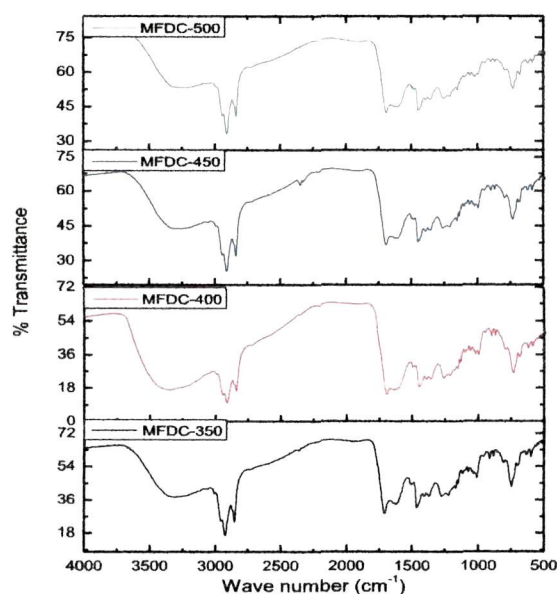


Figure 4.20: FTIR spectrum of MFDC bio-oil at different temperature.

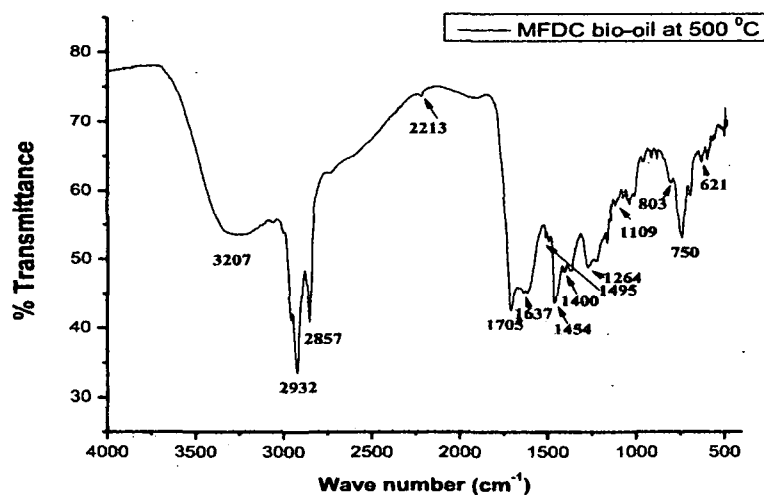


Figure 4.21: FTIR spectrum of MFDC bio-oil at 500°C.

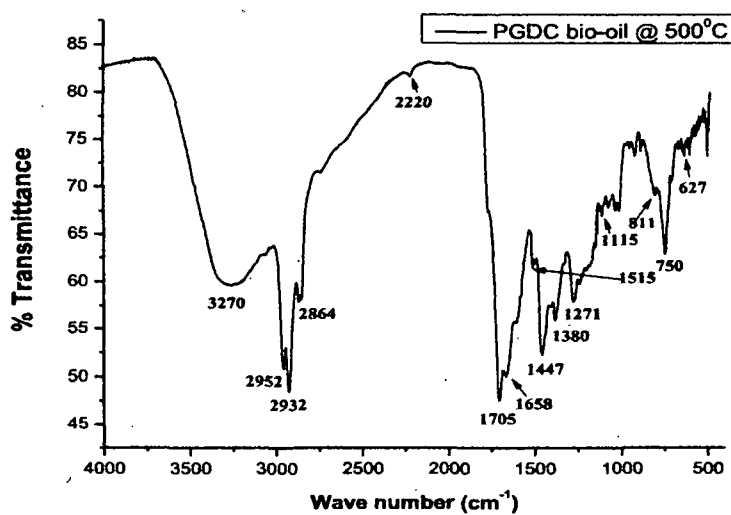


Figure 4.22: FTIR spectrum of PGDC bio-oil at 500°C.

Table 4.12: FTIR spectral data of bio-oil

Frequency range (cm ⁻¹)	Frequency (cm ⁻¹)		Group	Class of compounds
	MFDC bio-oil	PGDC bio-oil		
3200-3600	3270	3270	O-H stretching N-H stretching	Polymeric OH, water, -NH ₂
2800-2980	2857, 2932	2864, 2952, 2932	C-H stretching	Alkane
2000-2380	2213	2220	C≡C stretching	Alkynes, cyanides
1650-1850	1705	1705	C=O stretching	Aldehyde, ketone, carboxylic acid, esters etc
1580-1650	1637	1658	C=C stretching	Alkenes
1490-1550	1495	1515	N-H bending, aromatic C=C stretching	Nitrogenous compound, aromatic compounds
1350-1470	1400, 144	1380, 1447	C-H bending	Alkanes
950-1350	1109, 1264	1115, 1271	C-O stretching, O-H bending	Alcohol, ether
615-950	750, 803	760, 814	C-H in plane bending	Aromatic compound
>650	621	619		

Chemically bio-oil is a complex mixture of water, guaiacols, catechols, syringols, vanillins, furancarboxaldehydes, isoeugenol, pyrones, acetic acid, formic acid and other carboxylic acids. Bio-oils also contain other major groups of compounds including hydroxyaldehydes, hydroxyketones, sugars, carboxylic acids and phenolics [46]. Due to this chemical complexity of bio-oils, their characterization has been a challenging problem and in general requires the combined use of several analytical techniques, both chromatographic (GC, HPLC, GPC) and spectroscopic (IR, MS). In recent years, GC and IR analysis have been extensively used for assaying the chemical composition of bio-oils, but they have major lacunas in that they cannot provide insights into the overall chemical make-up of bio-oils. Only 25 – 40% of bio-oil compounds are observable by GC analysis since a significant fraction of these bio-oils comprise of lignin and carbohydrate oligomers, which are not volatile enough to be observed by GC [47]. On the other hand spectroscopic techniques like FTIR analysis can only provide qualitative insights (functional groups present in bio-oils). In a similar fashion, HPLC (for quantifying some water soluble species present in pyrolytic bio-oils) and gel

exclusion chromatography (for obtaining molecular weight distributions on higher molecular weight phenolic species derived from lignin) share similar disadvantages in that they are capable of characterizing only a fraction of bio-oils [47, 48]. With regard to these aforesaid limitations, NMR spectroscopy was carried out to examine, virtually the complete, intact, bio-oil rather than a selected fraction.

The $^1\text{H-NMR}$ spectra of petrol and diesel (international road fuels), crude oil (conventional petrofuel feedstock), MFDC and PGDC bio-oils (samples under investigation) are presented in Table 4.13 with the respective integral values of the selected regions of the spectra on percentage basis. The integrated regions in the spectra were from 0.5 – 1.5, 1.5 – 3.0, 3.0 – 4.5, 4.5 – 6.0, 6.0 – 8.5 and 8.5 – 10 ppm, respectively. From the spectra (Appendix figures), it is quite evident that both bio-oils have significant differences in their chemical make-over and their respective comparison standards (petrol, diesel and crude oil). A higher aliphatic content (presence of short, long and/or branched chain hydrocarbons) in MFDC bio-oil (Table 4.13) is indicative of high energy content compared to PGDC bio-oil. For catalytic pyrolysis of MFDC and PGDC, this region showed a slight lower percentage of resonating protons for all the catalyst used (Figures. 4.23 and 4.25). From Table 4.13, it is clear that petrol, diesel and crude oil had a higher aliphatic content which accounts for their superior energy content when compared to bio-oils. MFDC and PGDC bio-oils have high percentage of resonating protons in the integrated region from 1.5 – 3.0 ppm. This clearly indicates that aliphatic fractions of molecules (even those bonded to aromatic portions or near heteroatoms) are more prevalent for higher energy content. The integrated region 6.0 – 8.5 ppm corresponds to aromatic portion (aromatic carbon from benzene rings and heteroaromatics) of bio-oils. Both the bio-oil had a rather high proportion of aromatic ether protons (resultant from lignin derived methoxy phenols). However as shown in Figures 4.23 and 4.25, use of zeolite catalyst in the pyrolysis experiment increased the resonating percentage of proton in this region for both

bio-oils because acidic zeolite promotes aromatization reaction in catalytic pyrolysis of biomass [49, 50]. HZSM-5 catalyst showed a higher selectivity towards aromaticity than Mordenite and Y-zeolite which could be attributed to the presence of higher acid sites in HZSM-5 (0.81 mmol/g) than Mordenite (0.77 mmol/g) and Y-zeolite (0.71 mmol/g). The integrated region 8.5 – 10.0 ppm corresponds to oxygenated compounds (aldehydes, ketones, carboxylic acids, esters and amides). A higher proportion of resonating protons for MFDC and PGDC bio-oils in this region is suggestive of increased corrosive nature of both the bio-oils. It is noteworthy to mention that the comparison standards (petrol, diesel and crude oil) have no resonating protons in this region (no oxygenated compounds) which accounts for their comparatively higher energy content in comparison to MFDC and PGDC bio-oils. However, the use of zeolite catalyst decreased the resonating protons in this region. The information about relative abundance of oxygenated compounds may be useful information for applications involving the synthetic modification of bio-oils and their prospective utilization as a chemical feedstock.

¹³C-NMR spectra provide greater detail due to their large chemical shift regions. Signals in the 0 – 55 ppm range represent aliphatic carbon atoms that are separated from oxygen atoms by at least two bonds, although those adjacent to nitrogen atoms can also be found in this region. 60.7% (for MFDC) and 56.3% (for PGDC) of the carbon atoms resonate in the region from 0 – 55 ppm. This result is in accordance with the ¹H-NMR of the bio-oil which shows high proton percentage in the most upfield region. This could be due to two factors: (1) the presence of residual triglycerides in the pyrolysis feedstock and (2) the higher nitrogen content in these feedstock, as this region can also account for carbon adjacent to nitrogen atoms [51]. However, using zeolite catalyst, the percentage of resonating carbon decreased (Figures. 4.24 and 4.26) for both the MFDC and PGDC bio-oils, which is in accordance with ¹H-NMR spectra. This region is further subdivided into two regions, region from 0 – 28 ppm which is composed of

short aliphatics and region from 28 – 55 ppm comprising of the long and branched aliphatics. The presence of long aliphatics could be due to the presence of saturated and unsaturated free fatty acids and fatty acids derivatives [52]. The carbon percentage in the region ranging from 5-28 ppm is higher than that of 28 – 55 ppm region.

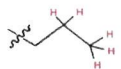
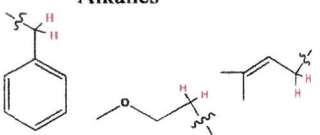
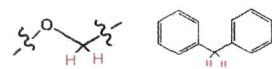
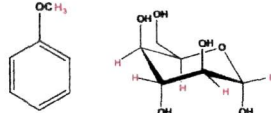

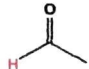
The next region of the spectrum is from 55 – 95 ppm which represents carbon adjacent to heteroatoms (mostly oxygen) in alcohols, ethers and anhydrous carbohydrates. Nearly all of the methyl groups in this region are probably methoxy groups on 2 and 6 positions of phenolic rings (structures derived from lignin). The solvent peak (CDCl₃) also appears in this region. Carbon percentage is 4.3 for MFDC and 20.6 for PGDC in this region. Using zeolite catalyst, showed a decrease in the resonating carbon percentage in this region as shown in Figure 4.26 for PGDC bio-oil which is in agreement with the elemental analysis of the bio-oil.

The aromatic region of the spectra (95 – 165 ppm) is the portion where most of the variability was seen in the pyrolysis oils obtained from lignocellulosic feedstock. This region includes aromatic carbon from both benzene rings and heteroaromatics (e.g., furans). The carbon percentage in this region was 34.2 for MFDC bio-oil and 21.1 for PGDC bio-oil. As observed in the ¹H-NMR integration region, using zeolite catalyst favored the aromatic production during catalytic pyrolysis of MFDC and PGDC. HZSM-5 catalyst showed a higher selectivity towards aromaticity than Mordenite and Y-zeolite which could be attributed to the presence of higher acid sites in HZSM-5 as mentioned above.

The extreme downfield end of the spectra represents carbonyl carbons with 165-180 ppm representing carboxylic acids, esters, and amides. Significant numbers of carbonyl groups are present in this region, mainly due to carboxylic acids, and to a minor extent to esters and amides. The region from 180 – 215 ppm represents ketones and aldehydes. The value of carbon percentage in 165 – 180

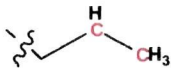
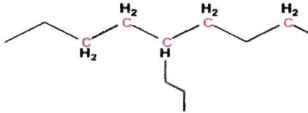
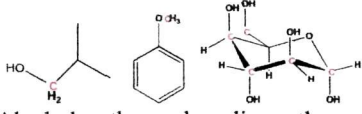
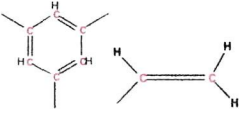
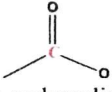
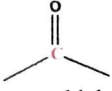
ppm region was 0.6 and 1.8 for MFDC and PGDC and in 180 – 215 ppm region, the carbon percentage was 0.3 and 0.7 for MFDC and PGDC bio-oils respectively. The presence of aldehydes and ketones was negligible in the bio-oil samples which were also evident from the $^1\text{H-NMR}$ spectrum which show negligible proton percentage in the downfield region from 8.5 to 10 ppm. Also, the presence of catalyst further decreased the percentage of carbon resonating in this region.

Table 4.13: Percentage of hydrogen based on $^1\text{H-NMR}$ analysis of MFDC, PGDC bio-oil and conventional petrol, diesel and crude oil, grouped according to chemical shift range^a

Chemical shift (ppm)	Proton assignment	MFDC bio-oil (%)	PGDC bio-oil (%)	Petrol (%)	Diesel (%)	Crude oil (%)
0.5-1.5	 Alkanes	51.65	49.54	70	82	67
1.5-3	 Aliphatics α -heteroatoms or unsaturation	27.19	19.65	19	16	17
3-4.5	 Alcohols, methylene diabenzene	5.19	20.35	2	0	2
4.5-6	 Methoxys, carbohydrates	7.87	4.15	2	0	3
6-8.5	 (Hetero)-aromatics	5.23	6.02	6	3	8
8.5-10	 ALdehydes	2.87	0.3	0	0	2

^a Highlighted atoms shown in representative chemical functional groups are intended only to indicate the potential types of chemical environments that may be present. The real mixtures may contain significant structural diversity

Table 4.14: Percentage of carbon based on ^{13}C -NMR analysis of MFDC, PGDC bio-oil and conventional petrol, diesel and crude oil, grouped according to chemical shift range^a

Chemical shift (ppm)	Carbon assignment	MFDC bio-oil (%)	PGDC bio-oil (%)	Petrol (%)	Diesel (%)	Crude oil (%)
0-28	 Short aliphatics	32.44	46.19	29	31	15
28-55	 Long and branched aliphatics	28.21	10.1	35	56	41
55-95	 Alcohols, ethers, phenolic-methoxys, carbohydrate sugars	4.28	20.6	7	7	30
95-165	 Aromatics, olefins	34.19	21.11	29	3	5
165-180	 Esters, carboxylic acids	0.60	1.8	0.3	1	3
180-215	 Ketones, aldehydes	0.28	0.67	0.4	5	5

^aHighlighted atoms shown in representative chemical functional groups are intended to only indicate the potential types of chemical environments that may be present. The real mixtures may contain significant structural diversity

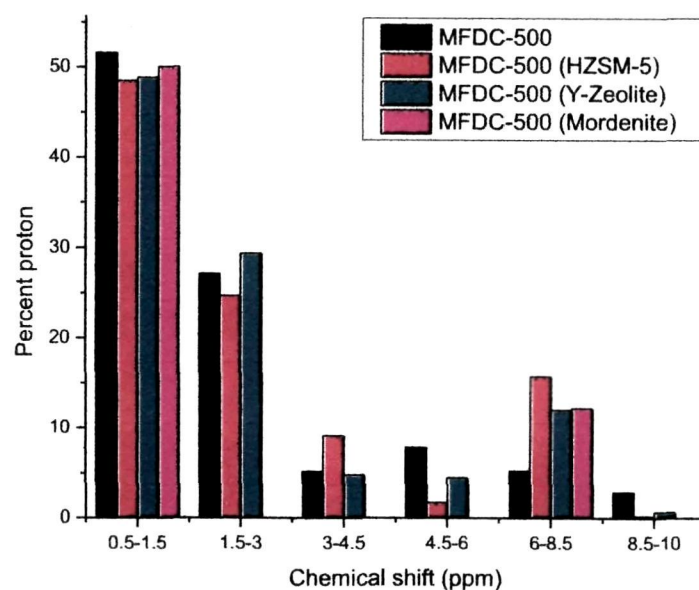


Figure 4.23: Comparison of ^1H -NMR spectral distribution of functional groups of MFDC bio-oil.

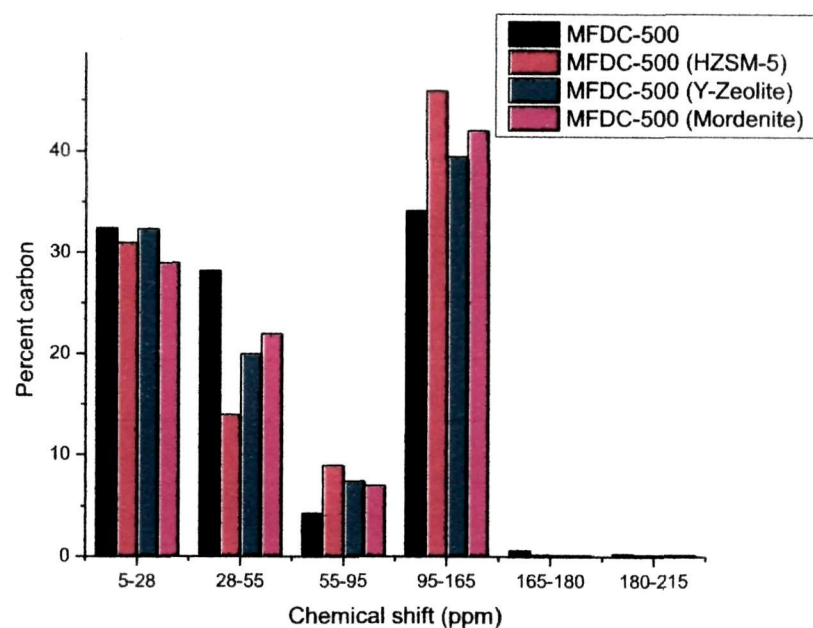


Figure 4.24: Comparison of ^{13}C -NMR spectral distribution of functional groups of MFDC bio-oil.

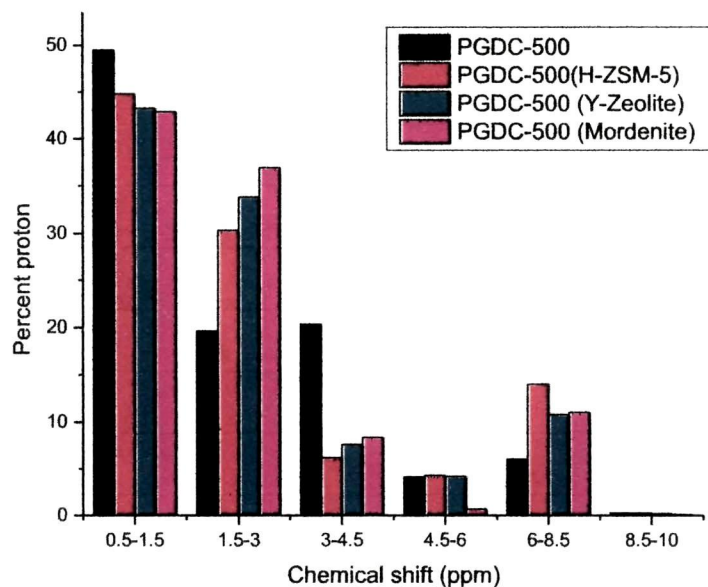


Figure 4.25: Comparison of ^1H -NMR spectral distribution of functional groups of PGDC bio-oil.

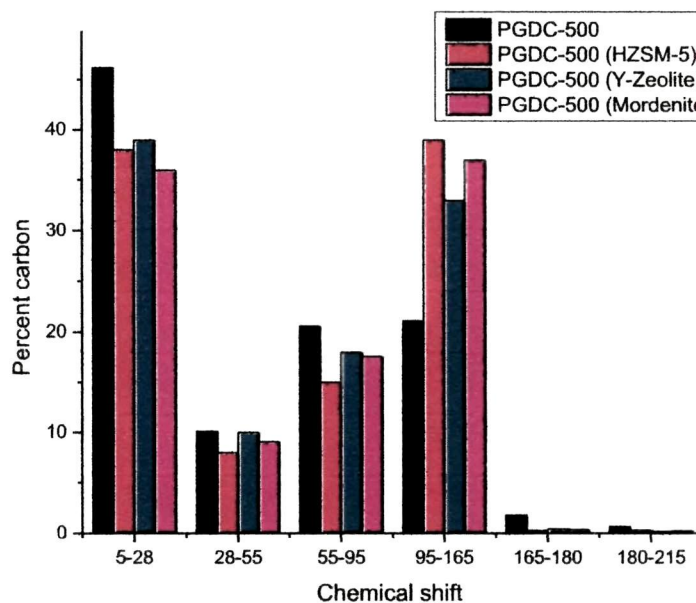


Figure 4.26: Comparison of ^{13}C -NMR spectral distribution of functional groups of PGDC bio-oil.

The TIC of MFDC and PGDC bio-oils are presented in Figures 4.27 and 4.28. GC-MS was applied to identify the organic compounds obtained from the bio-oils. Identification of the GC-MS peaks in most cases was based on comparison with spectra from the NIST 98 spectrum library. More than 100 peaks were displayed in the TIC of both the bio-oils (Figures 4.27 and 4.28). This implies the complex composition of the bio-oils; the results are consistent with both the FTIR and ^{13}C -NMR results. The perfect separation of all the peaks was impossible due to the intricate composition of bio-oils. Only those separated products that arose in considerable amounts, were semi-quantitatively evaluated, based on the peak areas of selected characteristic molecular or fragment ion chromatograms. Tables 4.15 and 4.16 show the details of the component of MFDC and PGDC bio-oils identified including retention time, compound name, peak area and molecular formula. The distribution of compounds was determined by using a semi-quantitative study by means of the percentage area of the chromatographic peak. As shown in Tables 4.14 and 4.15, most of the compounds formed during MFDC and PGDC pyrolysis are phenols. The presence of phenols is also evident from ^1H and ^{13}C NMR results. Substituted phenols are present in the bio-oil as monomeric units and oligomers derived from coniferyl and syringyl building blocks of lignin. The main phenolic compounds present in the bio-oils are phenols, alkylphenols, methoxyphenols and guaiacol (vanillin). The pyrolytic liquids are known to have an acidic nature. The presence of acids in bio-oil is undesirable due to its corrosive nature; however, they could be used as chemical feedstock if separated from bio-oil. Propionic acid methyl ester was also found in MFDC bio-oil.

Carbonyl groups are also oxygenated compounds and they affect the stability and heating value of bio-oil. Therefore, these compounds must be detached from bio-oil structure through efficient separation techniques so as to utilize the bio-oil effectively. The components present in MFDC and PGDC bio-oils were observed in other studies also [4, 53-55]. Phenols, carboxylic acids and

carbonyls were determined as main compounds forming pyrolytic liquid. Furthermore, nitrogenous compounds are also found in the final bio-oil product distribution from both the feedstock under investigation.

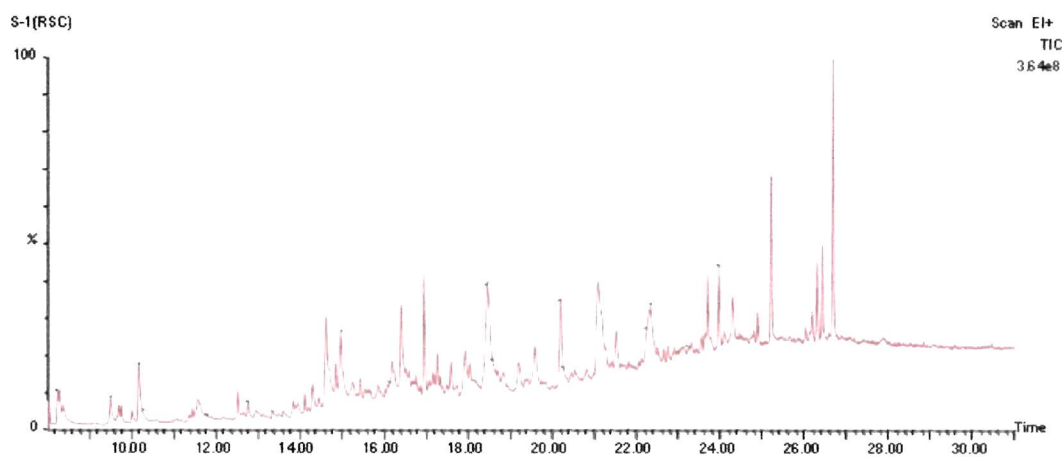


Figure 4.27: Total ion chromatogram of MFDC bio-oil.

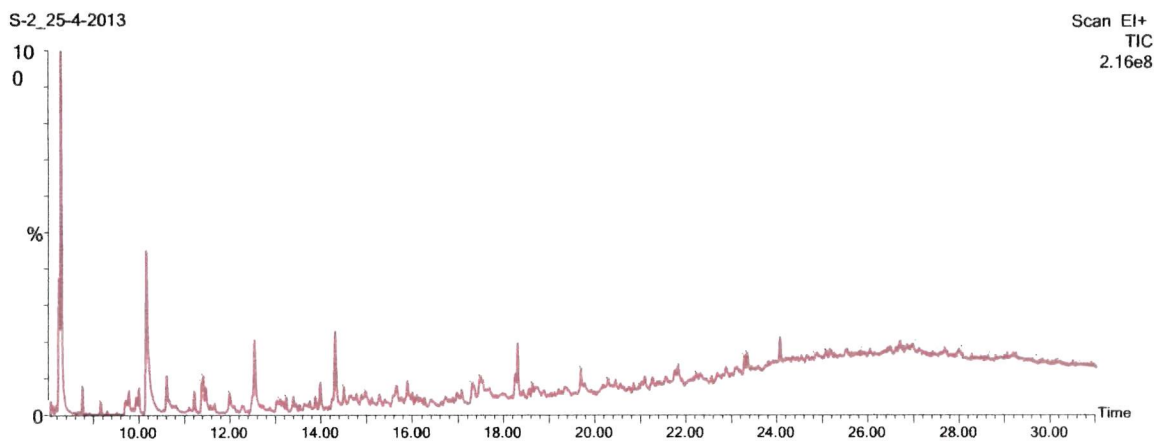


Figure 4.28: Total ion chromatogram of PGDC bio-oil.

Table 4.15: Chemical compounds in MFDC-500 bio-oil (GC-MS)

Sl. No.	RT	Area %	Name	MW	Molecular formula
1	8.23	0.57	3-pentanol	88	C ₅ H ₁₂ O
2	8.36	0.86	1,6-anhydro-b-D-glucopyranose	162	C ₅ H ₁₀ O ₅
3	9.48	0.74	Propionic acid methyl ester	88	C ₄ H ₈ O ₂
4	10.15	2.06	(1S,5R)-6,8-Dioxabicyclo[3.2.1]oct-2-en-4-one	126	C ₆ H ₆ O ₃
5	11.59	1.35	3-butene-2-one, 3-methyl	84	C ₅ H ₈ O
6	12.51	0.54	2-nitropyridin-3-ol	140	C ₅ H ₄ N ₂ O ₃
7	12.94	0.40	octanamide	143	C ₈ H ₁₇ NO
8	13.84	2.943	phenol	94	C ₆ H ₆ O
9	13.95	0.483	hydroxypropanone	74	C ₃ H ₆ O ₂
10	14.62	3.462	pyridin-3-ol	95	C ₅ H ₅ NO
11	14.96	1.933	2-buten-1-ol	72	C ₄ H ₈ O
12	15.86	0.605	3-methylphenol	108	C ₇ H ₈ O
13	16.38	3.160	5-ethylidihydrofuran-2(3H)-one	114	C ₆ H ₁₀ O ₂
14	18.48	0.632	1-morpholino-2-phenylethanone	205	C ₁₂ H ₁₅ NO ₂
15	19.56	2.237	Hydroxyl propanal	74	C ₃ H ₆ O ₂
16	20.18	0.406	5-hydroxymethylfurfural	126	C ₆ H ₆ O ₃
17	20.79	0.442	furan tetrahydro-2,5-dimethoxy	132	C ₆ H ₁₂ O ₃
18	21.07	6.656	D-allose	180	C ₆ H ₁₂ O ₆
19	21.49	1.293	butanedial	86	C ₄ H ₆ O ₂
20	22.31	4.423	3,4-dihydroxytoluene	124	C ₇ H ₈ O ₂
21	22.48	0.460	furan, tetrahydro-2,5-dimethoxy-	132	C ₆ H ₁₂ O ₃
22	23.94	1.56	3-ethoxy-4-methoxyphenol	168	C ₉ H ₁₂ O ₃
23	24.08	0.39	heptadecane	240	C ₁₇ H ₃₆
24	24.86	0.56	Furfuryl alcohol	97	C ₅ H ₅ O ₂
25	25.18	0.18	vanillin	152	C ₈ H ₈ O ₃
26	26.40	1.818	2-methoxy-4-methyl phenol (creosol)	138	C ₈ H ₁₀ O ₂

RT- Retention time, MW- Molecular weight

Table 4.16: Chemical compounds in PGDC-500 bio-oil (GC-MS)

Sl. No.	RT	Area%	Name	MW	Molecular formula
1	8.24	1.20	3-pentanol	88	C ₅ H ₁₂ O
2	8.72	0.84	Toluene	92	C ₇ H ₈
3	9.12	0.76	2-butenal, 2-methyl-	84	C ₅ H ₈ O
4	10.12	5.54	3-furanmethanol	98	C ₅ H ₆ O ₂
5	10.15	1.01	(1S,5R)-6,8-Dioxabicyclo[3.2.1]oct-2-en-4-one	126	C ₆ H ₆ O ₃
6	11.18	0.31	Styrene	104	C ₈ H ₈
7	11.34	0.56	2-cyclopenten-1-one, 2-methyl-	96	C ₆ H ₈ O
8	11.37	1.13	Ethanone, 1-(2-furanyl)-	110	C ₆ H ₆ O ₂
9	11.43	0.68	2,3,4-trimethylpyrrole	109	C ₇ H ₁₁ N
10	11.96	0.64	Pyridine, 3,4-dimethyl-	107	C ₇ H ₉ N
11	12.51	2.31	3-pyridinol, 2-nitro-	140	C ₅ H ₄ N ₂ O ₃
12	12.99	-	Pyrrole, 4-ethyl-2-methyl-	109	C ₇ H ₁₁ N
13	13.07	-	2,4-hexadiene, 2,5-dimethyl-	110	C ₈ H ₁₄
14	13.11	-	2-but-2-enyl-1H-imidazole	122	C ₇ H ₁₀ N ₂
15	13.20	0.51	3-hexene, 2,5-dimethyl-3,4-bis(1-methylethyl)-	196	C ₁₄ H ₂₈
16	13.84	0.43	2-cyclopenten-1-one, 2,3-dimethyl-	110	C ₇ H ₁₀ O
17	13.95	0.59	Phenol, 2-methyl-	108	C ₇ H ₈ O
18	14.28	1.67	Phenol, 4-methyl-	108	C ₇ H ₈ O
19	14.47	0.57	1-pentanone, 1-phenyl-	162	C ₁₁ H ₁₄ O
20	14.94	-	1-(1-butynyl)cyclopentanol	138	C ₉ H ₁₄ O
21	15.24	-	1,3-cyclopentanedione, 2,4-dimethyl-	126	C ₇ H ₁₀ O ₂
22	15.61	0.94	Phenol, 3,4-dimethyl-	122	C ₈ H ₁₀ O
23	15.63	-	Benzene, 1-methoxy-2-methyl-	122	C ₈ H ₁₀ O
24	15.86	0.70	Phenol, 4-ethyl-	122	C ₈ H ₁₀ O
25	17.44	1.59	Hydroquinone	110	C ₆ H ₆ O ₂
26	18.21	0.64	2,2'-bifuran	134	C ₈ H ₆ O ₂
27	18.27	1.07	Indole	117	C ₈ H ₇ N
28	18.59	-	1,3-benzenediol, 2-methyl-	124	C ₇ H ₈ O ₂
29	19.65	0.68	Indolizine, 2-methyl-	131	C ₉ H ₉ N
30	20.26	0.76	5-hydroxymethylfurfural	126	C ₆ H ₆ O ₃
31	21.79	0.68	Indole-2-carboxylic acid	161	C ₉ H ₇ NO ₂
32	24.03	1.04	3-ethoxy-4-methoxyphenol	168	C ₉ H ₁₂ O ₃
33	26.45	2.91	Phenol, 3,5-dimethoxy-	154	C ₈ H ₁₀ O ₃

RT- Retention time, MW- Molecular weight

4-1.4 Characterization of biochar

The proximate and elemental compositions of the biochars obtained from MFDC and PGDC pyrolysis at different temperatures with heating rate of 40°C/min are presented in Tables 4.17 and 4.18.

Table 4.17: Elemental analysis of biochar co-produced from pyrolysis of MFDC

	MFDC biochar				
	350°C	400°C	450°C	500°C	600°C
Water content	5.10	4.70	4.10	3.80	3.12
Volatile matter	25.56	21.34	15.70	13.45	11.70
Ash content	8.60	8.93	10.40	11.50	12.30
Fixed carbon	59.74	65.03	69.80	71.25	72.88
p ^H	7.20	8.83	10.10	11.30	11.78
Elemental analysis (wt%)					
C	63.20	66.90	73.03	75.80	80
H	3.97	3.95	3.87	3.84	2.71
N	3.00	4.97	4.98	4.36	2.71
O ^b	25.01	19.36	13.30	11.18	8.87
HHV (MJ/kg)	-	-	-	28.19	-

^b By difference

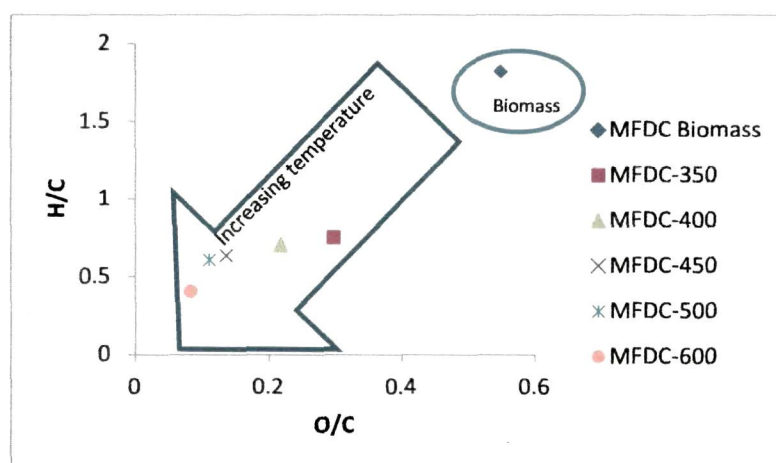


Figure 4.29: Van-krevelen diagram for MFDC biochar.

It was observed that the biochar from both feedstocks contain less oxygen than the original feedstock and a high carbon content. A Van-kraeven diagram (Figures 4.29 and 4.30) was constructed using the data in Tables 4.17 and 4.18. Biochar is often assessed through changes in the elemental concentrations of C, H, O and N and their associated ratios. Specifically, H/C and O/C ratios are used to measure the degree of aromaticity, carbonization and maturation, as is often illustrated in Van-kraeven diagrams. As observed from the Van-kraeven diagram, atomic O/C and H/C ratios of biochar decreased with increase in pyrolysis temperature for both the feedstock under investigation. Decrease in O/C ratio with increasing temperature is due to the fact that oxygen containing functionalities are decomposed by decarbonylation and decarboxylation, followed by transformation to the alkyl-aryl C-C bonds as a cross-linking between small aromatic rings [24, 56]. There occurs a significant increase of the calorific value of the biochar i.e. 28.2 MJ/kg from the original biomass having calorific value of 18.7 MJ/kg for MFDC and 24.3 MJ/kg from the original biomass having calorific value 16.9 MJ/kg for PGDC. Thus, the biochar obtained from MFDC and PGDC biomass can be used as a solid fuel upon densification. The pH of MFDC biochar increased from 7.2 to 11.8 and PGDC biochar from 7.3 to 11.6 with increase in pyrolysis temperature. The highly basic biochar obtained at higher temperatures may be potentially used in the agricultural soils in north-eastern region of India for liming, where the soil are highly acidic nature.

Table 4.18: Elemental analysis of biochar co-produced from pyrolysis of PGDC

	PGDC biochar				
	350°C	400°C	450°C	500°C	600°C
Water content	6.1	4.83	4.76	4.3	3.7
Volatile matter	27.5	22	15.8	14.6	11.7
Ash content	8.1	9.2	10.4	11.6	12.7
Fixed carbon	58.3	63.97	69.04	69.5	71.9
pH	7.3	7.5	9.8	11.2	11.6
Elemental analysis (wt%)					
C	63	65.7	72.3	75	79
H	4.29	4.35	4.21	3.26	2.7
N	4.77	5.25	4.96	5	4.78
O ^b	23.78	20.54	14.37	12.58	9.36
HHV (MJ/kg)	-	-	-	24.30	-

^b By difference

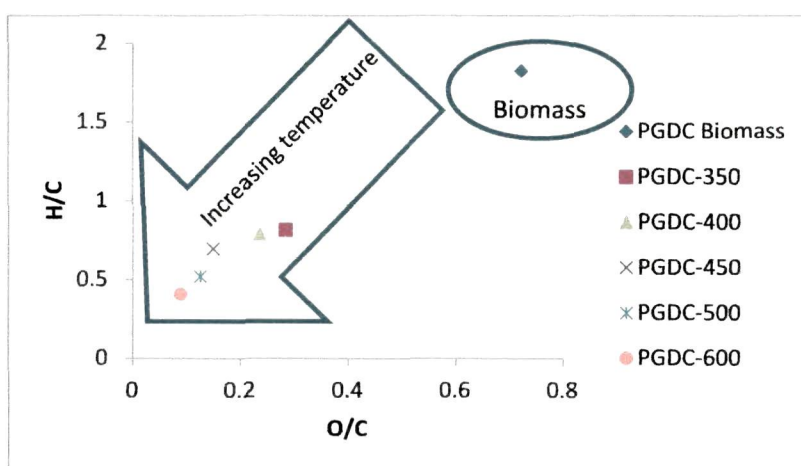


Figure 4.30: Van-krevelen diagram for PGDC biochar.

Figures 4.31 and 4.32 present the inorganic composition (Ca, K, Mg, Zn, Mn, Na) of the MFDC and PGDC biochar. It was observed that concentration of Ca, K, Mg increased with the pyrolysis temperature. The biochar containing inorganic nutrients can play an important role in soil fertility and crop production [24]. However, the proposition of biochar with high ash content and low surface area applicable as soil amendment entirely depends upon the economic circumstances and the local soil properties [57].

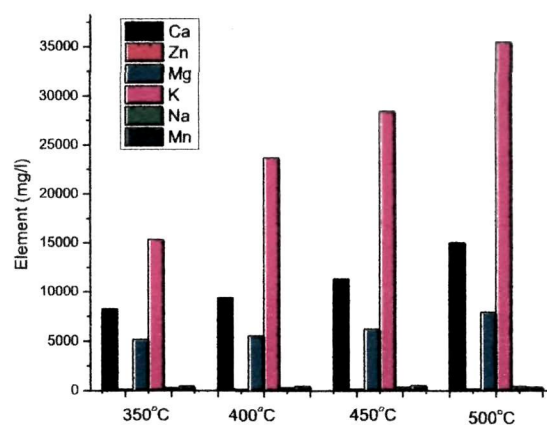


Figure 4.31: Inorganic element constituents of MFDC biochar at different temperature.

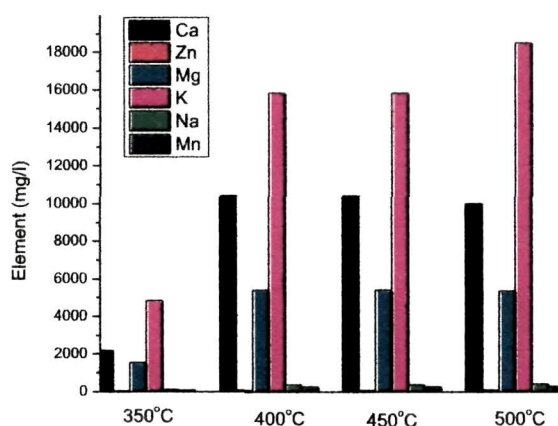


Figure 4.32: Inorganic element constituents of PGDC biochar at different temperature.

The thermal decomposition of biomass represents the chemical bonds presenting in biomass to break and release volatile gases as temperature increases to a specific point. Therefore, there might be a relationship between the chemical structure of solid charcoal (identified by FTIR) and the composition of released gases at different final temperatures. The FTIR spectra of solid char from MFDC pyrolysis at different final temperatures are plotted in Figure 4.33. It can be observed in Figure 4.33 that the broad band appears near 3400 cm^{-1} of O-H absorbance diminished sharply to zero with the increase in final temperature, which might be attributed to the dehydration of biomass, and at the same time, a large amount of water was released [58, 59]. The C-H (alkenes) absorbance amount also decreased to zero as temperature increased to 500°C , possibly caused by the break of the weak bonds between C and H of alkyl. The breaking of C-H functional groups brought some CH_4 and C_2H_4 being released and gave rise to the contents of CH_4 and C_2 hydrocarbon in the gas products [60]. The functional groups of C=O in biomass are easy to break with a large amount of CO and CO_2 evolving out and the absorbance of C=O (1700 cm^{-1}) decreased significantly as temperature increased. With the increase in final pyrolysis temperature, the peaks of C=C ar. (1620 cm^{-1}), C-H ar. (790 cm^{-1}) start to break stepwise to form volatiles. The cracking and reforming of aromatic rings give rise to H_2 and it is in accordance with the previous experimental finding of Yang *et al.*, where it was observed that H_2 yield increased with increase in final pyrolysis temperature [60].

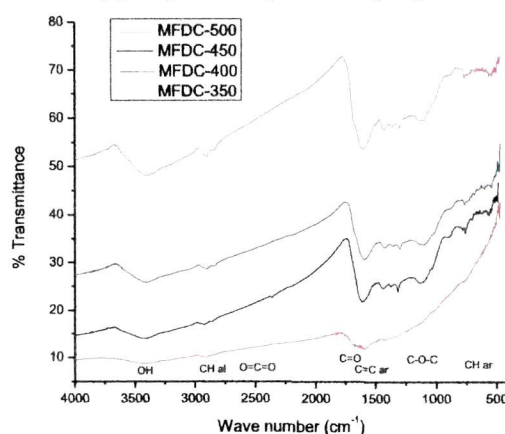


Figure 4.33: FTIR spectra of MFDC biochar at different temperature.

X-ray diffraction is a widely applicable technique for analyzing the biomass crystallinity and the biochar structure. The XRD spectra (Figures 4.34 and 4.35) of biochar show a broad peak at the 2θ values of around 20 – 30. The peak appeared for biochar, indicated the development of increasingly carbonized material [61] and gives evidence of presence of graphitic structure in the biochar. This peak comes from the formation and successive ordering of aromatic carbon in the biochar [62]. The presence of higher amount of aromatic compound in the biochar as evidenced from FTIR spectra was further supported by the XRD pattern.

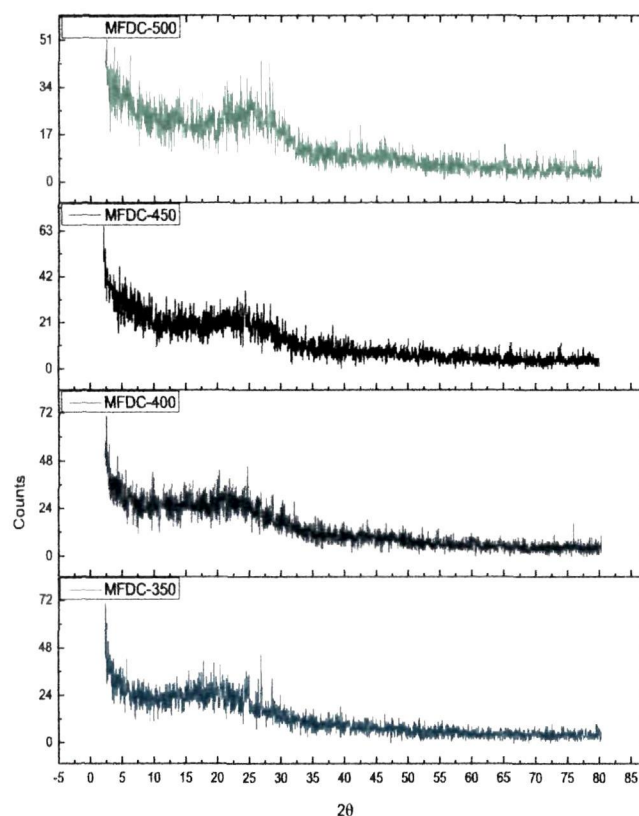


Figure 4.34: XRD pattern of MFDC biochar at different temperature.

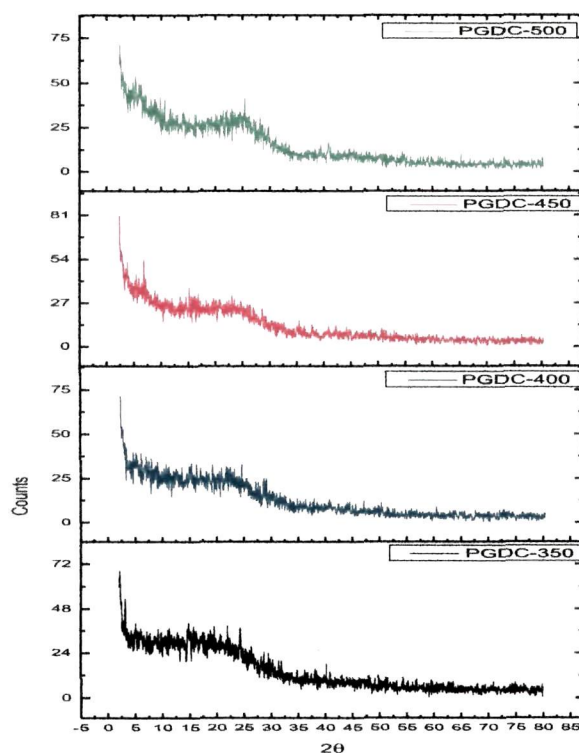


Figure 4.35: XRD pattern of PGDC biochar at different temperature.

The surface morphology of the biochar was studied by Scanning Electron Microscopy (SEM). The SEM images of the MFDC and PGDC biochars obtained at different temperatures at a heating rate of 40°C/min are shown in Figures 4.36 and 4.37. The SEM images confirmed the amorphous and heterogeneous structure of the biochars obtained from both the feedstock. It was observed that the biochars of MFDC and PGDC obtained at 500°C have a porous structure with identical surface area of $\sim 7 \text{ m}^2/\text{g}$. The pore volumes of MFDC and PGDC biochars were found to be 0.051 and 0.046 cm^3/g respectively. These properties of the biochars argues well for not being appropriate for direct usage as activated carbon application, however these co-products of biomass pyrolysis provides a scope for activation further through chemical or physical treatment for their usage as activated carbon or as a support material for solid catalyst.

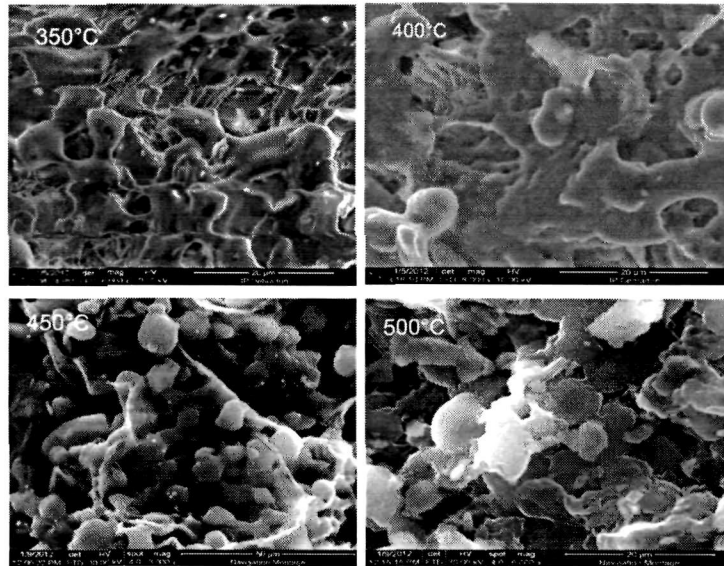


Figure 4.36: SEM micrographs of MFDC biochar at different temperature.

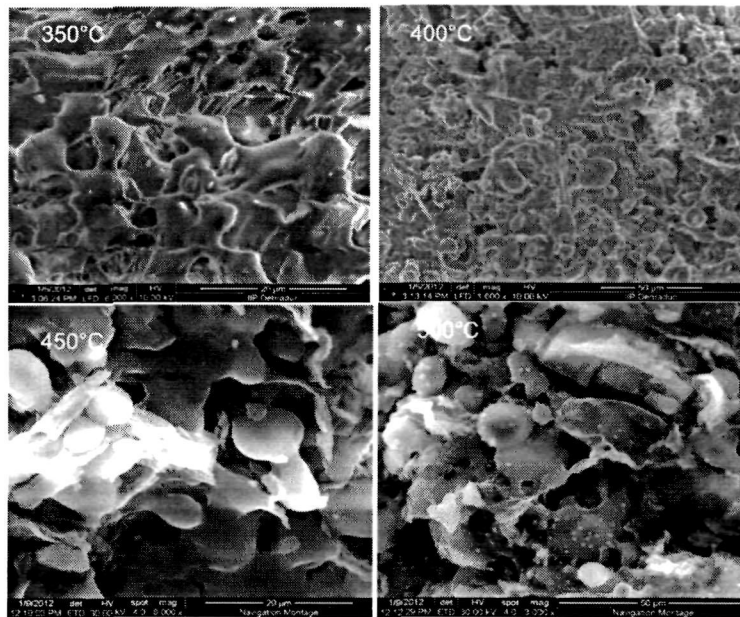


Figure 4.37: SEM micrographs of PGDC biochar at different temperature.

4-1.5 Pyrolysis of mixed feedstock

As discussed in the first chapter, the existent available bio-energy feedstock cannot suffice for the petro-crude reservoirs; consequently new feedstock for the same will serve as a cumulative step for addressing the long documented problem of energy production and supply. Therefore, this section of the study targets to investigate the potentiality of mixed type of feedstock for pyrolysis. For this purpose, MFDC and PGDC feedstock with particle size of 420 μ were mixed in a 1:1 ratio and pyrolyzed at 500°C with a heating rate of 40°C/min, as both the feedstock showed a maximum liquid product yield at this pyrolytic condition. The liquid, solid and gaseous product yield from this mixed feedstock was found to be 30.4%, 29.8% and 39.8%, respectively.

Table 4.19: Comparison of properties of the (MFDC+PGDC) with MFDC and PGDC bio-oil

Properties	MFDC Bio-oil ^a	PGDC Bio-oil ^a	Mixed feedstock (MFDC+PGDC) bio-oil ^a
Ultimate analysis			
C	59.3	55.4	58.57
H	8.8	7.6	7.78
N	6.4	6.7	7.7
O ^b	25.5	30.3	25.95
Empirical formula	C _{10.81} H _{19.25} NO _{3.49}	C _{9.65} H _{15.88} NO _{3.95}	C _{8.87} H _{14.15} NO _{2.95}
H/C molar ratio	1.78	1.65	1.59
O/C molar ratio	0.32	0.41	0.33
Higher heating value (MJ/kg)	30.63	28.19	30.26
Ash	0.30	0.39	0.43
Density (kg/m ³)	1075	1051	1075
Acid number (mg KOH/g)	42.71	45.20	45.12

^a Obtained at 500°C with heating rate 40°C/min

^b By difference

The bio-oil from mixed feedstock showed similar properties with individual bio-oil (Table 4.18). However, differences in composition to that of PGDC and MFDC bio-oil are found through NMR (Tables 4.20 and 4.21) and GC-MS (Figure 4.39 and Table 4.22). This is expected as feedstock composition greatly influences the bio-oil composition as discussed in chapter 2.

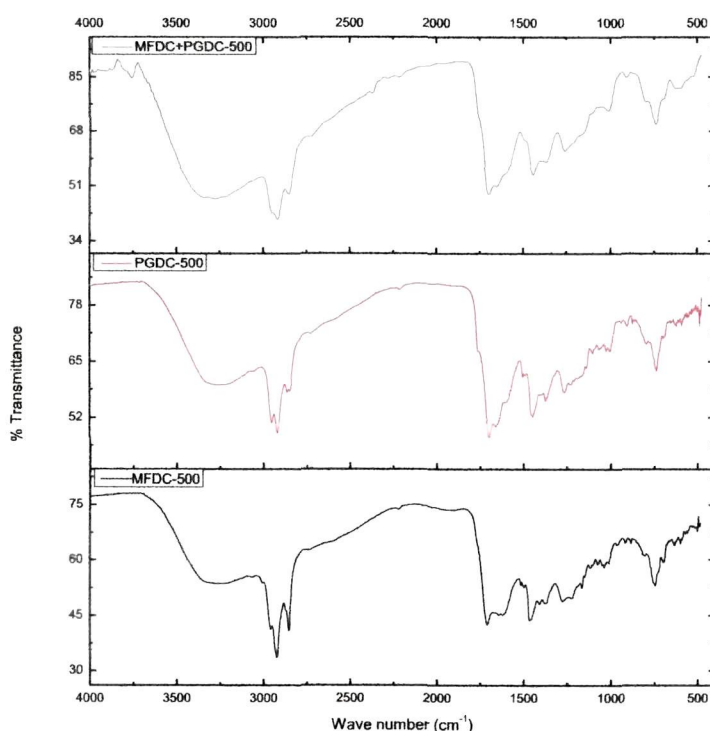
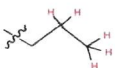
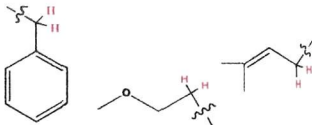
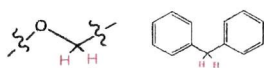
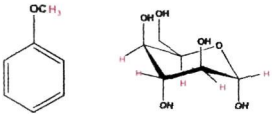
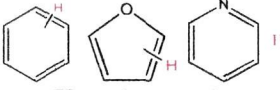
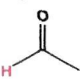


Figure 4.38: FTIR spectrum of (MFDC+PGDC) bio-oil compared with bio-oil from MFDC and PGDC.


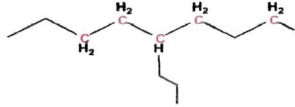
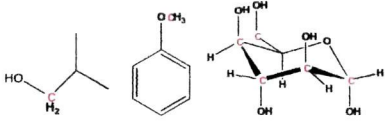
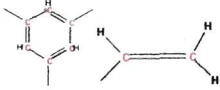
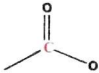
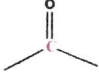
Figure 4.38 shows the FTIR spectrum of mixed feedstock bio-oil compared with individual bio-oil from MFDC and PGDC. The spectrum shows the presence of similar types of functionalities present in the mixed feedstock bio-oil. Presence of different functionalities according to wave number is already discussed in the previous section.

Table 4.20: Percentage of hydrogen based on ¹H-NMR analysis of (MFDC+PGDC) bio-oil and individual bio-oil, grouped according to chemical shift range^a

Chemical shift (ppm)	Proton assignment	MFDC bio-oil (%)	PGDC bio-oil (%)	MFDC+PGDC bio-oil (%)
0.5-1.5	 Alkanes	51.65	46.19	52
1.5-3	 Aliphatics α -heteroatoms or unsaturation	27.19	10.1	31
3-4.5	 Alcohols, methylene diabenzene	5.19	20.6	4
4.5-6	 Methoxys, carbohydrates	7.87	21.11	8
6-8.5	 (Hetero)-aromatics	5.23	1.8	4
8.5-10	 ALdehydes	2.87	0.67	2

^a Highlighted atoms shown in representative chemical functional groups are intended only to indicate the potential types of chemical environments that may be present. The real mixtures may contain significant structural diversity

Table 4.21: Percentage of carbon based on ^{13}C -NMR analysis of (MFDC+PGDC) bio-oil and individual bio-oil, grouped according to chemical shift range^a

Chemical shift (ppm)	Carbon assignment	MFDC bio-oil (%)	PGDC bio-oil (%)	MFDC+PGDC bio-oil (%)
0-28		32.44	46.19	36
28-55	 Long and branched aliphatics	28.21	10.10	20
55-95	 Alcohols, ethers, phenolic-methoxys, carbohydrate sugars	4.28	22.60	21
95-165	 Aromatics, olefins	34.19	21.11	21
165-180	 Esters, carboxylic acids	0.60	1.80	1
180-215	 Ketones, aldehydes	0.28	0.67	1

^aHighlighted atoms shown in representative chemical functional groups are intended to only indicate the potential types of chemical environments that may be present. The real mixtures may contain significant structural diversity

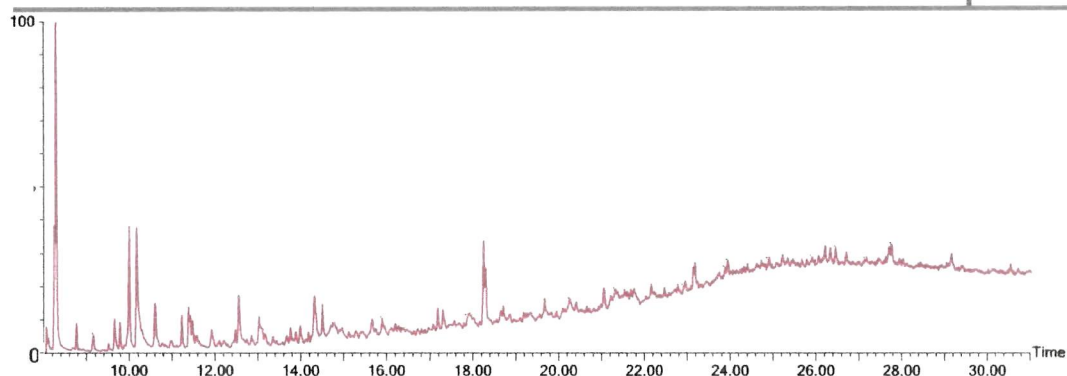


Figure 4.39: Total ion chromatogram of MFDC+PGDC (1:1) bio-oil.

Table 4.22: Chemical compounds in (MFDC+PGDC) bio-oil (GC-MS)

Sl. No.	RT	Area%	Name	MW	Formula
1	8.73	0.76	Toluene	92	C ₇ H ₈
2	9.12	0.53	2-butenal, 2-methyl-	84	C ₅ H ₈ O
3	9.96	2.34	Ethanol, pentamethyl-	116	C ₇ H ₁₆ O
4	10.13	3.76	(1S,5R)-6,8-Dioxabicyclo[3.2.1]oct-2-en-4-one or	126	C ₆ H ₆ O ₃
5	11.19	-	Styrene	104	C ₈ H ₈
6	11.35	0.60	2-methylcyclopent-2-enone	96	C ₆ H ₈ O
7	11.38	-	4-pyridinol	95	C ₅ H ₅ N ₀
8	11.43	0.61	1,2,5-trimethylpyrrole	109	C ₇ H ₁₁ N
9	11.88	-	Pyridine, 3,4-dimethyl-	107	C ₇ H ₉ N
10	12.44	-	Pyridine, 3-ethyl-	107	C ₇ H ₉ N
11	12.52	1.47	1h-pyrrole, 2,4-dimethyl-	95	C ₆ H ₉ N
12	12.99	1.02	Benzaldehyde, oxime	121	C ₇ H ₇ NO
13	13.72	-	Benzeneethanol, .beta.-ethenyl-	148	C ₁₀ H ₁₂ O
14	13.95	0.82	Phenol, 3-methyl-	108	C ₇ H ₈ O
15	14.29	1.39	Phenol, 4-methyl-	108	C ₇ H ₈ O
16	14.47	0.76	Benzeneacetic acid, .alpha.-oxo-, methyl ester	164	C ₉ H ₈ O ₃
17	15.62	0.87	Phenol, 2,4-dimethyl-	122	C ₈ H ₁₀ O
18	15.86	0.78	Phenol, 4-ethyl-	122	C ₈ H ₁₀ O
19	14.14	0.99	2-ethyl-5-propylcyclopentanone		C ₁₀ H ₁₈ O
20	18.21	1.45	2,2'-bifuran	134	C ₈ H ₆ O ₂
21	18.26	1.08	Indole	117	C ₈ H ₇ N
22	19.63	0.58	Indolizine, 2-methyl-	131	C ₉ H ₉ N
23	20.22	0.953	5-hydroxymethylfurfural	126	C ₆ H ₆ O ₃
24	21.72	0.62	Indole-2-carboxylic acid	161	C ₉ H ₇ NO ₂
25	23.91	0.77	3-ethoxy-4-methoxyphenol	168	C ₉ H ₁₂ O ₃
26	24.87	1.50	Furfuryl alcohol	97	C ₅ H ₅ O ₂
27	26.42	1.22	Phenol, 3,5-dimethoxy-	154	C ₈ H ₁₀ O ₃

RT-Retention time, MW- Molecular weight

Figure 4.40 shows the distillation characteristics of MFDC, PGDC and mixed feedstock (MFDC+PGDC) bio-oil obtained via simulated distillation. Table 4.23 shows percent mass of material recovered in the analysis, IBP and FBP. The IBP is the temperature at which a cumulative yield is equal to 0.5% of the total sample. The FBP is the temperature at which a cumulative yield is equal to 99.5% of the total sample.

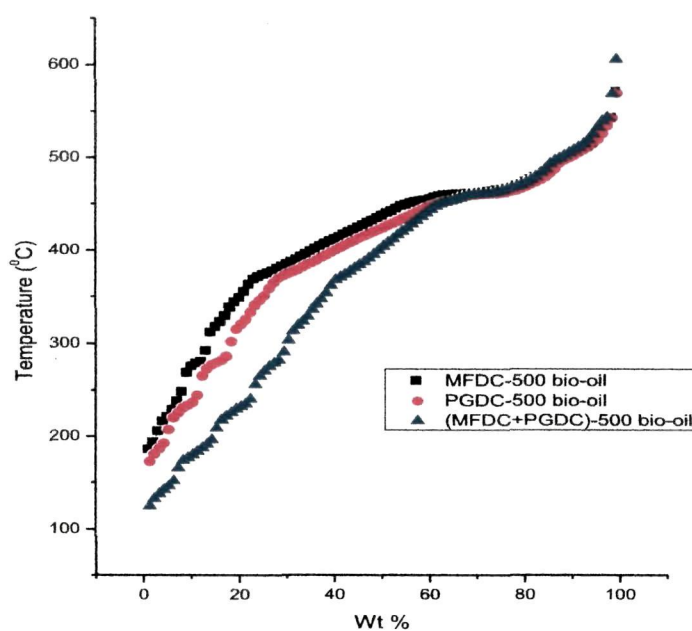


Figure 4.40: Distillation characteristics of bio-oil obtained via simulated distillation.

Table 4.23: Percentage of distillation cut point of bio-oil obtained via simulated distillation

Cut point (°C)	% (MFDC-500 bio-oil)	% (PGDC-500 bio-oil)	Cut point (°C)	% [(MFDC+PGDC)-500 bio-oil]	Description as per petro-crude
9	<IBP	<IBP	9	<IBP	C4
170	<IBP	<IBP	IBP-170	7.37	Naphtha type
IBP-350	20.1	24.66	170-350	29.91	Kerosene type
350-FBP	78.9	74.34	350-FBP	61.72	Residue 350+

Due to the complex nature, all the bio-oil exhibited a broader range of boiling points as shown in Figure 4.40 and Table 4.23. The IBP and FBP for bio-oil were (180 & 598.8°C), (135 & 598.2°C) and (83.4 & 613.3°C) for MFDC, PGDC and MFDC+PGDC bio-oil, respectively. It can be observed from the SimDist analysis that more than 60% compounds of all the bio-oil have boiling point above 350°C.

A robust pyrolytic system should be able to withstand feedstock of similar nature. In the present attempt, it was of interest to know, the probable variation if any in the pyrolytic products distribution and their characteristics, when individual feedstock are mixed. The information generated indicates that by mixing feedstock of similar nature, pyrolytic product distribution and their characteristics are not significantly varied. This is important as a pyrolytic system should have inbuilt flexibility to handle a mixture of feedstock of similar nature for its sustainable operation. This is also important from the point of view of biomass supply.

References:

- [1] Naik, S., et al. Characterization of Canadian biomass for alternative renewable biofuel. *Renewable Energy*, **35** (8), 1624-1631, 2010.
- [2] Choudhury, N.D., et al. Pyrolysis of jute dust: effect of reaction parameters and analysis of products. *Journal of Material Cycles and Waste Management*, **16** (3), 449-459, 2014.
- [3] Gu, S., et al. A detailed study of the effects of pyrolysis temperature and feedstock particle size on the preparation of nanosilica from rice husk. *Industrial Crops and Products*, **50** (0), 540-549, 2013.
- [4] Ates, F. & Isakdag, M.A. Evaluation of the role of the pyrolysis temperature in straw biomass samples and characterization of the oils by GC/MS. *Energy & Fuels*, **22** (3), 1936-1943, 2008.
- [5] Putun, A.E., Apaydin, E., & Putun, E. Rice straw as a bio-oil source via pyrolysis and steam pyrolysis. *Energy*, **29** (12-15), 2171-2180, 2004.
- [6] Mangut, V., et al. Thermogravimetric study of the pyrolysis of biomass residues from tomato processing industry. *Fuel Processing Technology*, **87** (2), 109-115, 2006.
- [7] McKendry, P. Energy production from biomass (Part 1): Overview of biomass. *Bioresource Technology*, **83** (1), 37-46, 2002.
- [8] Bilba, K., Arsene, M.A., & Ouensanga, A. Study of banana and coconut fibers Botanical composition, thermal degradation and textural observations. *Bioresource Technology*, **98** (1), 58-68, 2007.
- [9] Stuart, B.H., *Infrared Spectroscopy: Fundamentals and Applications*, John Wiley & Sons, 2004.
- [10] Dumas, P. & Miller, L. The use of synchrotron infrared microspectroscopy in biological and biomedical investigations. *Vibrational Spectroscopy*, **32** (1), 3-21, 2003.

- [11] Backmann, J., et al. Thermally induced hydrogen exchange processes in small proteins as seen by FTIR spectroscopy. *Proteins: Structure, Function, and Bioinformatics*, **24** (3), 379-387, 1996.
- [12] Fischer, G., et al. FT-IR spectroscopy as a tool for rapid identification and intra-species characterization of airborne filamentous fungi. *Journal of Microbiological Methods*, **64** (1), 63-77, 2006.
- [13] Wolkers, W.F., et al. A Fourier-transform infrared spectroscopy study of sugar glasses. *Carbohydrate Research*, **339** (6), 1077-85, 2004.
- [14] Yee, N., et al. Characterization of metal-cyanobacteria sorption reactions: a combined macroscopic and infrared spectroscopic investigation. *Environmental Science & Technology*, **38** (3), 775-82, 2004.
- [15] Wolpert, M. & Hellwig, P. Infrared spectra and molar absorption coefficients of the 20 alpha amino acids in aqueous solutions in the spectral range from 1800 to 500 cm^{-1} . *Spectrochimica Acta Part A: Molecular and Biomolecular Spectroscopy*, **64** (4), 987-1001, 2006.
- [16] Hujuri, U., Ghoshal, A.K., & Gumma, S. Modeling pyrolysis kinetics of plastic mixtures. *Polymer Degradation and Stability*, **93** (10), 1832-1837, 2008.
- [17] Hu, S., Jess, A., & Xu, M.H. Kinetic study of Chinese biomass slow pyrolysis: Comparison of different kinetic models. *Fuel*, **86** (17-18), 2778-2788, 2007.
- [18] Li, D., et al. Pyrolytic characteristics and kinetics of two brown algae and sodium alginate. *Bioresource Technology*, **101** (18), 7131-7136, 2010.
- [19] Li, D., et al. Pyrolytic characteristics and kinetic studies of three kinds of red algae. *Biomass & Bioenergy*, **35** (5), 1765-1772, 2011.
- [20] Idris, S.S., et al. Investigation on thermochemical behaviour of low rank Malaysian coal, oil palm biomass and their blends during pyrolysis via thermogravimetric analysis (TGA). *Bioresource Technology*, **101** (12), 4584-4592, 2010.

- [21] Lapuerta, M., Hernandez, J.J., & Rodriguez, J. Kinetics of devolatilisation of forestry wastes from thermogravimetric analysis. *Biomass & Bioenergy*, **27** (4), 385-391, 2004.
- [22] Açıklın, K. Pyrolytic characteristics and kinetics of pistachio shell by thermogravimetric analysis. *Journal of Thermal Analysis and Calorimetry*, **109** (1), 227-235, 2011.
- [23] Tonbul, Y. Pyrolysis of pistachio shell as a biomass. *Journal of Thermal Analysis and Calorimetry*, **91** (2), 641-647, 2008.
- [24] Kim, P., et al. Surface functionality and carbon structures in lignocellulosic-derived biochars produced by fast pyrolysis. *Energy & Fuels*, **25** (10), 4693-4703, 2011.
- [25] Onay, O. Influence of pyrolysis temperature and heating rate on the production of bio-oil and char from safflower seed by pyrolysis, using a well-swept fixed-bed reactor. *Fuel Processing Technology*, **88** (5), 523-531, 2007.
- [26] Chen, G., Yu, Q., & Sjöström, K. Reactivity of char from pyrolysis of birch wood. *Journal of Analytical and Applied Pyrolysis*, **40-41** (0), 491-499, 1997.
- [27] Sensoz, S. & Angin, D. Pyrolysis of safflower (*Charthamus tinctorius* L.) seed press cake: part 1. The effects of pyrolysis parameters on the product yields. *Bioresource Technology*, **99** (13), 5492-7, 2008.
- [28] Horne, P.A. & Williams, P.T. Influence of temperature on the products from the flash pyrolysis of biomass. *Fuel*, **75** (9), 1051-1059, 1996.
- [29] Zanzi, R., Sjöström, K., & Björnbom, E. Rapid pyrolysis of agricultural residues at high temperature. *Biomass and Bioenergy*, **23** (5), 357-366, 2002.
- [30] Laresgoiti, M.F., et al. Characterization of the liquid products obtained in tyre pyrolysis. *Journal of Analytical and Applied Pyrolysis*, **71** (2), 917-934, 2004.
- [31] Encinar, J.M., González, J.F., & González, J. Fixed-bed pyrolysis of *Cynara cardunculus* L. Product yields and compositions. *Fuel Processing Technology*, **68** (3), 209-222, 2000.

- [32] Chan, W.C.R., Kelbon, M., & Krieger-Brockett, B. Single-particle biomass pyrolysis: correlations of reaction products with process conditions. *Industrial & Engineering Chemistry Research*, **27** (12), 2261-2275, 1988.
- [33] Haykiri-Acma, H. The role of particle size in the non-isothermal pyrolysis of hazelnut shell. *Journal of Analytical and Applied Pyrolysis*, **75** (2), 211-216, 2006.
- [34] Shen, J., et al. Effects of particle size on the fast pyrolysis of oil mallee woody biomass. *Fuel*, **88** (10), 1810-1817, 2009.
- [35] Pütün, A.E., et al. Fixed-bed pyrolysis and hydrolysis of sunflower bagasse: Product yields and compositions. *Fuel Processing Technology*, **46** (1), 49-62, 1996.
- [36] Encinar, J.M., et al. Pyrolysis of two agricultural residues: Olive and grape bagasse. Influence of particle size and temperature. *Biomass and Bioenergy*, **11** (5), 397-409, 1996.
- [37] Şensöz, S., Angın, D., & Yorgun, S. Influence of particle size on the pyrolysis of rapeseed (*Brassica napus* L.): fuel properties of bio-oil. *Biomass and Bioenergy*, **19** (4), 271-279, 2000.
- [38] Onay, O. & Mete Koçkar, O. Fixed-bed pyrolysis of rapeseed (*Brassica napus* L.). *Biomass and Bioenergy*, **26** (3), 289-299, 2004.
- [39] Bridgwater, A.V. & Peacocke, G.V.C. Fast pyrolysis processes for biomass. *Renewable and Sustainable Energy Reviews*, **4** (1), 1-73, 2000.
- [40] Carlson, T.R., Vispute, T.P., & Huber, G.W. Green gasoline by catalytic fast pyrolysis of solid biomass derived compounds. *ChemSusChem*, **1** (5), 397-400, 2008.
- [41] Wang, P., et al. The effects of temperature and catalysts on the pyrolysis of industrial wastes (herb residue). *Bioresource Technology*, **101** (9), 3236-3241, 2010.
- [42] Demiral, İ., Eryazıcı, A., & Şensöz, S. Bio-oil production from pyrolysis of corncob (*Zea mays* L.). *Biomass and Bioenergy*, **36** 43-49, 2012.

- [43] Zou, S., et al. Thermochemical catalytic liquefaction of the marine microalgae *Dunaliella tertiolecta* and characterization of bio-oils. *Energy & Fuels*, **23** (7), 3753-3758, 2009.
- [44] Lu, Q., Yang, X.-l., & Zhu, X.-f. Analysis on chemical and physical properties of bio-oil pyrolyzed from rice husk. *Journal of Analytical and Applied Pyrolysis*, **82** (2), 191-198, 2008.
- [45] Göring, M., Larsson, M., & Alvfors, P. Bio-methane via fast pyrolysis of biomass. *Applied Energy*, **112** (0), 440-447, 2013.
- [46] Mohan, D., Pittman, C.U., & Steele, P.H. Pyrolysis of wood/biomass for bio-oil: A critical review. *Energy & Fuels*, **20** (3), 848-889, 2006.
- [47] Mullen, C.A., Strahan, G.D., & Boateng, A.A. Characterization of various fast-pyrolysis bio-oils by NMR spectroscopy. *Energy & Fuels*, **23** (5), 2707-2718, 2009.
- [48] Joseph, J., et al. Chemical shifts and lifetimes for nuclear magnetic resonance (NMR) analysis of biofuels. *Energy & Fuels*, **24** (9), 5153-5162, 2010.
- [49] Thring, R.W., Katikaneni, S.P.R., & Bakhshi, N.N. The production of gasoline range hydrocarbons from Alcell® lignin using HZSM-5 catalyst. *Fuel Processing Technology*, **62** (1), 17-30, 2000.
- [50] Carlson, T.R., et al. Aromatic production from catalytic fast pyrolysis of biomass-derived feedstocks. *Topics in Catalysis*, **52** (3), 241-252, 2009.
- [51] Strahan, G.D., Mullen, C.A., & Boateng, A.A. Characterizing biomass fast pyrolysis oils by ¹³C NMR and chemometric analysis. *Energy & Fuels*, **25** (11), 5452-5461, 2011.
- [52] Leonardis, I., et al. Characterization of bio-oil from hydrothermal liquefaction of organic waste by NMR spectroscopy and FTICR mass spectrometry. *ChemSusChem*, **6** (1), 160-7, 2013.
- [53] Ucar, S. & Ozkan, A.R. Characterization of products from the pyrolysis of rapeseed oil cake. *Bioresource Technology*, **99** (18), 8771-6, 2008.

- [54] Agrawalla, A., Kumar, S., & Singh, R.K. Pyrolysis of groundnut de-oiled cake and characterization of the liquid product. *Bioresource Technology*, **102** (22), 10711-10716, 2011.
- [55] Branca, C., Giudicianni, P., & Di Blasi, C. GC/MS characterization of liquids generated from low-temperature pyrolysis of wood. *Industrial & Engineering Chemistry Research*, **42** (14), 3190-3202, 2003.
- [56] Tang, M.M. & Bacon, R. Carbonization of cellulose fibers—I. Low temperature pyrolysis. *Carbon*, **2** (3), 211-220, 1964.
- [57] Brewer, C.E., et al. Characterization of biochar from fast pyrolysis and gasification systems. *Environmental Progress & Sustainable Energy*, **28** (3), 386-396, 2009.
- [58] Bilba, K. & Ouensanga, A. Fourier transform infrared spectroscopic study of thermal degradation of sugar cane bagasse. *Journal of Analytical and Applied Pyrolysis*, **38** (1-2), 61-73, 1996.
- [59] Yang, H., et al. Thermogravimetric analysis-fourier transform infrared analysis of palm oil waste pyrolysis. *Energy & Fuels*, **18** (6), 1814-1821, 2004.
- [60] Yang, H.P., et al. Mechanism of palm oil waste pyrolysis in a packed bed. *Energy & Fuels*, **20** (3), 1321-1328, 2006.
- [61] Keiluweit, M., et al. Dynamic molecular structure of plant biomass-derived black carbon (biochar). *Environmental Science & Technology*, **44** (4), 1247-1253, 2010.
- [62] Kim, K.H., et al. Influence of pyrolysis temperature on physicochemical properties of biochar obtained from the fast pyrolysis of pitch pine (*Pinus rigida*). *Bioresource Technology*, **118** (0), 158-162, 2012.

Chapter 4 (b)

Prospect of utilization of bio-oil

Chapter 4 (b): Prospect of utilization of bio-oil

4-2.1 Prospect of utilization of bio-oil

The energy intensive future research scenario has high lightened the importance of biomass conversion as a promising route for biofuel production. In wake of recent advancements in bioenergy research, bio-oils have already gathered the attention of the scientific community in that they offer prospective applicability as a source of value added chemical apart from being an increasingly attractive fuel option.

Antibiotics have always been considered as one of greatest discoveries of the past century. However, owing to the cost effectiveness, safety, increasing failure of chemotherapy and antibiotic resistance, search for plant resources has considerably increased for their potential antimicrobial activity [1]. The most significant bioactive compounds reported from plants are alkaloids, tannins, flavonoids, and phenolic compounds [2]. Alkaloids possesses antimicrobial, anticancer, antimalarial and cytotoxic properties while flavonoids have high antibacterial activity and are more efficient in treatment of inflammation, allergy, cancer, viral infection and hypertension [3]. Tannin has high activities against bacterial and viral infections and also acts as strong antioxidant [4]. The chemical compounds responsible for the antibacterial activity in algae have been variously identified as organic and fatty acids, terpenes, carbonyls, bromophenols, halogenated aliphatic and sulfur-containing heterocyclic compounds, isoprenylated and brominated hydroquinones, as well as phlorotannins [5, 6]. The study of natural products from the plant kingdom has long been the source of pharmaceuticals, and as such it makes sense that bio-oil may possess new functional moieties with prospective pharmaceutical value. There is paucity of evidence regarding possession of antimicrobial activity by bio-oil. Only a few reports pertaining to antifungal activity of bio-oil have been reported till date [7, 8]. In this regard, the present study was carried out to investigate the utility of bio-oil, produced via pyrolysis process (from MFDC and PGDC), as an antimicrobial agent against gram

positive and gram negative bacteria [*Staphylococcus aureus* (MTCC96) and *Escherichia coli* (MTCC723)] with a view to sincerely realize the value addition of bio-oils. An attempt was also made to assess the antimicrobial activity against eukaryotic systems [*Candida albicans* (ATCC 183) and *Saccharomyces cerevisiae* (ATCC 4126)].

The bioassay results for antimicrobial activity of the respective bio-oil samples are shown in Figure 4.41.

Table 4.24: Bioassay results for antimicrobial activity of MFDC and PGDC bio-oil

Species	Bio-oil	ZOI (mm)	t-value
<i>S. cerevisiae</i>	MFDC	20.36±0.32	0.68
<i>S. cerevisiae</i>	PGDC	20.60±0.52	
<i>C. albicans</i>	MFDC	20.10±0.36	6.01
<i>C. albicans</i>	PGDC	22.47±0.45	
<i>S. aureus</i>	MFDC	29.20±0.43	3.12
<i>S. aureus</i>	PGDC	28.03±0.35	
<i>E. coli</i>	MFDC	15.37±0.40	23.52
<i>E. coli</i>	PGDC	22.17±0.30	

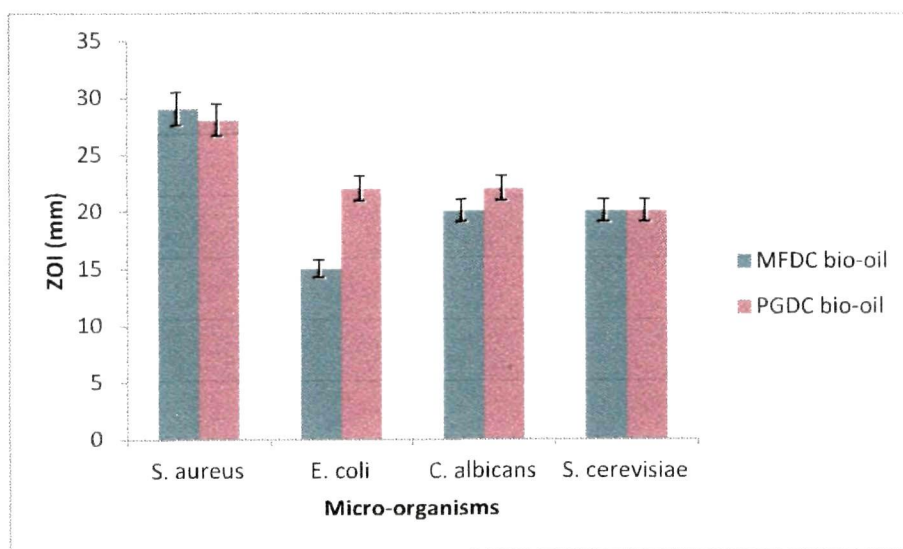


Figure 4.41: Antimicrobial activity histogram for MFDC and PGDC bio-oil samples.

Figures 4.42 and 4.43 shows the Zone of Inhibition (ZOI) produced by the bio-oil samples MFDC and PGDC on the test micro-organisms e.g. *S. cerevisiae*, *S. aureus*, *C. albicans* and *E. coli*. The ZOI of the sample extract was compared with the standard antibiotic chloramphenicol for antibacterial and Indofil M-45 (commercial antifungal) for antifungal and antiyeast assay. All the tested samples showed varying degree of antimicrobial activity against the tested micro-organisms. From Table 4.23 and Fig 4.42 it can be concluded that, MFDC bio-oil showed maximum ZOI against *S. aureus* (29 mm) and moderate against *E. coli* (15 mm). Similarly, PGDC bio-oil exhibited highest antibacterial activity against *S. aureus* (28 mm) and comparatively lesser activity against *E. coli* (22 mm). MFDC bio-oil was found to be more effective against gram positive bacteria whereas, PGDC bio-oil against gram negative bacteria.

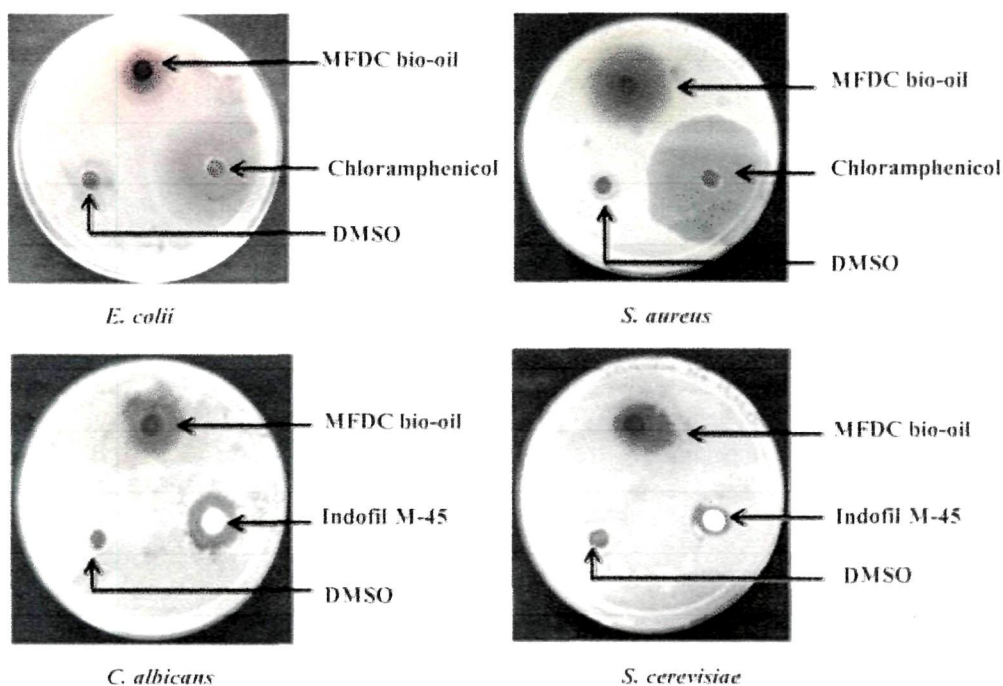


Figure 4.42: Inhibition zones of MFDC bio-oil against *E. coli*, *S. aureus*, *S. cerevisiae* and *C. albicans*.

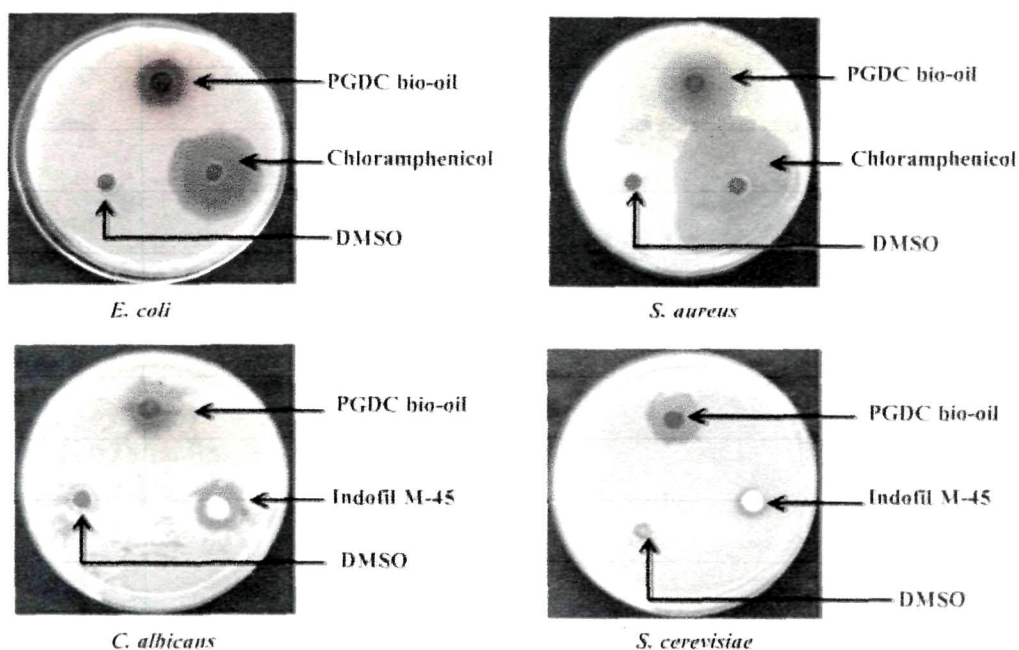


Figure 4.43: Inhibition zones of PGDC bio-oil against *E. coli*, *S. aureus*, *S. cerevisiae* and *C. albicans*.

Antifungal activity against human pathogens is highly sought after in pharmaceutical and pharmacological research. In this regard, antifungal assay was performed to evaluate the activity of the bio-oil samples against *C. albicans*. MFDC bio-oil showed a 20 mm ZOI against *C. albicans* whereas PGDC bio-oil showed a comparatively higher 22 mm zone. Both MFDC and PGDC bio-oil showed a 20 mm ZOI against *S. cerevisiae*. Performing the t-test for equality of two means it was observed that there is no significant difference between MFDC and PGDC bio-oil activity on *S. cerevisiae* ($t < \text{critical value } 2.132$ for 95% confidence level, Table 4.24). However, significant difference between both bio-oils were observed in case of activity on *C. albicans*, *S. aureus* and *E. coli*. ($t > \text{critical value } 2.132$ for 95% confidence level, Table 4.24).

Minimum inhibition concentration of both the bio-oil samples viz., MFDC and PGDC at different concentrations (100, 50, 25, 12.5, 6.25, 3.125, 1.56 and 0.78 $\mu\text{g/ml}$) was determined against two prokaryotic and two eukaryotic systems. After 24 hours / and 48 hours of incubation the cultures were subjected to MTT assay. Kanamycin (50mg/ml) and Indofil (50 mg/ml) were used as positive control and cells mixed with DMSO (1%) as negative control.

A concentration-dependent increase in inhibition of prokaryotic and eukaryotic cells was observed for all the three samples. MIC for MFDC bio-oil was minimum and it inhibits *E. coli* and *S. aureus* at concentrations of 1.56 and 3.12 $\mu\text{g/ml}$. On the contrary, higher concentration was required against eukaryotes viz., *C. albicans* (3.12 $\mu\text{g/ml}$) and *S. cerevisiae* (6.25 $\mu\text{g/ml}$). Antagonism of PGDC bio-oil against all the tested strains except *S. cerevisiae* was same. A concentration of 6.25 $\mu\text{g/ml}$ was required to inhibit the growth of *E. coli*, *S. aureus*, and *S. cerevisiae*, whereas for *C. albicans* a higher concentration of 12.5 $\mu\text{g/ml}$ was required.

Chemically, bio-oil is a complex mixture of water, guaiacols, syringols, furancarboxaldehydes, pyrones, isoeugenol, vanillins, catechols, acetic acid, formic acid and other carboxylic acids [9]. Bio-oils also contain other major group of compounds including hydroxyaldehydes, hydroxyketones, sugars, carboxylic acid and phenols [10]. Figure 4.44 presents the FTIR spectra for MFDC and PGDC bio-oils.

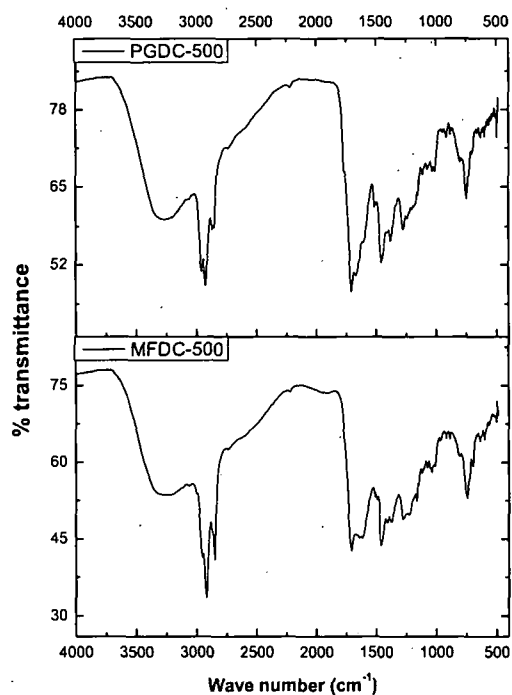


Figure 4.44: FTIR spectrum of MFDC and PGDC.

The FTIR spectra for both the bio-oils are almost similar due to the presence of similar functional groups. The major spectral assignments are C-H stretch (2928 cm^{-1}), CH_2 (bend) [1465 cm^{-1}], O-H (H bonded) [$3400\text{-}3200\text{ cm}^{-1}$], C=O ($1700\text{-}1725\text{ cm}^{-1}$) and CH_2 (rocking) [743 cm^{-1}]. The FTIR spectra of the bio-oil samples show the presence of hydroxyl group which is common in all phenolic compounds. The C=O (attributed to the presence of carboxylic acids) was another important functional component observed in the spectra of the bio-oils. Phenolic compounds have been reported to be associated with antifungal activity [11], whereas carboxylic acids with many antibacterial and antimicrobial activities [12].

Since, bio-oils are obtained from plant feedstock it is arguable to expect a diversity of compounds (obtainable by breakdown of larger polymers to simple compounds) in bio-oils with specific as well as broad-spectrum antimicrobial activity. The exploitation of bio-oil for the discovery of pharmaceutically important products is a futuristic top notch research area with tremendous biological prospects. Ongoing research

is currently focused on the isolation, identification and characterization of compounds responsible for bioactivity of bio-oils with high antimicrobial activity.

Bio-oils, if properly investigated may offer an unexplored repertoire for chemicals with huge potential to provide significant therapeutic benefits for the human civilization. From the above study, it can be concluded that MFDC bio-oil was found to be most effective against the growth of *S. aureus*, whereas PGDC bio-oil against *E. coli* and *C. albicans*. PGDC bio-oil was found to be moderately effective against prokaryotic system whereas, completely ineffective against eukaryotic systems. Antimicrobial activity exhibited by two of the bio-oil samples viz., MFDC and PGDC used in this study indicates that they possess bioactive natural products (may lead to development of new pharmaceuticals), and henceforth warrants further research investigations (greater research capacities would enable a better comprehensive understanding of drug discovery from fast pyrolysis technology). The study also suggests that bio-oil from different feedstocks which remain grossly unexplored should be evaluated for antimicrobial activity against multidrug resistant bacteria (MDR) and phytopathogens. There is every possibility that Mother Nature endowed with enormous biomass diversity may literally unfold the elixir of life against the worrisome trend of drug resistance.

References

- [1] Hammer, K.A., Carson, C.F., & Riley, T.V. Antimicrobial activity of essential oils and other plant extracts. *J Appl Microbiol*, **86** (6), 985-90.1999.
- [2] Duraipandiyan, V., Ayyanar, M., & Ignacimuthu, S. Antimicrobial activity of some ethnomedicinal plants used by Paliyar tribe from Tamil Nadu, India. *BMC Complement Altern Med*, **6** 35.2006.
- [3] Ahmad, B. & Ali, J. Physiochemical, minerals, phytochemical contents, antimicrobial activities evaluation and fourier transform infrared (FTIR) analysis of *Hippophae rhamnoides L.* leaves extracts. *African Journal of Pharmacy and Pharmacology*, **7** (7), 375-388
- [4] Jamil, M., et al. Pharmacological activities of selected plant species and their phytochemical analysis. *Journal of Medicinal Plants Research*, **37** (6), 5013-5022
- [5] Aubert, M., Aubert, J., & Gauthier, M., *Antibiotic substances from marine flora*, in *Marine Algae in Pharmaceutical Science*, H.A. Hoppe, T. Levring, and Y. Tanaka, Editors. 1979, Walter de Gruyter: Berlin. p. 267-291.
- [6] Glombitza, K.W., *Antibiotics from algae.*, in *Marine Algae in Pharmaceutical Science*, H.A. Hoppe, T. Levring, and Y. Tanaka, Editors. 1979, Walter de Gruyter: Berlin. p. 303-342.
- [7] Mohan, D., et al. Fungicidal values of bio-oils and their lignin-rich fractions obtained from wood/bark fast pyrolysis. *Chemosphere*, **71** (3), 456-465.2008.
- [8] Kim, K.H., et al. Evaluation of the antifungal effects of bio-oil prepared with lignocellulosic biomass using fast pyrolysis technology. *Chemosphere*, **89** (6), 688-93.2012.
- [9] Mohan, D., Pittman, C.U., & Steele, P.H. Pyrolysis of wood/biomass for bio-oil: A critical review. *Energy & Fuels*, **20** (3), 848-889.2006.
- [10] Piskorz, J., Scott, D.S., & Radlein, D., *Composition of Oils Obtained by Fast Pyrolysis of Different Woods*, in *Pyrolysis Oils from Biomass*, J. Soltes and T.A. Milne, Editors. 1988, American Chemical Society. p. 167-178.

- [11] Vijayarathna, S., et al. The Antimicrobial efficacy of *Elaeis guineensis*: characterization, in vitro and in vivo studies. *Molecules*, **17** (5), 4860-77.2012.
- [12] Sultana, T., et al. Hepatoprotective and Antibacterial Activity of Ursolic Acid Extracted from *Hedyotis corymbosa* L. *Bangladesh Journal of Scientific and Industrial Research*, **45** (1).2010.

Chapter 4 (c)

Prospect of utilization of biochar

Chapter 4(c): Prospect of utilization of biochar

4-3.1 Introduction

Biochar, the byproduct of pyrolysis process has got low surface area, pore size but higher percentage of inorganic constituents and pH value as discussed in chapter 4(a). Due to its high pH and ash content, biochar can be used as soil amendment without any further processing. However, if activated biochar becomes an excellent adsorbent with many uses. It has been used extensively for the removal of various pollutants, water treatment, as composite materials and as catalyst supports owing to desirable properties like high surface area, thermal stability and porous structure. The advantages of activated carbon derive from its large surface area, well-developed internal structure and presence of various surface functional groups. Moreover, carbon materials have recently gained attention as catalyst supports, owing to properties like: high stability in acidic, basic media and possibility of tailoring both their texture and surface chemistry and low material cost. In this context biochar is also a potential candidate as it mirrors charcoal in all aspects. Surface chemistry of biochar may be modified to have very high area (by physical or chemical activation) similar to charcoal [1]. A wide range of carbonaceous materials can be used as the carbon precursors such as coal, peat, wood and various agricultural by-products. Recently, agricultural by-products have received an increasing attention for the production of activated carbon due to their low-cost, renewability and wide prevalence. In the present impregnated biochar obtained from pyrolysis of MFDC with the CaO derived from waste shells obtained by calcination of waste *Turbonilla striatula* shells was used. The physical and chemical properties of this biochar-supported CaO material were evaluated and catalytic properties were studied in the model reaction transesterification of *Mesua ferrea* oil with methanol. The active phase of the catalyst, CaO was produced by the high temperature calcination of Waste shells of *T. striatula* as described elsewhere [2].

4-3.2 Preparation of catalyst and characterization

For preparing support, biochar produced from *Mesua ferrea* deoiled cakes were used, since biochar produced by pyrolysis have very low surface area [3, 4], it was than subjected to chemical activation (with 7 M KOH) in order to increase the surface area. The biochar-supported CaO (BCh-CaO) catalyst was prepared by the wet impregnation method. Typically, a Ca-containing solution was prepared by dissolving 20 g CaO produced earlier in minimum amount of dilute $\text{HNO}_3(\text{aq})$. To this solution, a 20 g of dried and powdered support was added and the resultant mixture was stirred for about 2 h at room temperature. Thereafter, it was heat treated at a calcination temperature of 600°C under atmospheric pressure. The resulting material formed hereafter was treated as catalyst. The catalyst changed the colour of phenolphthalein ($H_- = 8.2$) from colorless to pink, the colour of indigo carmine ($H_- = 12.2$) from blue to green and the colour of 2,4-dinitroaniline ($H_- = 15$) from yellow to mauve but failed to change the colour of 4-nitroaniline ($H_- = 18.4$). Therefore, the catalyst's basic strength was designated as $15 < H_- < 18.4$, and it was considered as a strong base for the transesterification reaction. Figure 4.45 shows the XRD patterns of shell-CaO and BCh-CaO, respectively. New peaks corresponding to the graphite carbon appeared in the XRD pattern of the prepared catalyst (BCh-CaO) along with the peaks of CaO. It was observed that major peaks corresponding to $2\theta = 32.14, 37.22, 53.57, 64.24$ and 67.49 are identified as the fundamental peaks for calcium oxide corresponding to JCPDS file no. 00-003-1123. The presence of carbon is indicated by the peak for $2\theta = 29.26$ which correspond to JCPDS file no. 01-074-2328. This indicates that the activated supported carbon catalyst consists of calcium oxide and carbon. Both shell-CaO and BCh-CaO shows peaks at $2\theta = 32.14, 37.22, 53.57, 64.24$ and 67.49 , which were the characteristic peaks for calcium oxide (JCPDS file no. 48-1467). The diffractograms of produced biochar was quite similar to biochars as per literature [4, 5], while the graphitic basal planes at a 2θ angle of 43° could only be seen in the spectrum of non-activated biochar but not in the activated samples.

The morphology of the catalyst (BCh-CaO) was observed by scanning electron micrographs. The SEM images of the samples showed a good dispersion of CaO on the surface of activated biochar (Figure 4.47). It was observed that although biochar could retain its initial structure [which is supported by XRD (Figure 4.45) pattern also] the CaO species were highly dispersed on the surface of the support. It could be seen that the particles distinctly filled up all the pores of the support indicating that the resulting sample may have high activity. This conclusion is also supported by the surface area measurements. It was observed that there was a significant reduction in BET surface area of activated biochar from (456 m²/g) to the BCh-CaO catalyst (58 m²/g) which indicates that the CaO molecules were successively impregnated into the pores of the activated carbon. The chemical composition of the catalyst was estimated by Energy-dispersive X-ray spectroscopy and the findings are shown in Figure 4.46. It was observed that the major constituent elements present in the BCh-CaO catalyst were calcium, carbon and oxygen having wt.% of 27.8, 17.7 and 54.6 respectively. This result supports the finding in XRD analysis and hence establishes that the catalyst proposed in this study is mainly composed of CaO particles dispersed on activated carbon. Biochar supported CaO (BCh-CaO) was found to be active in transesterification of *Mesua ferrea* oil. To study the influence of different parameters on activity (FAME yield), reactions were carried out at different temperatures with varying methanol to oil molar ratio and catalyst amounts. The results are presented in Table 4.25. From the results it was observed that the catalytic activity of prepared BCh-CaO catalyst was almost similar to the shell-CaO catalysts [6] which could be attributed to the very high loading (50% w/w of support) of active CaO particles. The key parameters affecting biodiesel yield were temperature and catalyst loading. In our study, use of 3. (Wt.%) catalyst loading produced the best results yield of 96% with 12:1 alcohol to oil ratio at 65 °C (Entry 6).

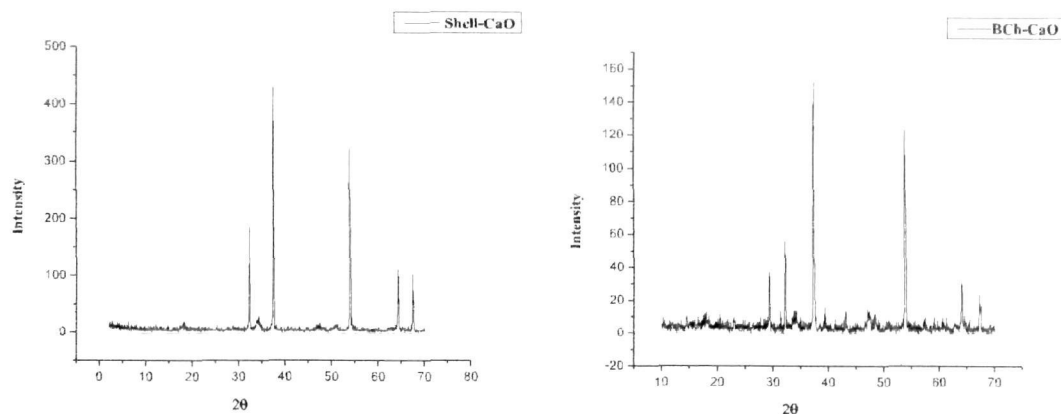


Figure 4.45: XRD patterns of active phase and supported catalyst.

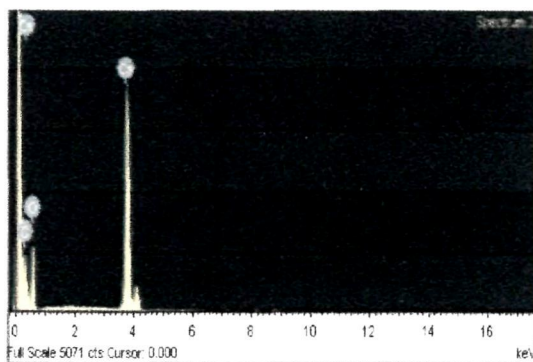


Figure 4.46: EDX spectra of BCh-CaO catalyst.

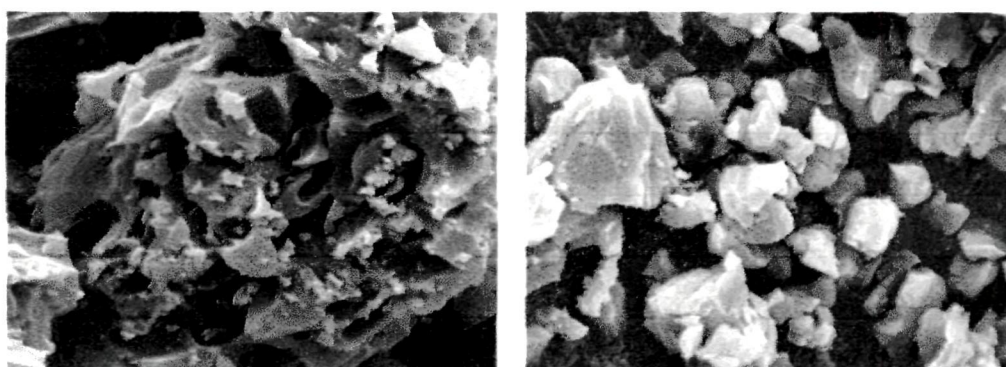


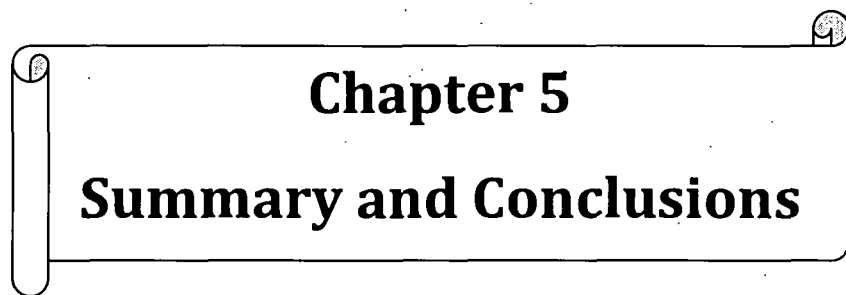
Figure 4.47: SEM images of activated biochar and BCh-CaO catalyst.

Table 4.25: Influence of different parameters on biodiesel yield

Entry no	Temperature (°C)	Catalyst (Wt.%)	Methanol/oil (molar ratio)	Time	Biodiesel Yield (%)
1	65	1	6/1	6	61
2	65	2	6/1	6	88
3	65	3	6/1	6	92.4
4	65	3	6/1	6	94.3
5	80	3	9/1	6	95.7
6	65	3	9/1	6	96
7	95	3	12/1	6	85.6
8	70	3	6/1	6	93
9	33	1	6/1	6	20
10	33	2	9/1	6	25.9
11	33	3	6/1	6	27.2
12	65	3	12/1	6	56
13	70	2	3/1	6	91
14	70	2	9/1	6	91.4

References

- [1] Azargohar, R. & Dalai, A.K. Biochar as a precursor of activated carbon. *Applied Biochemistry and Biotechnology*, **129-132** 762-773, 2006.
- [2] Boro, J., Thakur, A.J., & Deka, D. Solid oxide derived from waste shells of *Turbonilla striatula* as a renewable catalyst for biodiesel production. *Fuel Processing Technology*, **92** (10), 2061-2067, 2011.
- [3] R. Azargohar & Dalai, A.K. Biochar As a Precursor of Activated Carbon. *Applied Biochemistry and Biotechnology*, **129-132** 762-773, 2006.
- [4] Brewer, C.E., et al. Characterization of biochar from fast pyrolysis and gasification systems. *Environmental Progress & Sustainable Energy*, **28** (3), 386-396, 2009.
- [5] Sricharoenchaikul, V., et al. Preparation and Characterization of Activated Carbon from the Pyrolysis of Physic Nut (*Jatropha curcas* L.) Waste. *Energy & Fuels*, **22** (1), 31-37, 2007.
- [6] Boro, J., Deka, D., & Thakur, A.J. A review on solid oxide derived from waste shells as catalyst for biodiesel production. *Renewable and Sustainable Energy Reviews*, **16** (1), 904-910, 2012.



Chapter 5
Summary and Conclusions

Chapter 5: Summary and Conclusions

Biomass is the only renewable energy resources which can fulfill the mankind's need for hydrocarbons for manufacturing goods ranging from plastics and chemicals to biofuels and other products usually derived from modern petroleum refinery. However, successful implementation of any process for biomass conversion to fuels and chemicals primarily depends upon the availability of low cost, good quality feedstock. In this regard, the current work is an endeavor to investigate the prospect of two bioenergy byproducts viz. MFDC and PGDC for their potential use as feedstock for pyrolytic conversion. The prospect of utilization of products of pyrolysis i.e. bio-oil and biochar was also a part of the present investigation. The findings of the present investigations are summarized below.

5.1 MFDC and PGDC as potential bioenergy feedstock

Fundamental characterization of biomass as a feedstock is essential for bio-fuel and chemical production as different type of biomass has specific properties that determine its performance and reactivity during the conversion processes. The moisture and ash contents of MFDC and PGDC were found to be lower than many other similar feedstock currently being explored for pyrolytic conversion. Moisture and ash affect both the handling and processing costs of overall biomass energy conversion. The moisture content was found to be 4.08 and 6.8% and ash content was found to be 4.8 and 4.2% for MFDC and PGDC respectively which indicate that with MFDC and PGDC as feedstock for pyrolysis, there would be low handling and processing cost as compared to other feedstock containing higher moisture and ash contents. The volatile mater content was found to be 83.6 and 73.6% for MFDC and PGDC respectively. The fixed carbon content was 8.5% for MFDC and 13.3% for PGDC biomass. The high amount of volatile matter strongly influences its combustion behavior and thermal decomposition and thus, suggests good potential of the feedstock under investigation for energy production through thermochemical conversion route. The elemental content of carbon, hydrogen, oxygen and nitrogen was found to be 48.6,

7.4, 40.3 and 3.7% and 43.7, 6.6, 46.5 and 3.2% in MFDC and PGDC respectively. The GCV and NCV for MFDC were 18.7 and 16.3 MJ/kg and for PGDC the values were 16.9 MJ/kg and 14.3 MJ/kg respectively. The empirical formula of MFDC is $C_{15.58}H_{28.38}NO_{9.69}$ and PGDC is $C_{15.82}H_{28.52}NO_{12.6}$. Precise information regarding the composition of lignocellulosic biomass is yet another important parameter and is very essential for biomass to be used as a feedstock for pyrolysis system because the pyrolytic product distribution entirely depends upon the three major building blocks of biomass i.e. cellulose, hemicellulose and lignin. The cellulose, hemicellulose and lignin contents were found to be 56.9, 29 and 14.1% for MFDC and 59.3, 28.4 and 12.3% for PGDC biomass.

TGA is an extensively used technique to understand the decomposition behavior and study the reaction kinetics for pyrolysis process because of its simplicity and retrieval of a host of valuable information from a thermogram. On the basis of differential thermogram, the entire pyrolysis process was divided into four stages since every single slope change on a TG curve indicates the beginning of a new stage. It was observed from the study that all characteristic temperatures i.e. T_{onset} , T_{end} , T_{max} and W_{max} were laterally shifted to higher temperature values with increasing heating rate for both MFDC and PGDC. Kinetic parameters were calculated on the basis of four methods viz. Arrhenius, Coats and Redfern, FWO and Multilinear Regression Analysis method. The activation energy calculated on the basis of these methods was presented on average basis i.e. average of the results obtained at different heating rates. However, results from this study encountered variation which could be attributed to the approximations of the method used for determination of kinetic parameters. Thus, model-free method founded on an iso-conversional basis, such as Flynn-Wall-Ozawa (FWO) have gained more attractions in the kinetic analysis of biomass pyrolysis recently. By applying model-free approaches, the apparent activation energy can be estimated based on the fractional conversion of TG-DTG curves. On the basis of FWO method, activation energy of S_{II} and S_{III} was found to be 94.0 and 146.9 kJ/mol for

MFDC and 130.8 and 193.2 kJ/mol for PGDC. It was also observed that the activation energy at S_{III} was always higher than S_{II} as these two stages are characteristic of hemicellulose and cellulose decomposition and it is also well known that cellulose is thermally more stable than hemicelluloses.

5.2 Pyrolytic valorization of MFDC and PGDC

From MFDC and PGDC pyrolysis, maximum liquid yields of 32 and 30.6% at temperature 500°C with a heating rate of 40°C/min were obtained. With increasing temperature, the yield of liquid product increased upto 500°C, but further increase in temperature resulted in decrease in liquid yield. The yield of liquid product for both MFDC and PGDC was increased by increasing heating rate. The char yield was decreased by increasing both temperature and heating rate, while gaseous product yield was increased by increasing temperature and heating rate. The particle size did not show any significant effect on MFDC and PGDC pyrolysis. However, the liquid yield decreased with the application of catalyst while the char yield increased for both the feedstock.

The average chemical composition of bio-oil was found to be $C_{11.43}H_{19.46}NO_{4.18}$ and $C_{11.34}H_{19.16}NO_{4.77}$ for MFDC and PGDC bio-oil respectively. Both the bio-oils were characterized by lower oxygen content than that of original biomass feedstock. The significant decrease in oxygen content in bio-oil as compared to original feedstock is favorable for further processing of bio-oil into fuels and value added chemicals. The low ash content suggests that bio-oils have obvious advantages as a clean fuel oil. Further, it was observed that compared to non-catalytic pyrolysis experiment, the bio-oils obtained with catalyst, had higher C and H values and lower oxygen content.

The bio-oils from MFDC and PGDC are a mixture of complex compounds as evident from FTIR, NMR and GC-MS analysis. The NMR result showed that both the bio-oils are highly populated with carbon and proton in the most upfield region of ^{13}C

and $^1\text{H-NMR}$ spectra respectively. A higher aliphatic content (presence of short, long and/or branched chain hydrocarbons) in both MFDC and PGDC bio-oils is indicative of relatively high energy content in bio-oil (HHV of 30.6 MJ/kg for MFDC and 28.2 MJ/kg for PGDC bio-oil). Further, use of zeolite catalyst in the pyrolysis experiment increased the resonating percentage of proton in the aromatic region of NMR spectra for both the bio-oils because acidic zeolite promotes aromatization reaction in catalytic pyrolysis of biomass. HZSM-5 catalyst showed a higher selectivity towards aromaticity than Mordenite and Y-zeolite.

Mixed feedstock (MFDC+PGDC) pyrolysis at 500°C with a heating rate of 40°C/min showed comparable results with MFDC and PGDC pyrolysis singly. At this temperature, liquid, solid and gaseous products yield were 30.4%, 29.8% and 39.8% respectively. HHV of mixed feedstock bio-oil was found to be 30.3 MJ/kg. The bio-oil from mixed feedstock showed similar properties with individual bio-oils obtained from MFDC and PGDC. However, differences in composition among the bio-oils (bio-oil from mixed feedstock, MFDC and PGDC) are evident through NMR and GC-MS analysis. The IBP and FBP for bio-oil were (180 & 598.8°C), (135 & 598.2°C) and (83.4 & 613.3°C) for MFDC, PGDC and MFDC+PGDC bio-oil respectively. It can also be observed from the SimDist analysis that more than 60% compounds of all bio-oils have boiling point above 350°C.

Biochars obtained from pyrolysis of MFDC and PGDC at 500°C have a porous structure with identical surface area of $\sim 7 \text{ m}^2/\text{g}$. The pore volumes of MFDC and PGDC biochars were found to be 0.051 and 0.046 cm^3/g respectively. These properties of the biochars argues well for not being appropriate for direct usage as activated carbon application, however these co-products of biomass pyrolysis could be activated further through chemical or physical activation treatment for their usage as activated carbon or as a support material for solid catalyst. Furthermore, it was observed that pH and concentration of Ca, K, Mg in

both the biochars increased with the pyrolysis temperature. The biochar with higher contents of inorganic nutrients can play an important role in soil fertility and crop production, and due to their high basic nature, biochars may be potentially used in the agricultural soils of north-eastern region of India for liming, where the soil is predominantly acidic in nature.

5.3 Prospect of utilization of bio-oil and biochar

In the wake of recent advancements in bioenergy research, bio-oils have already gathered the attention of the scientific community in that they offer prospective applicability as a source of value added chemicals apart from being an increasingly attractive fuel option. For this purpose, the antimicrobial activity (antibacterial and antifungal) of bio-oil from MFDC and PGDC was studied. Bio-oil from MFDC and PGDC recorded the most effective zone of inhibition (ZOI) (28 and 29 mm respectively) against *S. aureus*. Both the bio-oils were more effective in terms of antimicrobial efficacy. The results of this study indicate the presence of bio-active agents in bio-oil which may lead to development of new pharmaceuticals.

The biochar obtained from MFDC and PGDC pyrolysis can be used as a support matrix for heterogeneous catalysts like CaO. This biochar supported CaO, used in the production of biodiesel from *Mesua ferrea* oil was found to be effective. The catalyst reported was synthesized entirely by processing waste materials. The active part of the catalyst (i.e. CaO) was derived from waste shells of *Turbonilla striatula* and the support (i.e. activated biochar) was prepared from MFDC. Use of this novel approach makes the biodiesel synthesis process environmentally benign. It showed a high activity and a comparatively higher yield upto 96% was achieved in 6 h using 3 wt.% catalyst in 12:1 methanol:oil molar ratio at a reaction temperature of 65°C.

5.4 Conclusions

From the present investigation, following conclusions can be drawn:

- I. Both MFDC and PGDC have potential for bio-oil production. Deoiled seed cakes which are otherwise low-value bioenergy derived refuse constitute a distinct type of biomass and can be value added through pyrolytic conversion to fuels/source of chemicals and biomaterials.
- II. Model-free method established on an iso-conversional basis, such as (FWO) is more attractive in kinetic parameter calculation. By applying model-free approaches, the apparent activation energy can be estimated based on the fractional conversion of TG–DTG curves.
- III. Use of zeolite catalysts in MFDC and PGDC pyrolysis promoted aromatics production. HZSM-5 catalyst showed a higher selectivity towards aromaticity than Mordenite and Y-zeolite.
- IV. The bio-oil obtained from mixed feedstock (MFDC + PGDC in 1:1 ratio) showed similar properties with individual bio-oils obtained from MFDC and PGDC having fewer differences in composition with PGDC and MFDC bio-oil. However, the compatibility of mixing of these feedstocks would be highly beneficial for fulfilling the criteria of “**feedstock availability**”. This indicates towards feasibility of mixing feedstock with similar properties to obtain the required volume of feedstock for sustainable and continuous operation of the pyrolysis system. This is important as supply of a particular biomass type alone may not be sufficient to fulfill the required volume in large scale operation of a pyrolysis unit continuously.
- V. The biochar containing higher amount inorganic nutrients can play an important role in soil fertility and crop production, and also due to their high basic nature, biochars may be potentially used in the agricultural soils of north-eastern region of India for liming, where the soil is predominantly acidic in nature.

- VI. Study of antimicrobial activity of bio-oil showed that bio-oil offer prospective applicability as a source of value added chemicals apart from being an increasingly attractive fuel option.
- VII. Further, biochar as a means of catalyst support confirmed that this could be a potential source of bio-material for a bio-based society.

5.5 Scope of future work

- I. Optimizations of process parameters for both non-catalytic as well as catalytic pyrolysis are important in MFDC and PGDC pyrolysis. In this study, limited number of parameters is varied for maximum liquid production. Future study is recommended to optimize the process parameters incorporating all possible variable combinations of process parameters such as sweeping gas flow rate, higher heating rate etc.
- II. Zeolites seem to be very promising since they crack biomass pyrolytic vapours or oil, producing higher aromatics albeit with lower yield. Further, non-noble metal incorporated zeolites could be a subject of future study. Conventional zeolite has certain limitations (e.g. formation of coke on the catalyst surface, lower product yield etc.), so development of new class of catalysts/catalysts support is essential and recommended.
- III. Further research is also recommended for extraction of value added chemicals/pharmaceuticals from bio-oil.
- IV. Techno-economic aspects of availability of feedstock, logistic issues, selection of technology, pricing issues of end products and by-product utilization needs to be carried out.

A horizontal rectangular box with a black border and rounded corners. The left side of the box is a vertical bar with a rounded top and bottom, resembling a scroll binding. The right side of the box has a small circular detail at the top right corner, also resembling a scroll binding. The word "Appendix" is centered within the box in a bold, black, serif font.

Appendix

¹H and ¹³C-NMR spectra

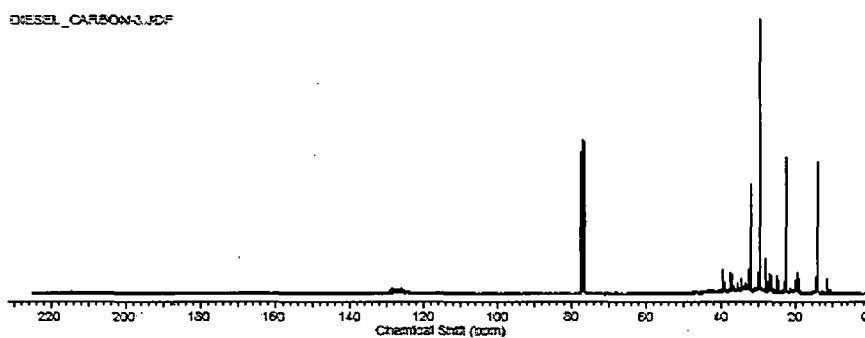


Figure A-1: ¹³C-NMR spectra of Diesel

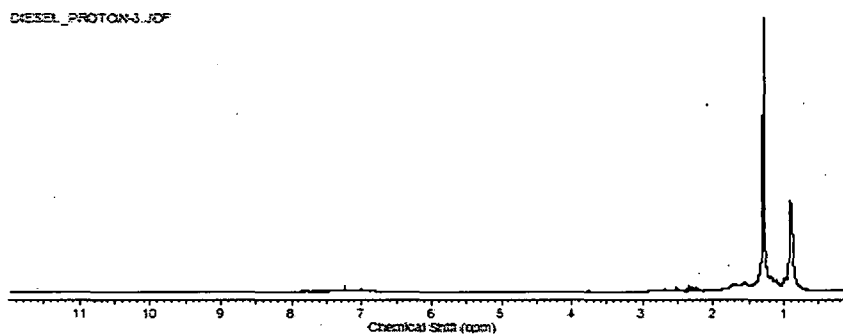


Figure A-2: ¹H-NMR of Diesel

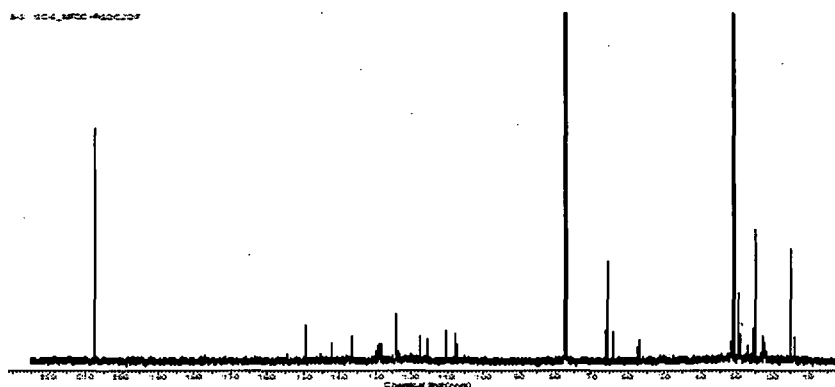


Figure A-3: ¹³C- NMR of bio-oil of MFDC+PGDC (1:1)



Figure A-4: ¹H-NMR of bio-oil of MFDC+PGDC (1:1)

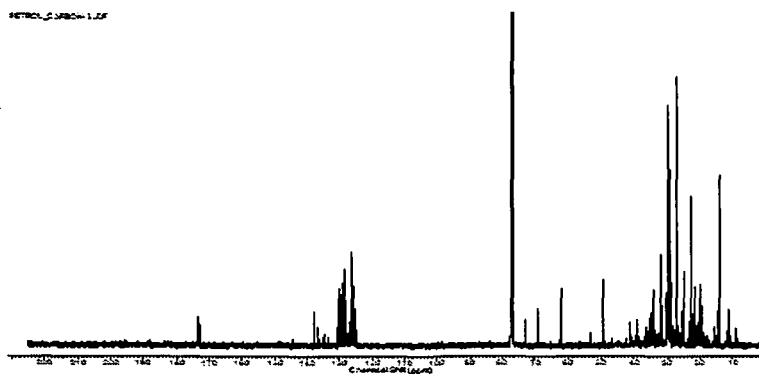


Figure A-5: ¹³C- NMR of bio-oil of petrol

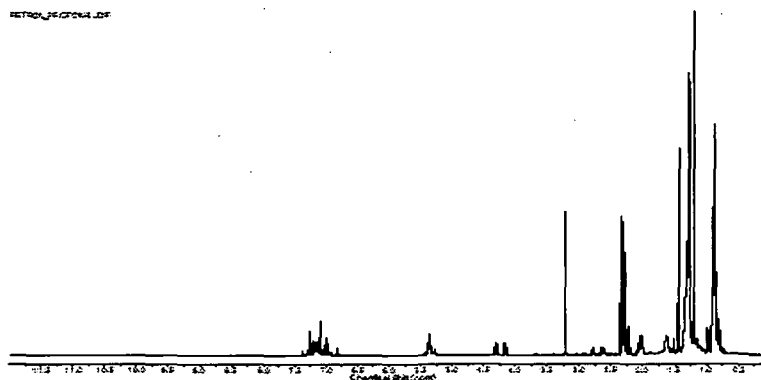


Figure A-6: ¹H-NMR of petrol

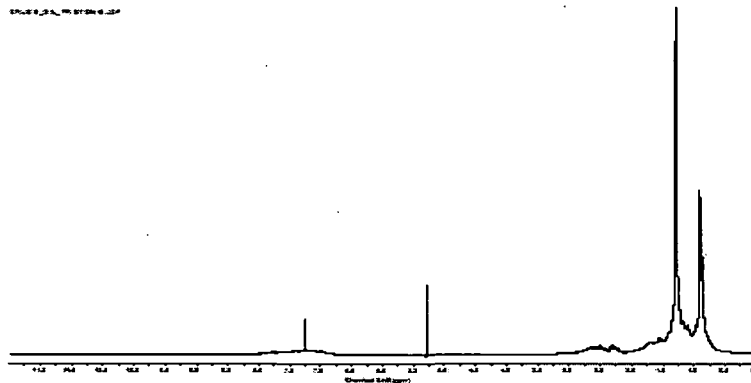


Figure A-7: ¹H-NMR of crude oil

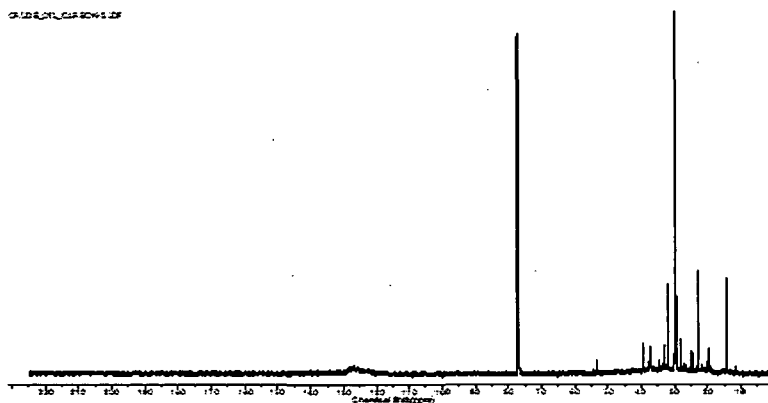


Figure A-8: ¹³C-NMR of Crude oil

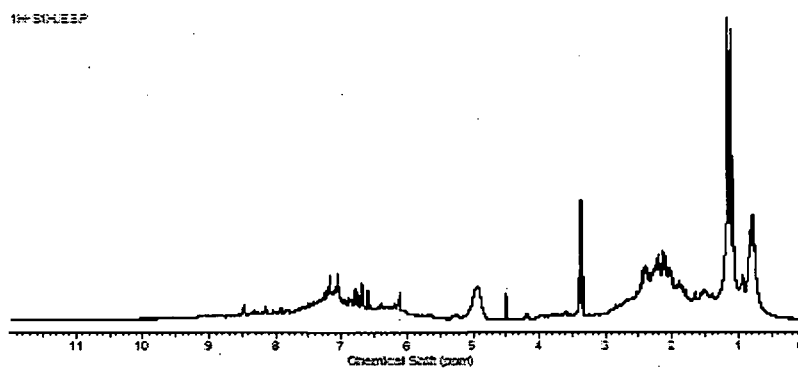


Figure A-9: ¹H-NMR of bio-oil of MFDC with HZSM5 catalyst

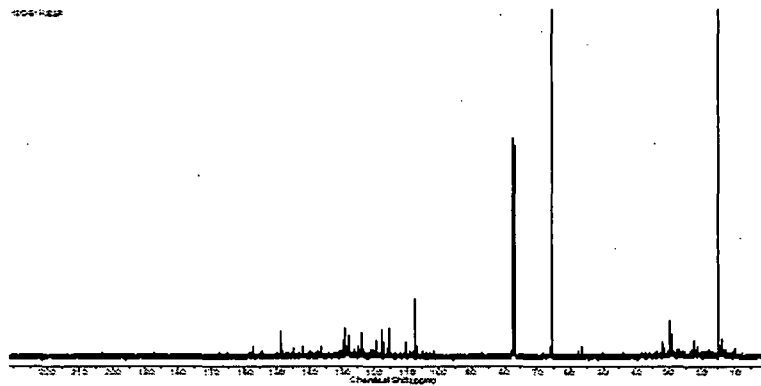


Figure A-10: ^{13}C -NMR of bio-oil of MFDC with HZSM5 catalyst

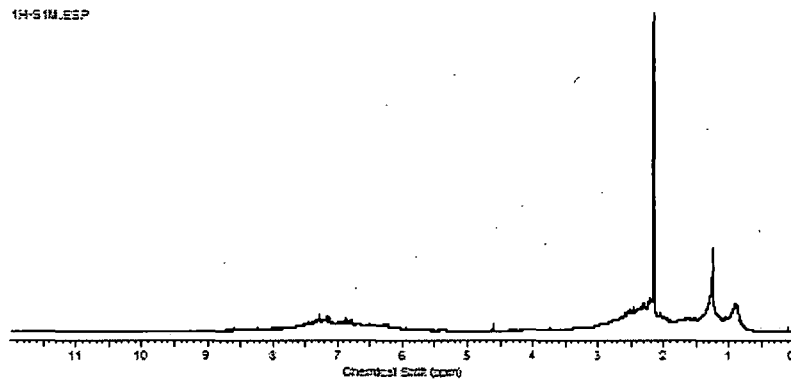


Figure A-11: ^1H -NMR of bio-oil of MFDC with Mordenite catalyst

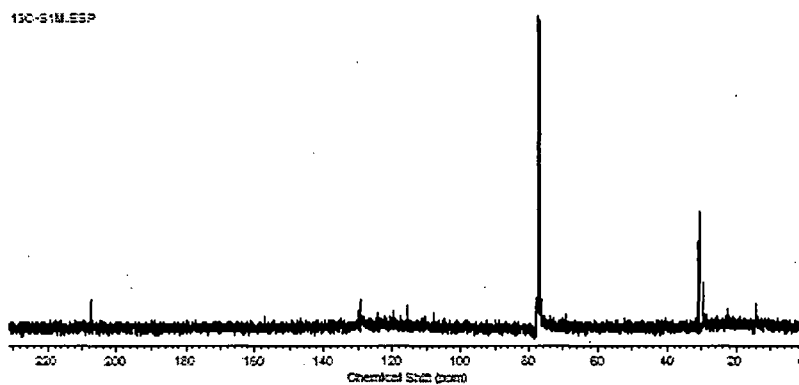


Figure A-12: ^{13}C -NMR of bio-oil of MFDC with Mordenite catalyst

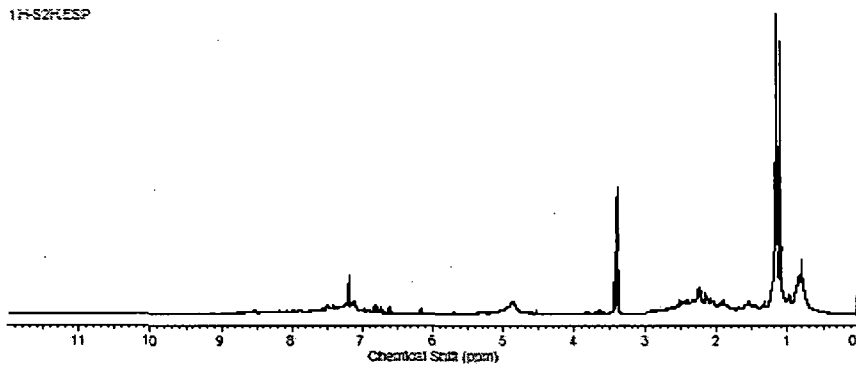


Figure A-13: ^1H -NMR of bio-oil of PGDC with HZSM-5 catalyst

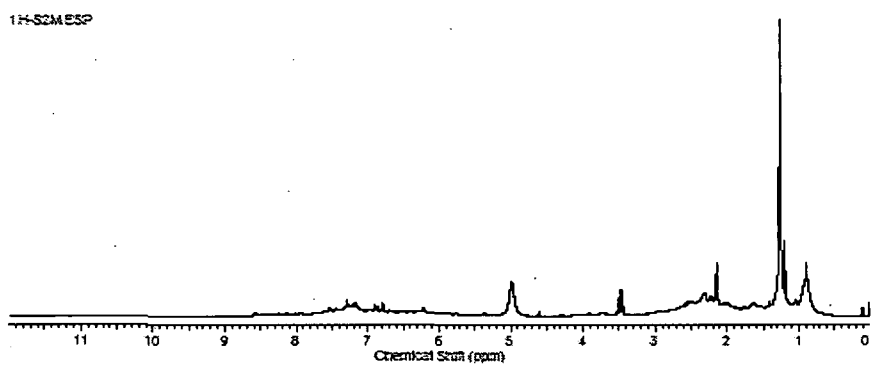


Figure A-14: ^1H -NMR of bio-oil of PGDC with Mordenite

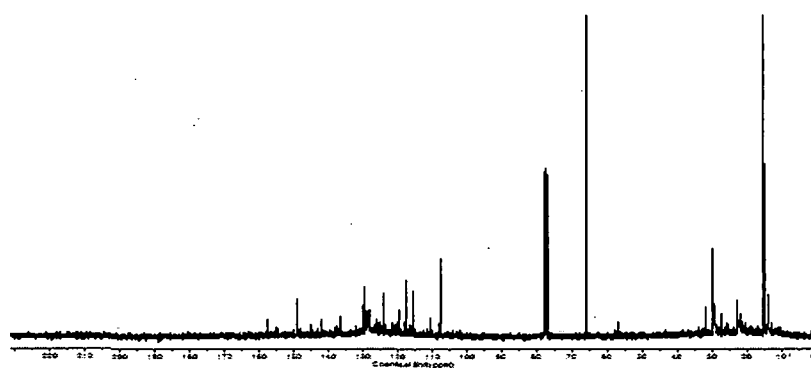


Figure A-15: ^{13}C -NMR of bio-oil of MFDC with Y-Zeolite catalyst

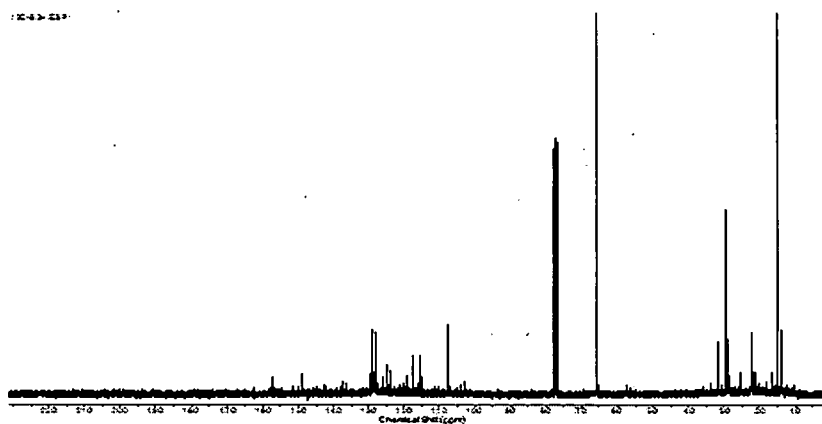


Figure A-16: ^{13}C -NMR of bio-oil of PGDC with HZSM-5 catalyst

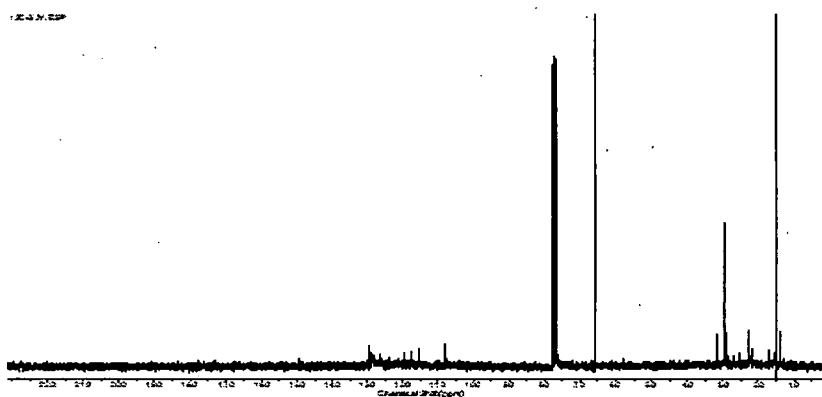


Figure A-17: ^{13}C -NMR of bio-oil of PGDC with Y-Zeolite catalyst

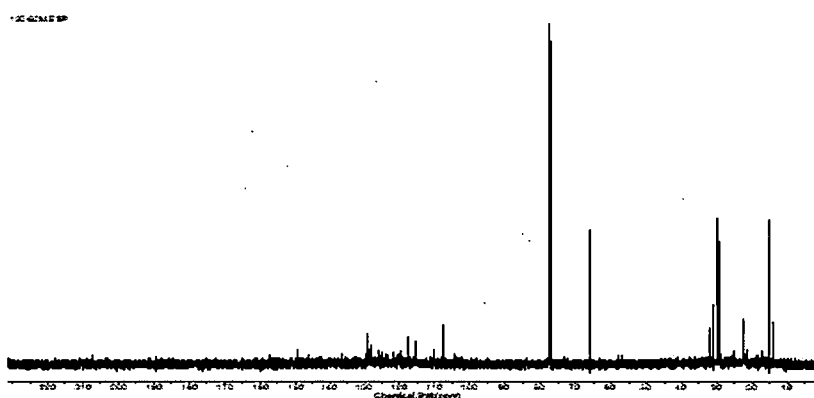


Figure A-18: ^{13}C -NMR of bio-oil of PGDC with Mordenite catalyst



List of Publications

LIST OF PUBLICATIONS

Journal (Published)

1. Bordoloi, N., Narzari, R., **Chutia, R. S.**, Bhaskar, T. and Kataki, R. (2014). "Pyrolysis of *Mesua ferrea* and *Pongamia glabra* seed cover: Characterization of bio-oil and its sub-fractions." *Bioresource Technology*, **In press**, DOI:10.1016/j.biortech.2014.10.079.
2. Choudhury, N. D., **Chutia, R. S.**, Bhaskar, T. and Kataki, R. (2014). "Pyrolysis of jute dust: effect of reaction parameters and analysis of products." *Journal of material cycles and waste management*, **16** (3), 449-459.
3. **Chutia, R. S.**, Kataki, R. and Bhaskar, T. (2014). "Characterization of liquid and solid product from pyrolysis of *Pongamia glabra* deoiled cake." *Bioresource technology*, **165**, 336-342.
4. **Chutia, R. S.**, Bhaskar, T. and Kataki, R. (2013). "Thermogravimetric and decomposition kinetic studies of *Mesua ferrea* L. deoiled cake." *Bioresource Technology*, **139**, 66-72.
5. Phukan, M. M., **Chutia, R. S.**, Kumar, R., Kalita, D., Konwar, B. K. and Kataki, R. (2013). "Assessment of antimicrobial activity of bio-oil from *Pongamia glabra*, *Mesua ferrea* and *parachlorella spp* deoiled cake." *International Journal of Pharma and Bio Sciences*, **4**(4), 910-918.
6. **Chutia, R. S.**, Borah, M., Nath, T. and Kataki, R. (2012). "Biomass fast pyrolysis: A Sustainable Renewable Energy Technology." *International Journal of Engineering Sciences Research*, **03**, 534-539.
7. Phukan, M. M., **Chutia, R. S.**, Konwar, B. K. and Kataki, R. (2011). "Microalgae *Chlorella* as a potential bio-energy feedstock." *Applied Energy*, **88**(10), 3307-3312.
8. **Chutia, R.**, Phukan, M. M., Kataki, R., Bhaskar, T. and Konwar, B. K. "Exploitation of *Pongamia glabra* deoiled cake for alternate energy: Physico-chemical characterization and Thermogravimetric studies." *Energy Sources, Part A: Recovery, Utilization, and Environmental Effects*. Accepted for publication. DOI:10.1080/15567036.2012.744117

9. Katak, R., **Chutia, R. S.** and Borah, M. "Woody shrubs as a potential source of domestic energy in the eastern Himalayan region of India." *Energy Sources, Part A: Recovery, Utilization, and Environmental Effects*. Accepted for publication. DOI:10.1080/15567036.2011.603027
10. Deka, D., Sedai, P. and **Chutia, R. S.** 2014. Investigating woods and barks of some indigenous tree species in North East India for fuel value analysis. *Energy Sources, Part A: Recovery, Utilization, and Environmental Effects*. **36** (17), 1913-1920.

Publications (Conference)

1. **Chutia, R. S.**, Katak, R. and Bhaskar, T. Characterization of liquid and solid product from pyrolysis of Pongamia glabra deoiled cake, in International Conference on Advances in Biotechnology & Bioinformatics & X Convention of The Biotech Research Society, India (ICABB 2013), Pune, India, 25-27 November, 2013
2. **Chutia, R. S.**, Katak, R. and Bhaskar, T. Production of renewable hydrocarbon through catalytic pyrolysis of large bio-polymers: A review, in 7th International Symposium on Feedstock Recycling of Polymeric Materials (ISFR-2013), New Delhi, India, 23-26 October, 2013.
3. **Chutia, R. S.**, Katak, R. Thermochemical conversion of agricultural waste to bio-oil, in National Convention of National Renewable Energy Fellows organized by Ministry of New and Renewable Energy, Govt. of India, 6-7 March, 2013.
4. Konwar, L. J., **Chutia, R. S.**, Boro, J., Katak, R. and Deka, D. Biochar supported CaO as heterogeneous catalyst for biodiesel production, in International Seminar and Workshop on Energy, Sustainability and Development (ISWED- 2012), Sibsagar College, Assam, 12-14 October, 2012.
5. **Chutia, R. S.** and Katak, R. Biomass Fast Pyrolysis: A Sustainable Renewable Energy Technology" in the National Seminar on New and Innovative Renewable Energy and Energy Efficiency, Guwahati, 10-11 July, 2010.
6. **Chutia, R. S.** and Katak, R. Biochar production as a byproduct of bio-oil production through pyrolysis of bio-wastes, in National Workshop on Biochar Production and Uses, Pune, India, 16-17 September, 2010.

7. **Chutia, R. S.** and Katak, R. Study of Pyrolytic Behaviour of Deoiled Seed Cakes of *Pongamia glabra* and *Mesua ferrea* by TGA for their Potential Use as Bio-oil, in National Seminar on Renewable Energy Technology: Issues and Prospects (RETIP-2010), NERIST, Nirjuli, Arunachal Pradesh. 24-25 September, 2010.
8. Katak, R., **Chutia, R. S.** And Saikia, P. Weeds Utilization for Energy Production. National Consultation on Weed Utilization, DWSR (ICAR), Jabalpur, M.P., 20-21 Oct., 2009.
9. Katak, R., **Chutia, R.S.** and Deka, D. (2009). A study on the fuel characteristics of some solid biofuels produced from some indigenous tree species of north-east India. In the proceedings of the 8th International oil & Gas Conference & Exhibition (Petrotech 2009), New Delhi, India.
10. Katak, R., **Chutia, R. S.** and Kashyap, S. Charcoal Production in North-East India : A Case Study on Biomass Utilization and Charcoal Production in Traditional Kilns, Proceedings of the World Renewable Energy Congress 2009, Asia, pp. 464-469, 19-22 May, 2009, Bangkok.

Book Chapter(s)

1. Katak, R., **Chutia, R. S.**, Mishra, M., Bordoloi, N., Saikia, R. and Bhaskar, T. *Feedstock suitability for thermochemical processes*. In Advances in thermochemical conversion of biomass, Pandey, A., Bhaskar, T. and Stocker, M., eds. Elsevier. In press. ISBN: 978-0-444-63289-0, DOI:10.1016/B978-0-444-63289-0.00002-8.
2. **Chutia, R. S.** and Katak, R. *Biowastes as a potential feed-stocks for thermochemical conversion to bio-oil and biochar*. In *Renewable Energy and Sustainable Development*, Katak R. and Borah A. C., eds.. 2012. EBH publishers (India). ISBN: 978-93-80261-78-2.
3. **Chutia, R. S.** and Katak, R. *Study of pyrolytic behavior of de-oiled seed cakes of Pongamia glabra and Mesua ferrea by TGA for their potential use as Bio-oil*. In *Renewable Energy Technology: Issues and Prospects*, Shankar, G., Das, B., & Blange, R., eds.. 2011, Excel India Publishers. New Delhi. 2011. ISBN: 978-93-80697-95-6.

4. Katak, R., Das, M., Chutia, R. S., Borah, M. "Biochar for C-sequestration and soil amelioration". In: *Renewable Energy Technology: Issues and Prospects*, (Eds. Shankar, G., Das, B., and Blange, R.), Excell India Publishers: New Delhi, 2011, pp. 131-137. ISBN: 978-93-80697-95-6.